January 2016

ASSESSING THE IMPACT OF EMERGING CONTAMINANTS ON ANAEROBIC MICROBIAL COMMUNITIES

Leila M. Nyberg
Purdue University

PURDUE UNIVERSITY
GRADUATE SCHOOL
Thesis/Dissertation Acceptance

This is to certify that the thesis/dissertation prepared

By LEILA M NYBERG

Entitled
ASSESSING THE IMPACT OF EMERGING CONTAMINANTS ON ANAEROBIC MICROBIAL COMMUNITIES

For the degree of Doctor of Philosophy

Is approved by the final examining committee:

Loring F. Nies Chair	Von Sigler
Chad T. Jafvert	
Ronald F. Turco	
Brett R. Baldwin	

To the best of my knowledge and as understood by the student in the Thesis/Dissertation Agreement, Publication Delay, and Certification Disclaimer (Graduate School Form 32), this thesis/dissertation adheres to the provisions of Purdue University's "Policy of Integrity in Research" and the use of copyright material.

Approved by Major Professor(s): Loring F. Nies

Approved by: Dulcy M. Abraham 8/1/2016

Head of the Departmental Graduate Program Date

ASSESSING THE IMPACT OF EMERGING CONTAMINANTS ON ANAEROBIC MICROBIAL COMMUNITIES

A Dissertation

Submitted to the Faculty

of

Purdue University

by

Leila Nyberg

In Partial Fulfillment of the

Requirements for the Degree

of

Doctor of Philosophy

August 2016

Purdue University

West Lafayette, Indiana

ACKNOWLEDGEMENTS

I would first like to thank my major professor Dr. Loring Nies, as well as my committee members Dr. Ronald F. Turco, Dr. Chad T. Jafvert, Dr. Brett R. Baldwin, and Dr. Von Sigler. I am grateful that they found it worthwhile to invest their time and share their expertise with me. I also thank them for their patient and constructive approach in helping me improve my work.

I extend special thanks to Dr. Changhe Xiao for ongoing technical and moral support since my first day in the Environmental area. I have been fortunate for the guidance of Dr. Linda Lee, as well as the friendship and collaboration of several members of her research group. I thank Dr. Corinne Ackerman, Judy Lindell, Dr. Rebecca Lindell, Militza Carrero-Colon, Dr. Joanna Barton, Fred Beasley, Dr. Marta Vargha, Dr. John Cupp, Darek Bulinksi, Jennifer Fizer, and Marcie Duffin for their encouragement and mentorship that laid the groundwork for my success in the program. Dr. Nadya Zyaykina has been a stabilizing presence and invaluable resource as I completed the last phase of my lab work under the auspices of Murphy's Law. Being a joint ESE/Civil Engineering student presented special challenges and I thank Jenny Ricksy and Christal Musser for their expert coordination in guiding me through the process.

Marianne Bischoff Gray assisted with microcosm headspace analysis. I especially thank her for her time spent with me on method development. I have had the honor of mentoring several talented undergraduate students over the years. Among them, Shruti Mishra and Allison Kloiber contributed directly to the sediment project described here. Purdue Dairy Farm, specifically cow #4421, graciously provided rumen inoculum. Dr. Robert J. Moon provided cellulose nanomaterials. Debby Sherman (Purdue Life Sciences Microscopy Facility) performed SEM imaging and EDX analysis. Timothy Miller at Birck Nanotechnology Center in Discovery Park provided ultrapure water for all microscopy including EDX. Greater Lafayette Wastewater Treatment Plant staff generously provided tours for student lab assistants and accommodated our frequent requests for digester samples. Thanks also to the microbial inhabitants of the wastewater treatment plant, Celery Bog Nature Area, and the digestive tract of cow # 4421 for all they have taught me by participating in my experiments.

This work was completed under STAR Fellowship Assistance Agreement no. FP: 917146 awarded by the U.S. Environmental Protection Agency (EPA). It has not been formally reviewed by EPA. The views expressed in this thesis are solely those of Leila Nyberg, and EPA does not endorse any products or commercial services mentioned in this publication.

Finally, I acknowledge the support of National Science Foundation Award EEC – 04040006 in the preliminary phase of this work.

TABLE OF CONTENTS

Page

Page

ABSTRACT

Nyberg, Leila M. Ph.D., Purdue University, August 2016. Assessing the Impact of Emerging Contaminants on Anaerobic Microbial Communities. Major Professor: Loring Nies.

The impact of emerging contaminants on anaerobic microbial communities is critical and under-explored. Anaerobic processes are foundational to ecosystem function. Routes of chemical exposure to anaerobic communities include wastewater discharge, drug delivery to ruminant livestock and land application of biosolids. Emerging contaminants are frequently used in consumer products; pharmaceuticals and nanomaterials are of particular concern because of their unique chemical and physical properties. Endocrine-disrupting nonylphenols, degradation by-products of surfactants found in consumer products, are established to be persistent and toxic to aquatic life in sediments. The research presented here consists of a survey of effects of these contaminants on anaerobic microorganisms. The relationship between microbial community structure and function was studied. Nanotube experiments were carried out with either digester sludge or cow rumen inoculum. Impact of a surfactant was examined in Celery Bog sediment. Microbial community function was measured with a biomethane potential assay. Sodium 2-bromoethanesulfonate, a known inhibitor of methanogenesis, was used as a toxic reference. Community structure was assessed with PCR-DGGE and 16s next-generation Illumina sequencing and metagenomics. Carbon nanotubes and their associated residual

elements were characterized by TEM and EDX. Metals analysis in both solid and aqueous phases of microcosms was performed by ICP-MS. None of the carbon nanomaterials were found to be toxic. Several of the manufactured nanotube products were found to accelerate gas production and shift the microbial communities. These effects appear to be independent of metal or amorphous carbon content, or degree of nanotube functionalization. A more pronounced effect was seen with increasing nanotube length, which is likely related to surface area. Surfactants in sediments resulted in significant enrichment of *Geothrix fermentans* in the presence of continuing methanogenesis but only moderate effects on community function. Carbon nanomaterials very substantially accelerate methanogenic activity, and may in fact facilitate biotransformation of recalcitrant biopolymeric material.

CHAPTER 1. INTRODUCTION

1.1 Introduction to Emerging Contaminants

Approximately 50,000 chemicals are used by industry with about 500 new chemicals deployed each year. The USGS targets almost 100 chemicals as "emerging contaminants" in surface waters while the CDC monitors human body burden of almost 150 chemicals found in the environment. Such direct chemical analysis and monitoring is certainly needed. However, it is infeasible to monitor the environment for every potential contaminant or its metabolites. Furthermore, analytical methods have not yet been developed for emerging nanomaterials in environmental matrices. Moreover, in the interest of long-term environmental protection and stewardship, we must improve our understanding of ecosystem function in response to chemical exposure. Due to their critical role in carbon and nutrient cycling, waste assimilation and water purification, microorganisms are important sentinel communities in ecosystems. Strengthening our assessment of the effects of new chemicals on microorganisms would enrich and supplement data obtained about chemical exposure to macroscopic organisms. Routes of exposure for emerging contaminants in anaerobic environments are illustrated in Fig. 1.1.

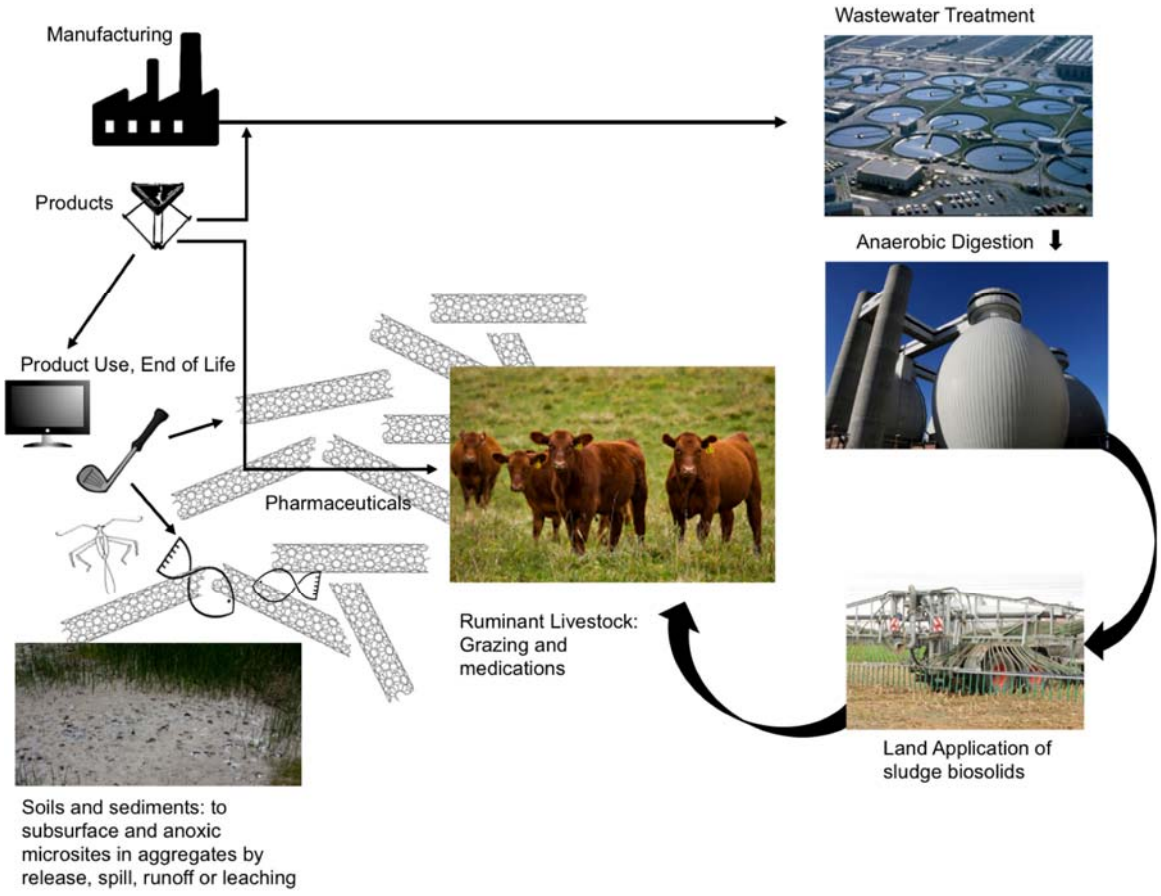

Figure 1.1. Routes of exposure for emerging contaminants in anaerobic systems. Image credits in Appendix Table 1.

This study employed functionalized carbon nanotubes (f-CNTs) as model emerging contaminants due to their theoretically increased bioavailability[1] compared with non-functionalized nanotubes that are more strongly hydrophobic. Expansion of this work included other chemicals of interest such as cellulose nanomaterials and alkylphenol

ethoxylate detergents. Of additional concern are the residual metals present in many engineered nanomaterials that will be released to the environment.

The effects of these contaminants on both natural and engineered anaerobic systems were explored. In Chapter 4, the effect of different manufactured nanotubes on the anaerobic microbial community in the ruminant digestive tract of a dairy cow was assessed. The predominant form of methanogenesis in cow rumen is hydrogenotrophic, as acetate and other volatile fatty acids (VFAs) are used directly by the cow as a nutrient source. Rumen microbial communities are adapted to degradation of complex biopolymers such as lignin, cellulose, and hemicellulose. It seemed plausible that any biodegradation of nanotubes that could potentially occur at defect sites in the carbon cage structure would occur via some of the same pathways used by these microorganisms. This inoculum source was of further interest due to the potential exposure of livestock to nanomaterials by way of veterinary drug delivery technology, or by grazing on cropland with applied biosolids from wastewater treatment sludge.

The latter was the inoculum of choice for the nanotoxicology study described in Chapter 5. The wastewater treatment digester is the receptor for emerging contaminants at every stage of their life cycle; from manufacturing waste streams to discharges resulting from end use, such as domestic, biomedical, or industrial. Hydrophobic contaminants such as carbon nanotubes would be likely to accumulate in biosolids and be transported to soils through land application.

Finally, in Chapter 6, the effect of a known chemical of concern on wetland sediment is studied. Sediment was the appropriate matrix for this assessment because the hydrophobic metabolite of this detergent compound is known to accumulate and exert toxic, particularly endocrine-disrupting effects on aquatic life.

Many common species between all these anaerobic environments were detected by next-generation DNA sequencing and metagenomics. Another shared element between all these studies is the relative hydrophobicity of either the reference material (e.g. carbon nanotubes without functional groups), or a known toxic metabolite (the nonylphenol moiety of the nonylphenol ethoxylate surfactant). Finally, in each of these studies a complex relationship between microbial community structure and function is revealed.

CHAPTER 2. LITERATURE REVIEW

2.1 Nanotubes: functionalization, application, and environmental concern

Research and development for applications of carbon-based manufactured nanoparticles (CMNP) continue to outpace scientific investigations of potential toxicity and negative environmental impacts of these new materials[2]. The focus for new applications that are likely to lead to large-volume manufacturing has shifted from fullerenes to carbon nanotubes (CNTs)[3]. It is urgent that environmental scientists respond to this trend by refocusing ecotoxicological assessment of nanomaterials on nanotubes. It is important to place the highest priority on study of those with routes of exposure and mass fluxes most likely to exert a toxic effect. Development of nanotechnology research priorities is ongoing, but consistently published objectives aimed at environmental and ecosystem health are i) detection methods in biological matrices, ii) effects on species and test methods, iii) ecosystem wide effects, and iv) transformation under different environmental conditions (e.g. NNI, 2006). This work described in this thesis was aimed at advancing discovery specifically in these national research priority areas. If nanomaterials were determined to have any hazardous characteristics (e.g. toxic), they would be regulated under the Solid Waste Disposal Act (SWDA), the Toxic Substances

Control Act (TSCA) or the Clean Water Act (CWA) depending on the use, treatment, or discharge scenario.

Of particular concern for ecotoxicity are functionalized single-wall nanotubes, which are being explored for a variety of biomedical applications such as imaging and drug delivery, because of their theoretical capability to penetrate cell membranes. Introduction of polar functional groups significantly increases their solubility, and as a result, their potential bioavailability[4]. These materials may have great potential to increase safety and efficacy of medical treatments by delivering drugs or imaging molecules with targeted precision. However, virtually nothing is known about their long-term effects if they remain in the human body, or alternatively, their environmental impact if they are excreted and released to wastewater treatment plants (WWTP). Additional waste streams from manufacturing and industrial release must be considered as well. From the standpoint of environmental risk assessment, the potential toxicity of attached functional groups must be considered in addition to the unknown effects of the base nanomaterial. Both abiotic and biological processes may lead to hydrolytic cleavage and subsequent degradation of functional groups in the environment, perhaps altering the toxicity and behavior of nanomaterials in the environment. These transformations might facilitate biodegradation of the nanotubes over the long term. The lipophilic nature of nanotubes[5] and their ability to act as metals or as semiconductors depending on their chirality[6] raise additional concerns about possible accumulation up the food chain, or unpredictable reactivity in both natural and engineered ecosystems.

Since SWNT are extremely hydrophobic, they will strongly partition into the biomass in wastewater treatment plants, and ultimately anaerobic sludge digesters. Even soluble functionalized f-CNTs will sorb to organic matter (e.g. biomass) through molecular interactions[7, 8]. Therefore, anaerobic digester sludge is the ultimate receptor for f-CNTs and via land application of digested sludge, a possible vector to the environment. Any new chemicals released during manufacturing or to an industrial waste stream will follow this route to the environment[9]. Moreover, as receptors and vectors of CMNPs, microbial communities in anaerobic digesters are excellent sentinel communities for evaluation of their effects.

Biodegradation potential of a chemical in anaerobic systems is important for environmental risk assessment[10]. The objectives of this study are to assess toxicity and potential for anaerobic biodegradation of CNTs by examining their effect on structure and function of anaerobic microbial communities and to advance applications of molecular genetic tools for assessing complex environmental matrices. This study attempts to address several important issues in experimental design of risk assessment for nanomaterials, such as the range of forms in which CMNPs may be found in the environment, their bioavailability, and the additional effect of their manufacturing byproducts such as solvents, PAHs and other possible components of a CMNP waste stream. The expected production volume of nanotubes has been projected to reach millions of tons within the next few decades. With the prospect of large production volumes of nanotubes becoming a reality, a new research agenda has been proposed to address emerging risks that may accompany large commercial enterprises; such as

transportation of nanomaterial products, workplace health and safety, control of environmental releases and the need for emergency responders[11].

Recent reports have highlighted the need for a more standardized approach to nanomaterials assessment, including the choice of dose metrics (particle number, concentration, size), as well as a more complete understanding of the factors determining their toxicity and transport, such as preparation techniques, surface modifications, and pH[12]. The importance of potential microbial interactions with nanomaterials in the environment is generally appreciated by the research community. Fortner *et al.*[13] and Lyon *et al.*[14] accomplished the first studies of microbial effects of C_{60} under both aerobic and anaerobic conditions, with pure cultures and facilitated exposure to C_{60}. Tong *et al.*[15]showed that neither solid nor nC_{60} had any effect on soil microbial respiration, with a corresponding lack of impact on 16s rRNA gene and phospholipid profiles. It has also been shown that neither solid nor nC_{60} had any effect on methanogenesis, or 16s or 18s community profiles in anaerobic digester microcosms[16].

The pressing need for ecological risk assessment of nanomaterials is primarily driven by the unique chemical and physical properties conferred by the nanoscale, which remain poorly understood. Their high surface area to volume ratio possibly enhances their reactivity, which is expected to be an important factor in potential toxicity[17]. The potential for biodegradation to other organic products, particularly large aromatic structures, confounds the scenario of nanoscale effects of fullerenes and their derivatives. Partial transformations of PAHs[18] yield toxic metabolites, and a similar process could

occur with neat or functionalized nanotubes. Furthermore, PAHs are believed to be intermediates in and byproducts of fullerene and nanotube synthesis[19]. A small pilot study of a waste stream from synthesis of multi-wall nanotubes found at least 15 different PAHs as well as volatile organic compounds[20]. It is clear that common environmental contaminants such as these may present an environmental hazard at any step in the life cycle of CMNP.

Kang *et al*. showed a strong antimicrobial effect of SWNT on E. coli K12 (2007, 2008a) [21, 22]with changes in metabolic activity, morphology, and regulation of stress genes in response to SWNT, and, to a lesser extent, MWNT[21]. Their work highlights functionalization and stability in aqueous suspension as contributing factors to toxicity[23]. Experiments with different bacterial monocultures, river water, and wastewater treatment plant effluent supports their conclusion that SWNT are more toxic than aq-C_{60}, graphite, and MWNT[24]. They found that natural organic matter (NOM) mitigated direct contact between cells and SWNT, but it did not reduce toxicity of the nanomaterial to attached cells. Arias and Yang[25] have demonstrated antimicrobial activity of SWNT-COOH and SWNT-OH to bacteria in pure culture. This literature demonstrates the importance of studying the effect of CNT on microbial communities, because while it emphasizes the potential for toxicity, these studies underscore the importance of understanding the complexity of environmental interactions. More recent studies suggest that microbial populations in natural environments are capable of attenuating carbon nanotube toxicity, for example through biopolymer deposition on nanotube surfaces by river water bacteria[26].

Early assessment of the ecological impact of nanomaterials or any new chemicals must include anaerobic systems as well as aerobic in order to characterize their effects on biogeochemical cycles. Methanogens were once classified as bacteria, but are now included in the domain Archaea[27]. The global role of methanogenesis is a rapidly developing area of study, not only because of the impact of methane and other greenhouse gases on climate change, but also the potential to harness methane as an alternative energy source[28]. The complexity of community interactions among methanogens and other anaerobic microorganisms is of critical importance for understanding such ecosystems as wastewater treatment sludge, subsurface soil, sediment, and rumen. Shifts in the community profiles of any of the three domains may become ecologically significant.

Muyzer *et al*.[29] first described the PCR-DGGE technique for analysis of the V3 region of the 16s rRNA gene of bacteria. More recently, this technique has been used to target this region for Archaea[30], and the 18s rRNA gene for Eukarya, using primers for fungi[31], the domain Eukarya (Van Hannen *et al*.,1998)[32], and protists[33]. To our knowledge, our group is the first to use PCR-DGGE to study the effect of anthropogenic chemical input on all three branches of the universal phylogenetic tree in the same study[16].

Since persistent organic pollutants inevitably accumulate in anaerobic environmental compartments (sediments and WWTP sludge), improved tools are needed to better characterize the structure and function of anaerobic communities impacted by CNTs. The aim of this thesis research was to advance developments in microbial community

analysis to increase the robustness of assessment techniques and begin to answer pressing questions of great relevance to environmental and human health. It is also important to acknowledge that analytical techniques to measure CNTs in environmental matrices have not yet been developed. Therefore, developing methods to assess and understand response to CNT and other emerging chemical exposure is a rational approach.

2.2 Residual Metals in Carbon-based Nanomaterials

Ecological assessment of nanomaterials requires investigation of complex mixtures potentially released to the environment including organic solvents, metal catalysts, and other byproducts of manufacturing. Hull *et al.*[34] found that "process-associated" Fe, Gd, Cu and other metals had their toxicity eliminated or reduced to some extent by chelation with EDTA. Hard water also mitigated toxic effects of the metals. These authors cautioned against ignoring potential effects of residual metals in risk assessment of manufactured carbon nanomaterials.

Nickel and yttrium are the predominant (~5%) metals detected in many of the nanotube products used in my work. For the purpose of this study, it should be noted that the enzyme that catalyzes the final step of methanogenesis, methyl coenzyme M reductase (MCR), is a nickel enzyme, and according to recent work, it carries out both forward and reverse reactions[35].

2.3 Cellulose nanomaterials and biopolymer-degrading communities in cow rumen

According to Moon *et al*.[36], cellulose nanomaterials have the potential to replace many petroleum-based products (e.g. fibers and textiles, nanoelectronics, drug delivery and other biomedical applications). Nano-sized cellulose is biocompatible with the human body, and in many cases is produced by microorganisms, which gives the advantage of a higher-purity material[37]. Early research[38] suggests that ecological toxicity is not a pressing concern. However, environmental impact assessment of these new materials is very limited. Kovacs et al.[39] found that nanocrystalline cellulose (NCC) had equivalently low aquatic toxicity to carboxyl methyl cellulose (CMC), with a notable exception being its effect on fathead minnow reproduction at the IC25 dose of 0.29 g/L.

Theoretically, nano-sized cellulose products may be biodegraded by the same mechanisms as their bulk cellulose counterparts. Schwartz[40] describes the complex of multiple extracellular enzymes called the cellulosome, which enables anaerobic bacteria such as those in the cow rumen to degrade many forms of this biopolymer. The work with anaerobic microbial communities described in this thesis presents an opportunity to make an important contribution to biological assessment of these emerging "green" materials, by discovering their impact on cellulose-adapted rumen microcosms.

2.4 Alkylphenol ethoxylates in sediment

Alkylphenol ethoxylates (APEO) are anthropogenic chemicals that have been in use for more than 50 years, and are the second largest class of nonionic surfactants in

commercial production in North America[41]. The most widely used of this class of compounds are the nonylphenol ethyoxylates (NPEO), and the mechanisms for their biodegradation in the environment remain largely unknown[42]. Their ethoxylate chains typically degrade very readily under anaerobic conditions, with a wide range of chain lengths between different NPEO. Several studies, including Jonkers et al.[43] have found that longer-chain NPEO degrade faster in aquatic environments than shorter – chain NPEO, which may lead to accumulation of the latter in ecosystems. Shang et al.[44] reported that NPEO persist in sediment, with estimated half-life of greater than 60 years, and no significant degradation occurring by chain shortening. An inverse relationship has been reported between APEO chain length and toxicity of the alkylphenol moiety, with endocrine-disrupting effects on aquatic fauna[45]. These shorter-chain degradation products have been shown to be recalcitrant in aquatic environments[46]. Anaerobic biodegradation of APEO was studied by Lu et al.[47], who found that estrogenic metabolic intermediates accumulated with biodegradation of NPEO. Ying et al.[48] stated that degradation of APEO in sediment should be further studied in both aerobic and anaerobic systems.

This brief review of the literature reveals that knowledge about how emerging hydrophobic contaminants will affect the structure and function of anaerobic communities is lacking. It is evident that investigation into how these materials affect diverse anaerobic communities (e.g. rumen, digester sludge, sediment) would be prudent.

CHAPTER 3. MATERIALS AND METHODS

3.1 Elemental Analysis by Energy-dispersive X-ray spectroscopy (EDX)

SEM imaging and EDX for elemental analysis of commercially available nanotubes were performed at the Purdue University Life Science Microscopy Facility. Nanotubes were prepared by suspension in ultrapure water from Birck Nanotechnology Center. This was accomplished by water bath sonication for 15 -30 minutes, with the time depending on the nanotube dimensions and degree of functionalization for each manufactured product. Ultrapure water was also used as a blank for elemental analysis.

"The samples were imaged with an FEI Quanta 3D FEG scanning electron microscope (FEI Company, Hillsboro, OR). Parameters were 20kV, spot 6.5, and working distance of ~10mm. Magnifications for analysis were 250x-8K in full screen mode (30x26cm). X-ray analysis (EDX) was done with an Oxford INCA Xstream-2 with Xmax80 detector (Oxford Instruments, Peabody, MA) using above parameters, 50µm objective aperture, and P5. Spectra were collected for 120 sec."[49]

3.2 Anaerobic Microcosm Setup and Biomethane Potential (BMP) Assay

A biomethane potential assay[10] was used to assess the effect of treatments on microbial community function. Rumen inoculum was collected from Purdue Dairy. Anaerobic digester sludge was collected from the Greater Lafayette Wastewater Treatment Plant. Sediment was collected from Celery Bog Nature Area. Detailed information for microcosm setup is provided in each chapter. Anaerobic gas production was monitored over time (> 1 year).

Theoretical gas production for substrates and treatments in all experiments were calculated using the Buswell equation[50] (Equation 1) and the Ideal Gas Law (Equation 2):

1) $C_aH_bO_c + (a-(b/4) - c/2) H_2O \Rightarrow ((a/2)-(b/8)+(c/4)) CO_2 +((a/2)+(b/8)-(c/4))CH_4$

2) $PV=nRT$

3.3 Microcosm Headspace Analysis

Gas analysis was performed on an Agilent 7890 GC equipped with a FID detector and a TCD detector (Santa Clara, CA). A model 120 autosampler upgraded for headspace analysis (Quantum Analytics, Foster City, CA) was used to inject samples using 2 mL vials with crimp caps. Caps were fitted with PTFE/silicone septa (Thermo, Rockwood, TN). A 250 µl loop with 0.4 mm ports (Valco, Houston, TX) was used for autosampler

injection. The GC was further customized (Custom Solutions Group, Katy, TX) by the installation of two pneumatically actuated 10 port gas sampling and backflush-to-vent valves, and a 6 port series-bypass valve on Valco E rotors, and a switching solenoid valve for purge of valve loops between injection. Four columns were installed, a HayeSep N 80/10 mesh micro-pack stainless steel, a HayeSepQ 80/100 mesh micropack stainless steel column, a HayeSep N 80/100 mesh silcosteel and a HayeSepQ 80/100 mesh micropack silcosteel, all with the dimensions of 4' x 1/16". Helium was used as a carrier gas and make-up gas. Injector temperature was 100 °C and flow rate was set at 40 mL min^{-1}. The modifications allow for simultaneous analysis of CH_4 and CO_2.

3.4 DNA Extraction for Analysis of Microbial Community Structure

The MO BIO Powersoil® DNA Isolation Kit was used to extract total genomic DNA for all experiments. In the rumen study, subsamples of microcosms were taken at day 417 and after the end of the biomethane potential assay. These were transferred to 2 ml microcentrifuge tubes and spun at 16,000 x g. The supernatant was discarded and biosolids stored at -20 ° C until DNA extraction. Samples from the earlier time point taken during active gas production were used for library preparation for next-generation sequencing. Both sets of genomic DNA samples were used for PCR-DGGE.

In the sludge experiment, a similar procedure was followed except for the following modifications. Subsamples were taken for genomic DNA between each substrate feeding, except for the last two sampling days (592 and 644), which were taken during active

periods of anaerobic gas production. DNA sent for Illumina sequencing was taken on day 131, a single sample from reference and treated sets.

For sediment Experiment A, subsamples of microcosms were taken three times after the end of the biomethane potential assay designated T1, T2, and T3. T1 occurred approximately four years after the beginning of Experiment A, T2 occurred about six years into the experiment, and T3 occurred at about six years and two months. Between T2 and T3, microcosms received a third feeding of GME only, with no added treatments. For sediment Experiment B, microcosm subsamples were taken at time-zero, day 3, day 22, and day 35. These were transferred to 2 ml microcentrifuge tubes and spun at 16,000 x g. The supernatant was discarded and biosolids stored at -20 ° C until DNA extraction. The MO BIO Powersoil® DNA Isolation Kit was used to extract total genomic DNA. For Experiment A, the following samples were used for library preparation for next-generation sequencing: GME reference at T1, T2, and T3 (pooled duplicates at each time point), Tergitol® NP-9 + GME for T1, T2, and T3 (from a single microcosm), and Phenol + GME, and 4-NP + GME, both from T3 (pooled duplicates from each). For experiment B, microcosms were sacrificed as they were subsampled for DNA isolation. Genomic DNA subsamples sent for library preparation came from a single GME reference microcosm at T0 and another at 3 days. Corresponding subsamples (two pooled replicates each) with Tergitol® NP-9 addition + GME were sent from T0 and day 3. These and all other genomic DNA samples not sent for library preparation were used for PCR-DGGE.

3.5 Polymerase Chain Reaction and Denaturing Gradient Gel Electrophoresis

Small fragments of the V3 region of the 16s rRNA gene were amplified for phylogenetic domains Bacteria and Archaea. Bacteria primers were PRBA 338f [51]*(5'-ACT CCT ACG GGA GGC AGC AG-3') and PRUN 518r[29] (5'-ATT GCG GCT GCT GG-3'). Program parameters were initial denaturation at 94 ° C for 5 min., then 25 cycles of denaturation at 92 ° C for 30 sec, annealing at 55 ° C for 30 sec, then extension at 72 ° C for 30 sec, with final extension at 72 ° C for 15 min. For Archaea, a nested reaction was performed with the outer PRA 46f (5'-YTA AGC CAT GCR AGT-3') and PREA 1100r[52] (5'-YGG GTC TCG CTC GTT RCC– 3') amplifying a ~1100 bp fragment. This PCR product was used as template for the second reaction with PARCH 340f* (5'-CCC TAC GGG GGY GCA CAG-3') and PARCH 519r[30] (5'-TTA CCG CGG CKG CTG-3'). Both reactions used the following parameters: initial denaturation at 92 ° C for 2 min., then 30 cycles of 92 ° C for 1 min., 53.5 ° C for 30 sec., and 72 ° C for 1 min. Final extension was at 72 ° C for 6 min.

For the Eukarya 18s rRNA gene, the V8 region was targeted with primers 1427f* (5'-TCT GTG ATG CCC TTA GAT GTT CTG GG-3') and 1616r[53] (5'-TTA CCG CGG CKG CTG-3'). Initial denaturation was at 95 ° C for 5 min., followed by 30 cycles of: 95 ° C for 30 sec., 55 ° C for 30 sec., and 72 ° C for 30 sec. Final extension was at 72 ° C for 15 min.

*A 40-base GC-clamp was added to the 5' end of each forward primer (inner primer set only for the Archaea PCR)[29].

PCR fragment sizes were confirmed by running on 1% agarose gels. DGGE denaturants were prepared with 8% (v/v) acrylamide. Gradient for Bacteria was 35-65% (all experiments), For Archaea 50-70% (rumen) or 40-70% (sediment and sludge), and 35-55% and 35-60% (sediment) or 30-60% (sludge and rumen) for Eukarya. Gels were run at 75 V, for 16 h and stained with GelRed™ Nucleic Acid Gel Stain (10,000X in water, Biotium, Fremont, CA) before imaging with UVP BioDoc-It™ imaging system.

3.6 16S MetaVx™ Environmental Sequencing Library Preparation and Illumina MiSeq Sequencing

"16S MetaVx™ Environmental next generation sequencing library preparations and Illumina MiSeq sequencing were conducted at GENEWIZ, Inc. (South Plainfield, NJ, USA). DNA samples were quantified using a Qubit 2.0 Fluorometer (Invitrogen, Carlsbad, CA) and DNA quality was checked on a 0.6% agarose gel. Sequencing library was constructed using a 16S MetaVx™ Environmental Library Preparation kit (GENEWIZ, Inc., South Plainfield, NJ, USA). Briefly, 100 ng DNA was used to generate amplicons that cover V3, V4, and V5 hypervariable regions of bacteria and Archaea16S rDNA. Indexed adapters were added to the ends of the 16S rDNA amplicons by limited cycle PCR. Sequencing libraries were validated using an Agilent 2100 Bioanalyzer (Agilent Technologies, Palo Alto, CA, USA), and quantified by Qubit

and real time PCR (Applied Biosystems, Carlsbad, CA, USA). DNA libraries were multiplexed and loaded on an Illumina MiSeq instrument according to manufacturer's instructions (Illumina, San Diego, CA, USA). Sequencing was performed using a 2x250 paired-end (PE) configuration; image analysis and base calling were conducted by the MiSeq Control Software (MCS) on the MiSeq instrument. Initial taxonomy analysis was carried out on Illumina BaseSpace cloud computing platform"[54]. Shannon diversity indices[55] and evenness distributions were calculated for each sample using an Excel add-in developed by the University of Reading Statistical Services Center[56]

.

3.7 ICP-MS measurement of Nickel and Yttrium

Metal concentrations were measured in the aqueous and solid phases of representative microcosms. Subsamples were taken from microcosms so they would not be sacrificed while other analysis (e.g. sampling for DNA extraction) was ongoing. Phases were separated by centrifugation for 40 min. at 1,500 rpm in acid-washed 50 ml tubes (Falcon). Extraction and analysis was carried out by Galbraith Laboratories. Briefly, solid samples were wet-ashed and acid-extracted[57, 58] while aqueous samples were subjected to a test tube digestion using a hot plate and HNO_3[59]. Scandium and germanium were used as internal standards for ICP-MS. Concentrations were reported in parts per million.

CHAPTER 4. EFFECT OF CARBON NANOTUBES AND CELLULOSE NANOMATERIALS ON STRUCTURE AND FUNCTION OF ANAEROBIC MICROBIAL COMMUNITIES FROM COW RUMEN

4.1 Abstract

Digestive tracts of ruminant animals are important anaerobic ecosystems due to their crucial involvement in food production and contribution to greenhouse gas emissions. The effects of both functionalized and non-functionalized single- and multi-walled carbon nanotubes, as well as two different forms of cellulose nanomaterials on rumen microbial communities were assessed. Elemental Analysis was performed by scanning electron microscopy and energy-dispersive X-ray spectroscopy on most of the manufactured nanotube products used in the experiments. Indicators of both microbial community function and structure were used to assess the impact of exposure to nano-materials. A biomethane potential (BMP) assay was performed for 517 days and average cumulative gas production in treated samples were compared with untreated reference samples. No inhibition of anaerobic gas production occurred as a result of any nanomaterial treatment. Both functionalized and pristine, single- and multi-walled nanotube treatments were associated with accelerated gas production. Microcosm headspace analysis was performed by gas chromatography. Methane fraction increased in a cellulose reference set of microcosms late in the experiment, while a decrease in

methane fraction was seen in nanotube-treated microcosms that showed visual evidence of biomass depletion and loss of dissolved organic matter by 730 days. Molecular genetic community analysis was carried out by PCR-DGGE for16s and 18s rRNA genes, as well as 16s Illumina MiSeq Sequencing and metagenomics. Next-generation sequencing showed community shifts and increased diversity in pooled replicates of genomic DNA from nanotube-treated samples compared with pooled untreated reference samples. Results of this long-term study suggest enhanced oxidation of organic matter in nanotube-treated samples due to their surface catalytic properties and favorable conditions for biofilm formation in the microcosms.

4.2 Introduction

Anaerobic microbial communities are receptors for emerging environmental contaminants through multiple routes of exposure. They are relatively under-studied systems in ecotoxicology, where long-term interactions and biotransformations may be particularly relevant. Digestive tracts of ruminant animals are important natural anaerobic environments that are also highly engineered in domestic livestock. They play a significant role in greenhouse gas emissions, and much research and development has occurred with regard to abatement strategies[60]. Carbon-based nanomaterials represent an emerging class of contaminants of concern, owing to their unique chemical and physical properties at the nanoscale[61], wide range of potential applications[3], and the rapid progress of research and development that outpaces our understanding of ecological impacts[62]. Two major routes of chemical and nanomaterial exposure for ruminants are evident.

These are drug delivery[63], and grazing on land to which anaerobic sludge biosolids have been applied[64]. One consideration for assessment of microbiological effects of carbon nanomaterials in natural environments is that soil organic matter may attenuate any toxic effects measured under laboratory conditions[65]. The cellulose degradation capabilities of ruminant microorganisms are of interest for ecotoxicology studies of carbon nanomaterials because their adaptation to using complex biopolymers as substrate may predispose them to be affected differently than other microorganisms. Further, these capabilities are under assessment to be exploited for renewable energy production[66].

Long-term studies of exposure of carbon nanomaterials to anaerobic communities are not abundant in the literature. Nyberg et al.[16] found no effect of C_{60} fullerene on the structure or function of an anaerobic digester sludge community. Recent studies have focused on the effect of carbon nanotubes on anaerobic reactors. Li et al.[67] found that single-walled carbon nanotubes (1,000 mg/L) accelerated methanogenesis and increased secretion of extracellular polymeric substances (EPS). They cite evidence for direct interspecies electron transfer (DIET) in the microbial community, which may have been enhanced by nanotube exposure. The DIET phenomenon was first described in anaerobic digestion in the genera *Methanosaeta* and *Geobacter*[68] and has recently been suggested to occur in the family *Anaerolinaceae* and the genus *Clostridium*[69] in addition to the two previously mentioned genera between which DIET has been established to occur. The enhancing effect has also been seen with activated carbon[70], although to a lesser extent than with carbon nanotubes[71]. All of these studies were carried out with single-walled nanotubes (SWNT). Another group[72] found a toxic effect of multi-walled nanotubes on an upflow

anaerobic sludge blanket (UASB) reactor. They concluded that the most likely mechanism was physical disruption. Agitation of the culture flasks promoted penetration of the microbial cell membranes by the multi-walled nanotubes, which are less flexible compared with single-walled tubes.

In contrast with a wastewater treatment anaerobic digester, a different type of methanogenesis predominates in rumen; that is, hydrogenotrophic methanogenesis over acetoclastic[73]. Typical residence times in cow rumen have been found to be 49-59.6 hours[74], with heavier, smaller particles having residence times on the shorter end of the range. In normal cow physiology, methanogenesis is kept under control for both animal health and greenhouse gas emissions mitigation. Unlike in soils, sediments, and the anaerobic digester in which complete bioconversion to carbon dioxide and methane occurs, the animal is the primary consumer of acetate and other volatile fatty acids produced by its rumen microflora[75]. In the current study, long-term batch experiments were carried out by adding two different cellulose nanomaterials, a bulk cellulose reference, and eight different types of manufactured carbon nanotubes to cow rumen microcosms. These microcosms were enriched for methanogenesis by keeping them strictly anaerobic. Although a departure from typical conditions found in the digestive tract of a living cow, this enrichment provided for exploration of the metabolic capabilities of these microbial communities when methanogenesis became the dominant terminal metabolic process. By simultaneously testing materials with different properties, possible mechanisms of effects could be better elucidated. Total anaerobic gas production

was measured over 517 days, while headspace analysis was done two times in the later part of the experiment.

Carbon nanotubes from two different manufacturers were used in the experiment. Differences in manufacturing technique, carbonaceous purity, length, degree of functionalization if any, number of walls, bundle sizes, amorphous carbon content and presence of metal and other impurities could all potentially contribute to any biological effects observed. Two types of nanocellulose: freeze-dried nanocellulose and "CN film" were also studied, due to the wide variety of applications under research and development[76]. High concentrations of each material were used for two reasons. First, any toxic effect could be more easily detected than with lower concentrations, and second, higher concentrations would enable the measurement of substantial increases in gas production if any degree of anaerobic biodegradation of the materials should occur. Previous literature on carbon-based nanomaterials indicate that any effects on microorganisms, either toxic or beneficial, are likely multifactorial.

Possible contributions of metals and other residual byproducts of manufacturing were taken into account in this study. Nanotube characterization was accomplished by scanning electron microscopy (SEM) and x-ray spectroscopy (EDX). Nickel and yttrium catalyst used in production of nanotubes from one of the two manufacturers were of concern due to a small but significant increase in gas formation seen in an anaerobic digester sludge microcosm experiment (preliminary data for experiments in Chapter 5).

Therefore, both solid and aqueous phase concentrations of these metals were measured by ICP-MS in microcosm subsamples.

In ecotoxicological assessments, effects on both microbial community function and community structure are necessary. The two are often intrinsically linked. However, it is possible to observe complete inhibition of a measure of community function such as methanogenesis in response to a toxicant such as sodium 2-bromoethanesulfonate[77], while finding relatively subtle shifts in molecular genetic profiles. These results are described in Chapter 5. On the other hand, more dramatic effects on community structure may occur with overall maintenance of community function, indicating functional redundancy of different phylogenetic groups[78].

Microbial community structure was assessed in this study by two different techniques. PCR-DGGE[29] is a relatively inexpensive and quick screening technique for mutation detection in microbial communities. However, its limitations include a poor correlation between the number of DGGE bands detected and the number of species present[79]. It also lacks the high resolution possible with more state-of-the-art phylogenetic assessment techniques. DGGE results were compared with next-generation sequencing using the Illumina MiSeq platform and Metagenomic analysis. Sequencing results showed an overall increase in diversity and evenness of the microbial communities in response to exposure to carbon nanotubes, as well as enrichment of some groups of microorganisms. These were expressed in terms of relative abundance of sequences, not direct counts of microorganisms. Copy number for the 16s rRNA gene varies between species, with a

higher number and wider range of copies generally found for Bacteria (1-15) than Archaea (1-4)[80]. This pattern was apparent in our samples, by using the searchable *rrn*DB[81] to look up microorganisms of functional importance that were detected by DNA sequencing. However, copy number should be consistent for any given species, so it was still possible to determine differences between treated samples and the untreated reference. Nanocellulose-treated microcosms were not subjected to further genetic characterization beyond initial screening by DGGE profiles, due to their lack of effect on community function in this study.

No toxicity of any carbon nanotube or nanocellulose material was observed in this study. Instead, an acceleration of methanogenesis and associated microbial community shifts were seen with many types of carbon nanotubes, consistent with other studies.

Treatment with several types of carbon nanotubes were shown to accelerate gas production in the anaerobic microcosms, as well as shift the microbial community structure with an overall increase in diversity. No toxicity or inhibition was observed with any of the materials tested.

4.3 Experimental Design

Rumen material was collected from a fistulated cow at Purdue Dairy. Dietary information is shown in Table 4.1[82]. The sample included both solid and liquid rumen contents.

Table 4.1. Dietary information for a single cow source of rumen inoculum, on an as fed, wet weight basis.

Component	Dietary Fraction
Corn Silage	0.5714
Soybean Meal	0.0462
High-moisture shell corn	0.1092
Hay--Grass	0.0168
Haylage E	0.1597
High-protein supplement	0.1008

Rumen material was not homogenized before microcosm construction to minimize disruption to the microbial community. Glass serum bottles (125 ml, Wheaton) were filled with 75 ml potassium phosphate buffer (pH ~ 7.5), 25 ml rumen fluid, and 5 g +/- 0.15 g rumen solids (wet mass). The bottles were sealed with Teflon-coated septa and aluminum crimp caps and pre-incubated away from light at approximately 20 ° C for 65 days before adding carbon nanotube or cellulose nanomaterials treatments. Gas production was monitored during pre-treatment as well as post-treatment. Monitoring and adjustment of pH was carried out as needed, especially in the first months of the experiment. A sodium carbonate ($NaHCO_3$) and phosphate buffer solution of pH 9 was first added to restore buffering capacity to the microcosms. Later pH adjustments were made with dilute NaOH, and finally with small volumes of 10% NaOH[83]. Measurements of pH were carried out using pH paper (Hydrion) or a pH meter. Microcosm bottles were

not exposed to oxygen for pH measurements. Instead, up to 2 ml of the aqueous phase was extracted by syringe and transferred immediately to another container where a pH probe could be inserted.

Experimental design is shown in Table 4.2. Cellulose nanomaterials were provided by Dr. Robert J. Moon, Purdue University Materials Engineering. Carbon nanotubes were purchased from one of two different manufacturers, Carbon Solutions, Inc. (Manufacturer A) and Cheap Tubes, Inc. (Manufacturer B). Two different batches of the same product, single/double-walled nanotubes with carboxyl group functionalization (S/DWNT-COOH) are designated B1 and B2. Batch B2 was provided as a replacement by the supplier after it was found that their plasma generator was working at only 40% efficiency during production of B1.

Microcosms were randomly assigned to treatments or to the untreated reference set using the list randomizer function at Random.org[84]. Treatment additions were carried out in an anaerobic chamber. Three replicates of each treatment were used, with four replicates in the untreated reference set. A fifth bottle in the untreated set never established methanogenic function after multiple pH adjustments and was removed from the experiment. Three additional microcosms were air-dried and their average dry mass was used to calculate concentrations in Table 4.2. Target concentrations for each treatment were normalized to the mass of carbon from which 250 ml of total gas would theoretically be produced if the material were completely biodegraded. The exception

was amidated nanotubes (SWNT-CO(NH_2)) due to the higher cost of this material, and P2 SWNT due to limited availability.

Table 4.2. Experimental design for nanotube treatments, cellulose nanomaterials, and a bulk cellulose reference, for the rumen inoculum experiment.

Treatment	**Concentration (mg/kg biomass (dw))**
CN Film + RC	219,300
Freeze-dried CN + RC	219,300
P9 SWNT-$CONH_2$ (A) + RC	21,400
P3 SWNT-COOH (A) + RC	95,300
P2 SWNT (A) + RC	52,100
S/DWNT-COOH (B1) + RC	89,900
S/DWNT-COOH (B2) + RC	90,500
SWNT-O^+ (B) + RC	87,900
MWNT (B) + RC	87,900
MWNT-COOH (B) + RC	90,400
Microcrystalline Cellulose (MCC) + RC	219,300
Untreated reference*	n/a

* Rumen contents (RC) only

Representative microcosms from the rumen experiment are shown in Fig. 4.1. Just two days after nanotube addition, differences between the treatments are apparent. Microcosms treated with P2 neat SWNT and P9 amidated SWNT appeared similar to the untreated reference microcosms (not shown in Fig. 4.1), except for the nanotubes (black particles) visible in the solid phase. It should be noted that these treatments used a lower

concentration of nanotubes than the other treatments. Microcosms with other nanotube treatments show obvious changes in color, with some nanotubes visible in suspension

Figure 4.1. Microcosms with rumen inoculum at the end of the pre-incubation period and two days after addition of nanotube treatments.

Average actual masses of nanotubes for each treatment were as follows: P9 $CO(NH_2)$ (A) (30.2 mg), P3 SWNT-COOH (A) (133.2 mg), SWNT-COOH (B1 and B2) (126 mg), SWNT-O^+ (123.3 mg), MWNT-COOH (126.9 mg), MWNT (123.7 mg), P2 SWNT (50.1 mg). Single-walled nanotubes with "O^+" functionalization have a mix of –OH, -COOH, and C=O groups, as specified by the manufacturer. Both forms of nanocellulose and also microcrystalline cellulose (not shown) were added to microcosms at ~307 mg.

4.4 Results

4.4.1 Elemental Analysis by Energy-dispersive X-ray spectroscopy (EDX)

Characterization data for most of the carbon nanotube preparations used in the experiments are shown in Table 4.3. EDX was not performed for MWNT (B) or S/DWNT-COOH (B2). Reported functionalities (wt%) are from the manufacturers, as well as the dimensions listed. A dash (-) indicates that an element was not detected in the sample. Dimensions reported by the manufacturers indicate the longest of the range of tube lengths from Manufacturer A is the shortest of the length range of products purchased from Manufacturer B.

Table 4.3. Nanotube dimensions reported by manufacturer: L = length, BL = bundle length, D = diameter, BD = bundle diameter, OD = outer diameter, ID = inner diameter. Elemental Composition of f-CNTs and residual metals were measured by EDX at Purdue University. All elements are shown in weight percent. NA indicates "not analyzed". Manufacturer A is Carbon Solutions, Inc. Manufacturer B is Cheap Tubes, Inc. "S/DWNT-COOH" are a mixture of single- and double-walled tubes.

Nanotube	Manufacturer	Reported dimensions (average or range)	Reported functionality (wt%)	C	O	Ni	N	Y	S	Cl	Al	Ca	Co	Mo	F	Si	Fe
SWNT-COOH	A	D = 1.4 nm BD = 4 - 5 nm L= 0.5 – 3 µm BL = 500 nm – 1.5 µm	2.2	77.46	17.30	4.37	-	0.61	0.25	-	-	-	-	-	-	-	-
SWNT-CO(NH_2)	A	D = 1.4 nm L= 0.5 – 3 µm	2.2	72.22	19.04	1.37	4.49	0.23	0.08	1.02	-	-	-	-	1.39	0.16	-
MWNT-COOH*	B	OD ≤ 8nm ID = 2-5 nm L = 10-30 µm	2.8	90.49	8.16	0.17	-	-	-	-	0.09	0.11	0.35	0.61	-	-	-
MWNT	B	OD ≤ 8nm ID = 2-5 nm L = 10-30 µm	-	NA	NA	NA	NA	NA	NA	NA	NA	NA	NA	NA	NA	NA	NA
S/DWNT-COOH (1)	B	OD = 1-2 nm L = 3 – 30 µm	2.20	85.05	9.99	-	-	-	-	0.17	0.38	-	-	-	2.39	0.27	1.50
S/DWNT-COOH (2)	B	OD = 1-2 nm L = 3 – 30 µm	2.9	NA	NA	NA	NA	NA	NA	NA	NA	NA	NA	NA	NA	NA	NA

4.4.2 Biomethane Potential (BMP) assay

Anaerobic gas production data are shown in three separate groups due to the large number of materials tested. All treatments are compared with the untreated reference set in each of three time plots. Highest average cumulative gas production over time occurred in microcosms treated with nanotubes from Manufacturer B (Fig. 4.2). Single/double-walled nanotube (B2) treatment showed significantly higher gas production ($p < 0.05$) than the untreated reference microcosms from day 185 to day 446. These microcosms had the highest gas production rate in the experiment, at 4.67 ml/day around days 169 to 173. Microcosms with batch (B1) of the same material had

significantly higher gas volumes from day 185 to day 400. MWNT-COOH (B) also had significantly higher gas production from day 153 to day 169 and again from day 240 to day 472. Neat MWNT (B) microcosms' gas production was significantly higher than the average of the untreated reference from day 265 to day 494.

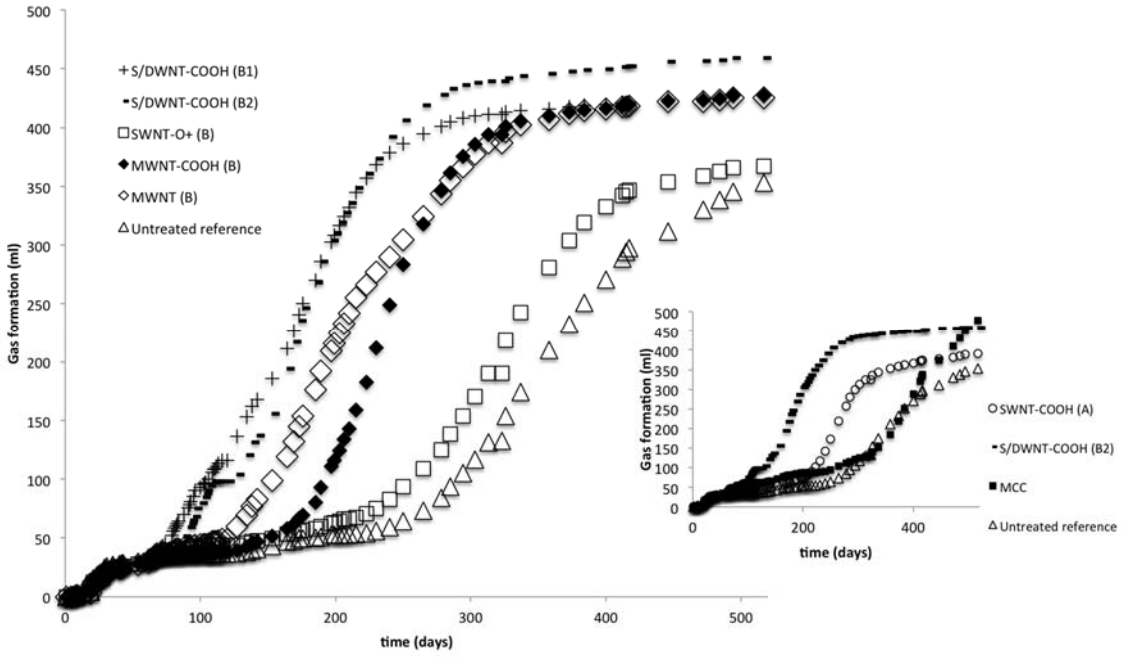

Figure 4.2. Average cumulative gas production over time, for microcosms treated with nanotubes from Manufacturer B. For scale (inset) the microcosms with the most accelerated gas production from each of the three groups is shown with the untreated reference set. For untreated reference set, n=4. For all other treatments, n=3. Error bars are omitted for clarity.

The SWNT-COOH and neat SWNT from Manufacturer A also had significantly higher ($p < 0.05$) gas production than untreated reference microcosms (Fig. 4.3). For SWNT-COOH samples this occurred at day 134 and again at day 153 to day 164 and finally from

day 240 to day 358. For SWNT, this time span was from day 265 to day 358. Microcosms treated with amidated tubes (SWNT-CO(NH_2)) did not produce different gas volumes from untreated microcosms.

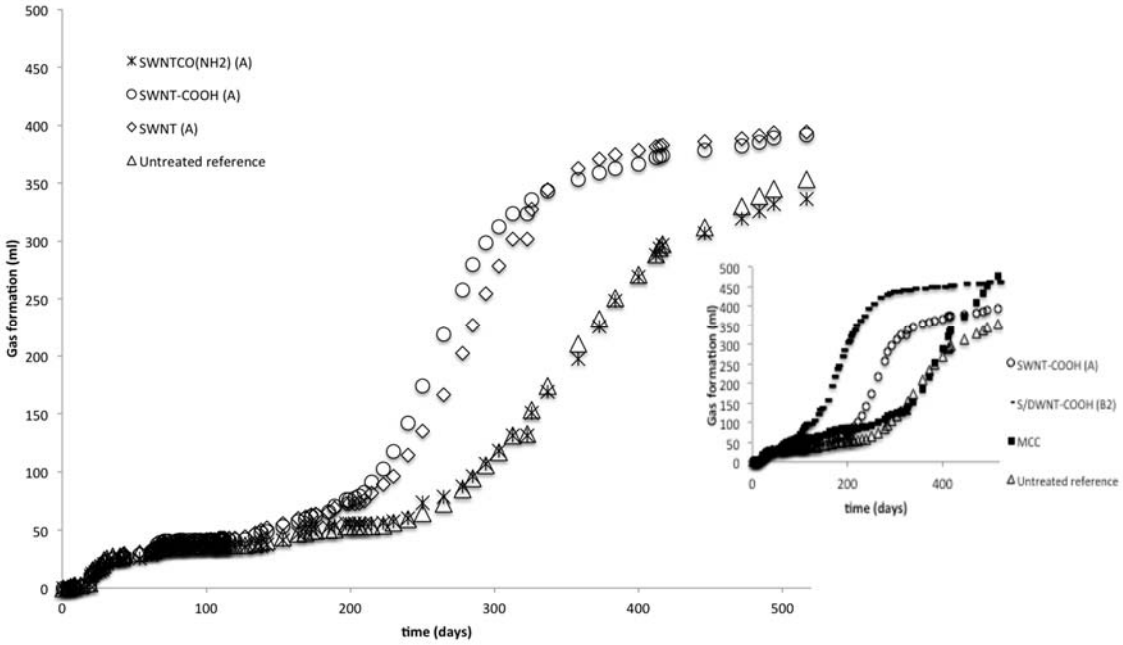

Figure 4.3. Average cumulative gas production over time, for microcosms treated with nanotubes from Manufacturer A. For scale (inset) the microcosms with the most accelerated gas production from each of the three groups is shown with the untreated reference set. For untreated reference set, n=4. For all other treatments, n=3. Error bars are omitted for clarity.

In Fig. 4.4., average cumulative gas formation is shown for microcosms treated with different forms of cellulose (other than rumen contents present in all samples). Only the microcrystalline cellulose (MCC) showed significantly higher gas formation ($p < 0.05$) than the untreated reference microcosms. This occurred from day 68 to 71, day 80 to day 134, day 164 to day 250, and finally from day 494 to day 517. These microcosms

produced the highest average cumulative gas volume of all the rumen treatments (477 ml). Microcosms treated with freeze-dried nanocellulose showed high variability in gas production within this treatment set, so this difference from the untreated reference was not significant. This variability is shown in Fig. 4.7.

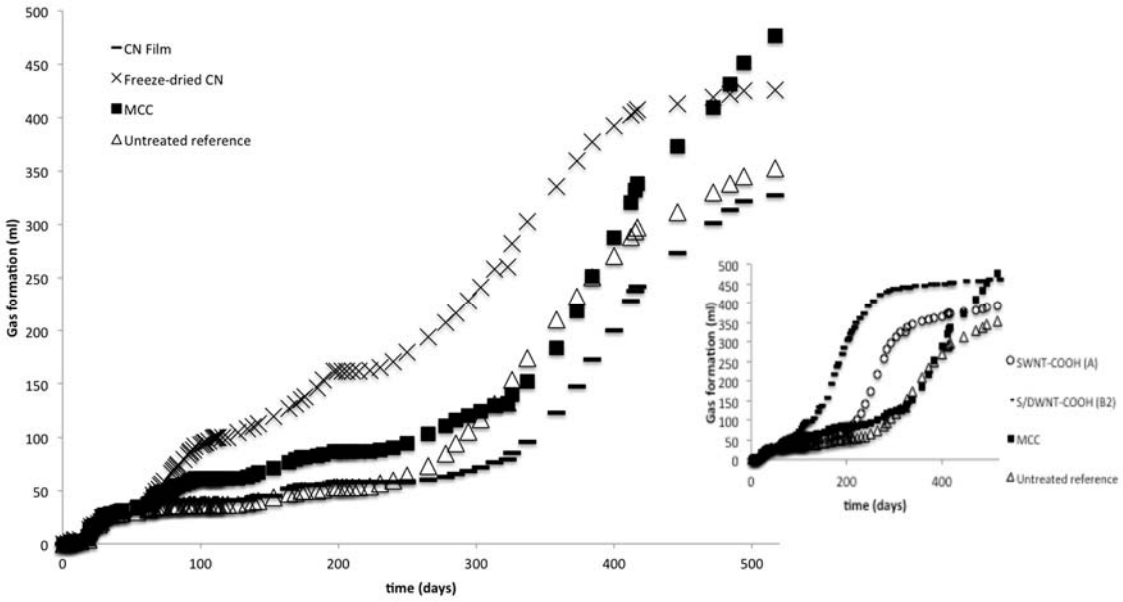

Figure 4.4. Average cumulative gas production over time, for microcosms treated with cellulose nanomaterials and microcrystalline cellulose. For scale (inset) the microcosms with the most accelerated gas production from each of the three groups is shown with the untreated reference set. For untreated reference set, n=4. For all other treatments, n=3. Error bars are omitted for clarity.

Average cumulative gas formation normalized to the untreated reference is shown at day 265 (Fig. 4.5) and day 517 (Fig. 4.6), with error bars. Microcosms treated with most of

the nanotube formulations had significantly higher gas formation at day 265 and for much of the experiment ($p < 0.05$). Exceptions were SWNT-$CO(NH_2)$ (A) and SWNT-O^+ (B). By day 517, the untreated reference microcosms had produced more gas while all the nanotube-treated microcosms' gas formation had reached a plateau. Therefore, any difference between them at day 517 was no longer significant. Samples with none of the cellulose treatments were significantly higher or lower than the untreated reference at day 265, but the microcrystalline cellulose (MCC) was significantly higher at day 517.

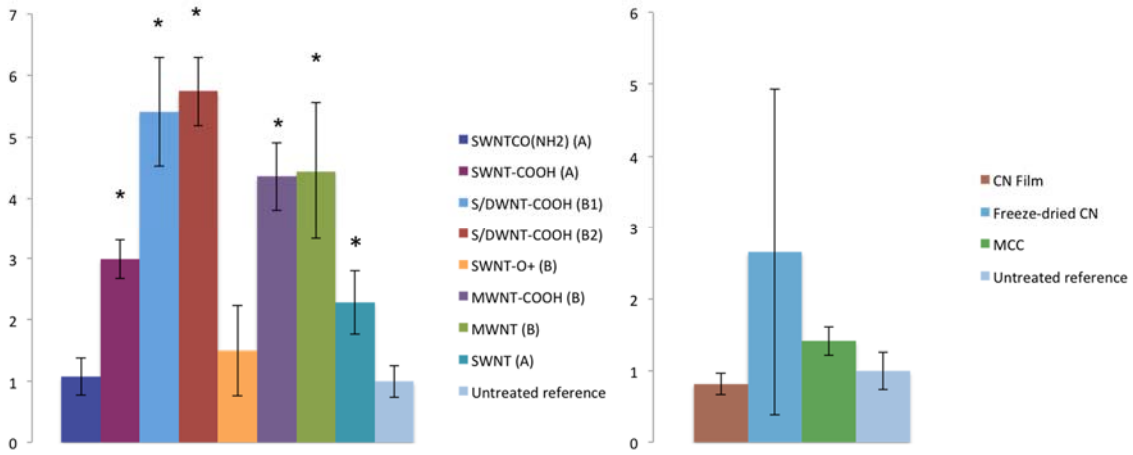

Figure 4.5. Average cumulative gas production, normalized to the untreated reference, at day 265. An asterix (*) shows significant difference from the untreated reference ($p < 0.05$).

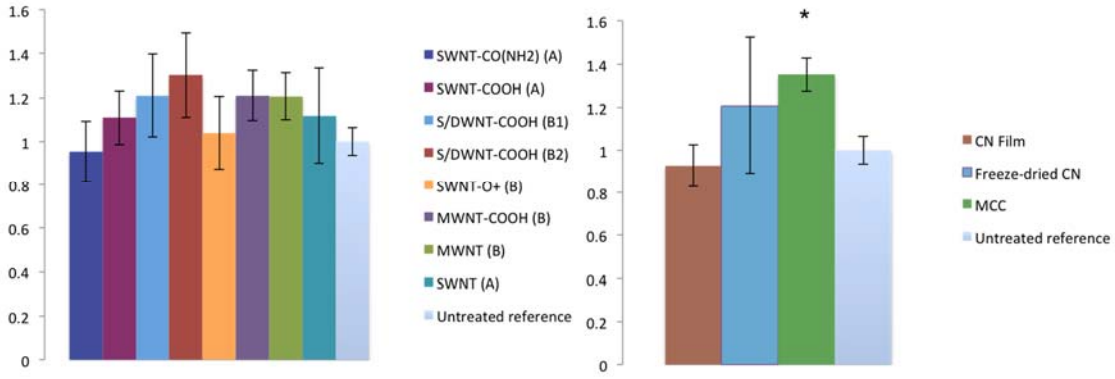

Figure 4.6. Average cumulative gas production, normalized to the untreated reference, at day 517. An asterix (*) shows significant difference from the untreated reference ($p < 0.05$).

Average error (%) for all treatments in the rumen experiment is shown in Table 4.4. Cumulative gas formation for two replicate treatment sets of three microcosms each is shown along with the four replicates of the untreated reference in Fig. 4.7. Much of the variability occurred during pH stress early in the experiment, with some microcosms recovering gas production sooner than others.

Table 4.4. Average error (%) for the rumen BMP assay, from treatment addition on day 65 to day 517.

Microcosm set	**Average % error**
CN Film	16.4
Freeze-dried CN	74.9
P9 SWNT-$CONH_2$ (A)	19.3
P3 SWNT (A)	10.1
0113 S/DWNT-COOH (B1)	50.7
0113 S/DWNT-COOH (B2)	37.1
0112 S/DWNT-O^+ (B)	23.2
030301 MWNT-COOH (B)	13.9
030101 MWNT (B)	30.6
P2 SWNT (A)	18.5
MCC	14.0
Untreated reference	18.3

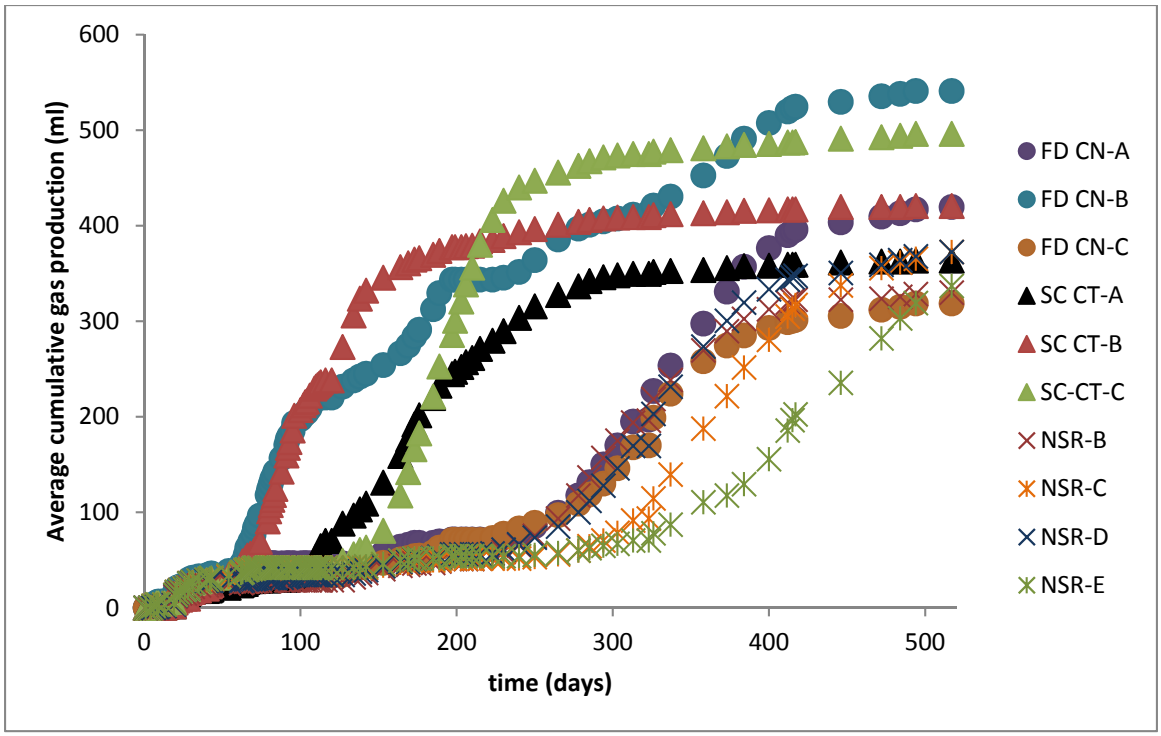

Figure 4.7. Cumulative gas production for n=3 replicates of Freeze-dried CN (FD CN), n=3 replicates of S/DWNT-COOH (B1) (SC CT), and n=4 replicates of the untreated reference set (NSR). Variability in pH early in the BMP assay contributed to higher error in some sets of microcosms.

A heatmap showing pH trends for the experiment is shown in Fig. 4.8. The highest daily gas production was measured at day 102, in a microcosm treated with S/DWNT-COOH (B2). The gas production was 15 ml, with two days between this volume measurement and the previous one. The pH measured in this sample on day 102 was 6.74. The lowest pH measured at any time was 6.00, at day 81, in a microcosm treated with microcrystalline cellulose (MCC). Gas volume measurement was 2 ml, with 1.5 ml having been measured the previous day. A different microcosm in the same set was not producing gas when its pH reached a maximum of 7.71. Methanogenesis in this bottle

recovered approximately 30 days later. By day 417 when the last pH measurement was taken, cumulative gas production had started to plateau for most sets of microcosms, with the exception of MCC. The pH in these three samples ranged from 7.00 to 7.21.

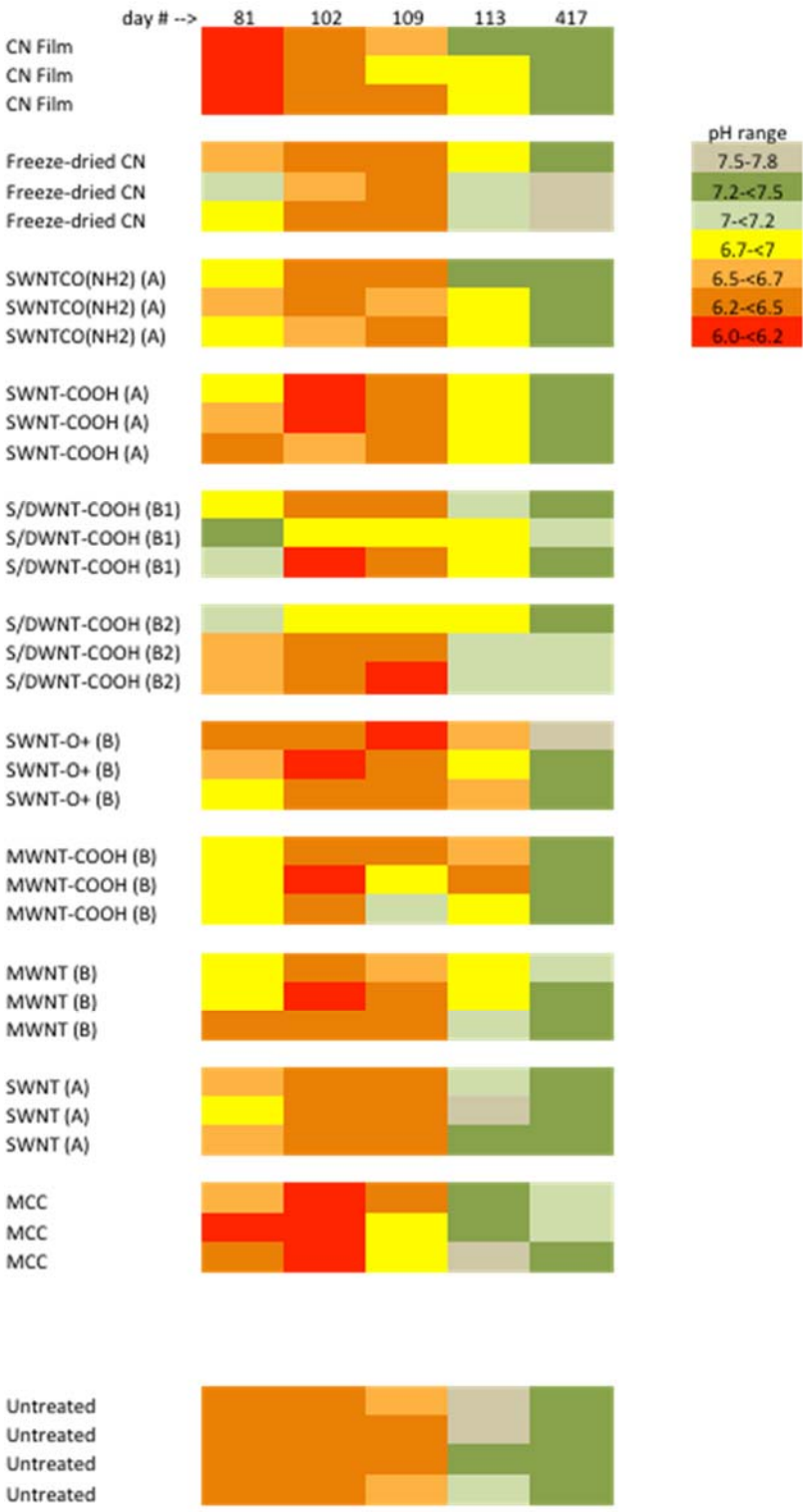

Figure 4.8. Heat map showing pH trends in replicate sets of microcosms through multiple pH adjustments. Microcosms with different treatments recovered gas formation at different times (approximately day 72 through day 230).

Photographs of representative microcosms are shown in Figures 4.9, 4.10, and 4.11. Day 67 was two days after adding treatments (Fig. 4.9). Nanotubes in treated microcosms are visible in the solid phase. Some darkening of the aqueous phase was already occurring in these samples as well, particularly in the MWNT-COOH (B) microcosms. The cloudy yellow appearance of rumen contents remained in all microcosms after more than two months' pre-incubation.

Figure 4.9. Microcosms at day 67, two days post-treatment. Untreated reference (top left), MWNT-COOH (B) at top right, SWNT-O^+ at bottom left, S/DWNT-COOH (B2) at bottom right.

In Figure 4.10, nanotube-treated microcosms have a very different appearance than the untreated references at day 730. A time series of images (not shown) illustrates the gradual progression of this phenomenon. The biomass blanket becomes depleted and the

color of the liquid phase is lost. Clarity of the liquid phase also increases in treated samples over time, with loss of suspended particulate matter. Detail of an MWNT-COOH (B)-treated microcosm shows what appears to be a biofilm formed with microbial biomass and nanotubes entrained in plant material of the rumen contents.

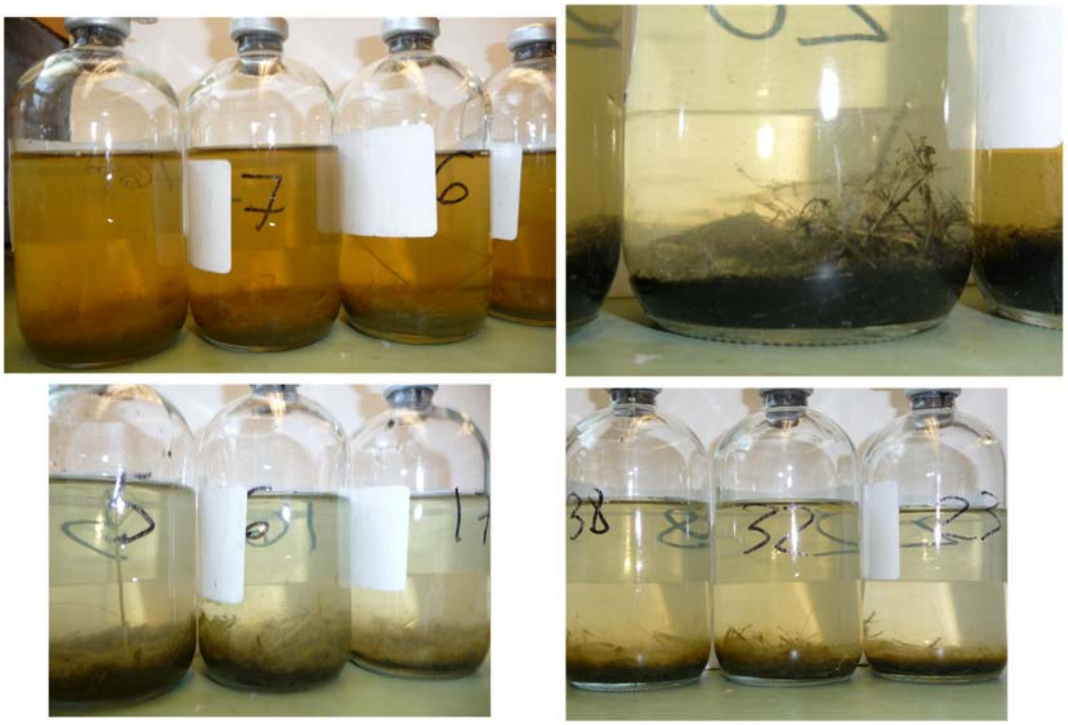

Figure 4.10. Microcosms at day 730 showing depleted biomass blanket and remaining nanotubes. Untreated reference (top left). MWNT-COOH detail (B) (top right). SWNT-O^+ (bottom left). S/DWNT-COOH (B2) (bottom right). Lines in center area of bottles are edges of labels.

In general, microcosms that started gas production earliest showed this effect most strongly (e.g. S/DWNT-COOH (B2). A weaker effect (somewhat less biomass depletion and a slight yellow color remaining in the liquid phase) is seen with treated microcosms (e.g. SWNT-COOH (A), not shown) that started gas production later, yet before the untreated reference.

Figure 4.11 shows a similar effect with microcosms treated with MWNT (B). The nanotubes appear to be a major fraction of all material remaining in the microcosms.

Figure 4.11. MWNT (B) microcosms showing depleted biomass blanket at 730 days. Each sample was treated with 123 mg of nanotubes. Gas formation for this set was significantly higher than the untreated reference from day 265 until day 494.

4.4.3 Microcosm Headspace Analysis

Figure 4.12 shows methane fraction normalized to the untreated reference for cellulose treatments and nanotube treatments, at day 446 (top) and day 736 (bottom). Results at day 446 are not significant due to high percent error in the untreated reference set. However, the pattern is the same as samples taken at the later time point. The methane fraction is significantly higher in MCC microcosms at 736 days. These still had yellow color and relatively less depleted biomass blanket, with similar appearance to untreated microcosms. Gas production in these microcosms was not noticeably accelerated compared with the untreated set, but their average cumulative gas volume was the highest and they were still producing gas at the end of the BMP assay.

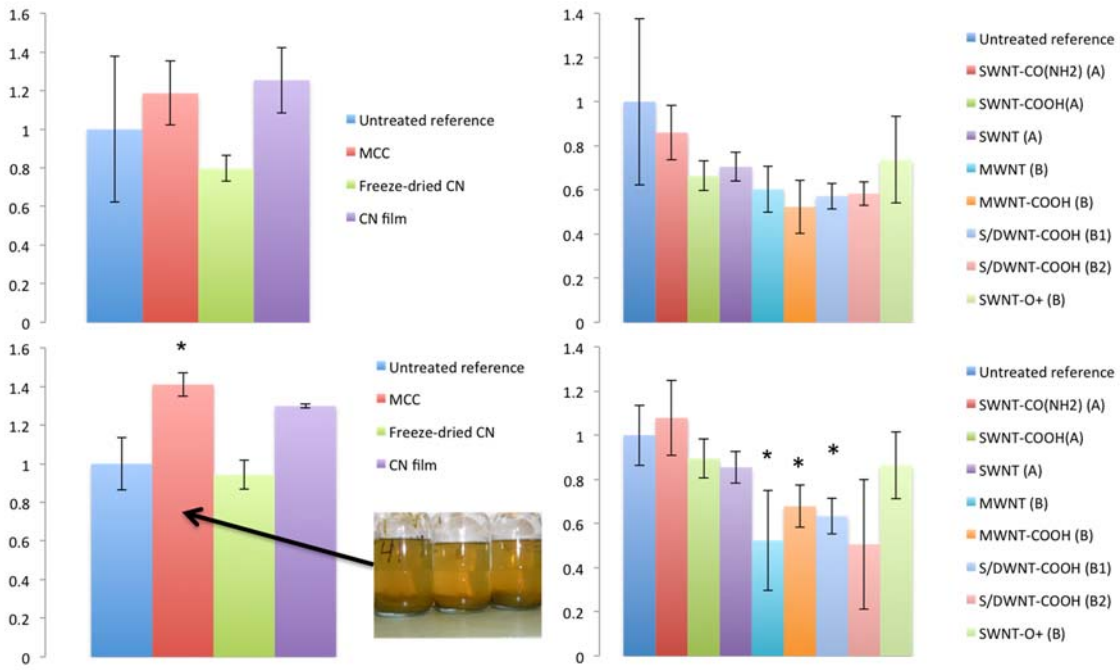

Figure 4.12. Methane normalized to untreated reference at 446 days (top) and near the end of the experiment (bottom). All with an asterix (*) are significantly lower than the reference at $p < 0.05$. Inset, bottom left: MCC microcosms with higher methane than untreated reference. Compare with images in Figures 8 and 9 taken the same day.

Methane fraction is lower in most sets of nanotube-treated samples. Some of these differences are significant at 736 days, for treatments MWNT (B), MWNT-COOH (B), and S/DWNT-COOH (B1). Methane fraction is also lower for S/DWNT-COOH (B2) treatment, but the difference is not significant due to high variability between replicates. The overall trend is that lower methane fraction late in the experiment is directly associated with treatments that accelerated gas production earlier in the experiment. Furthermore, it is correlated with visual evidence of biomass depletion and enhanced oxidation of organic matter in these microcosms.

4.4.4 DNA Extraction for Analysis of Microbial Community Structure

Figure 4.13 shows an interesting effect of nanotubes in the DNA extraction procedure. This effect is most apparent with MWNT (B) as shown in the previous figure. Nanotubes were gradually removed from microcosm subsamples during cell lysis, protein precipitation, DNA binding, washing, and elution. The DNA extraction kit uses proprietary surfactants, precipitating agents, and inhibitor-removing agents. At lysis and two separate protein precipitation steps, some nanotubes were visible in stable suspension even after centrifugation at 10,000 x g (not shown). A high-salt solution is then used to bind DNA to the spin filters, where it is washed with a solution containing ethanol. The final elution step occurs in 10 mM Tris buffer. All remaining color from the nanotubes was left on the spin filters with the eluted DNA (not shown) being clear and colorless.

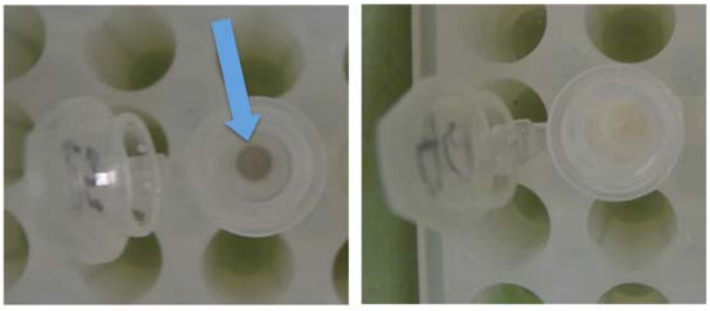

Figure 4.13. Spin filters in microcentrifuge tubes post-DNA extraction. DNA is bound to filters and washed before the last elution step, which yields clean PCR-ready DNA. Nanotubes were gradually removed from suspension and the solid phase at each step of the procedure, with some remaining on the filters. This is most noticeable with MWNT (B) at left. Untreated reference is shown at right.

4.4.5 Polymerase Chain Reaction and Denaturing Gradient Gel Electrophoresis (PCR-DGGE)

Representative community profiles generated by PCR-DGGE are shown for some replicates of different treatments in Figure 4.14, for each of three domains Bacteria, Archaea, and Eukarya. In general, replicates of different sets had differences in one or more dominant (brightest) bands, including the untreated reference (not shown). Therefore, it was not possible to determine the effect of any treatment on rumen microbial community structure using this technique.

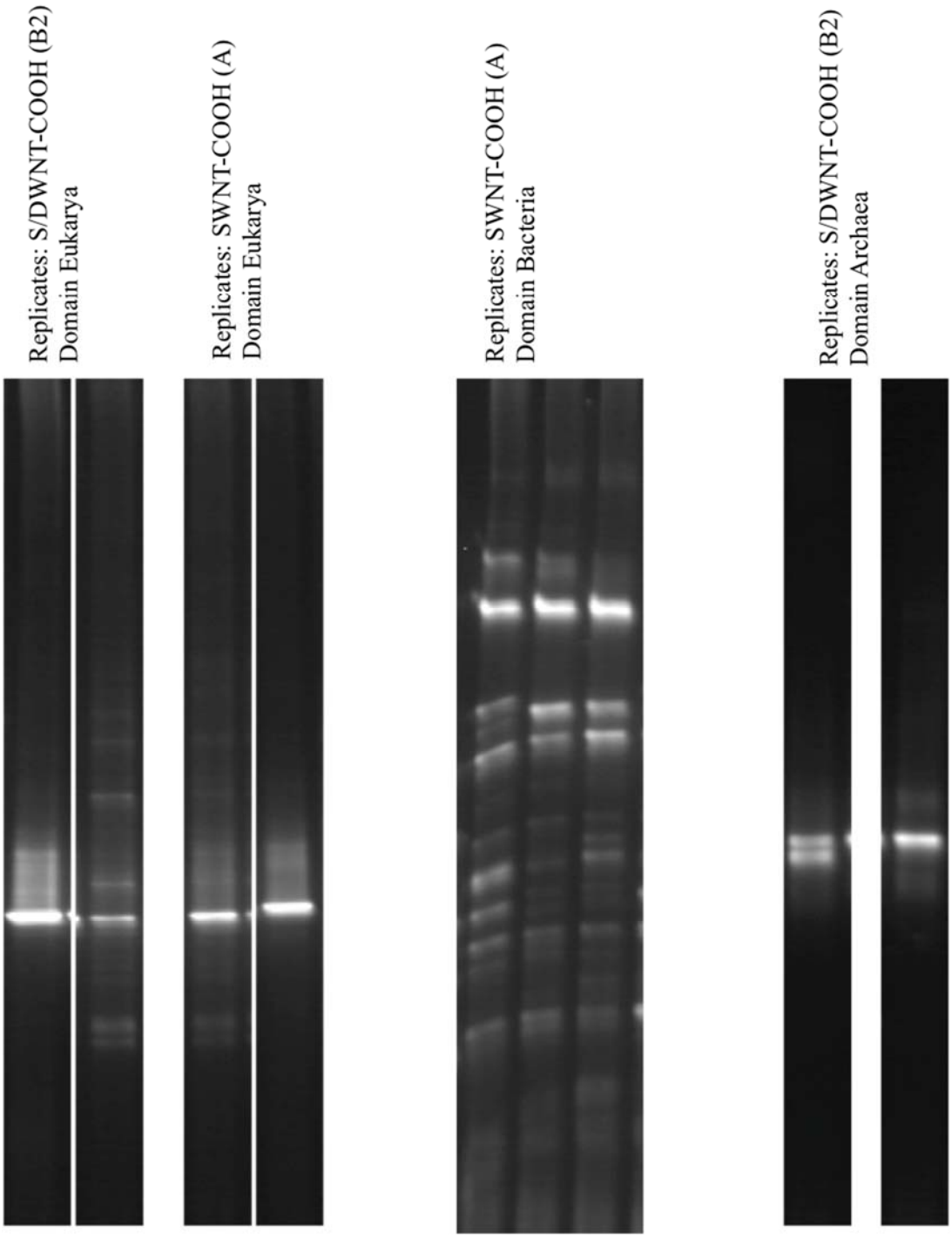

Figure 4.14. Differences between DGGE profiles for replicate samples in each of three domains. From left to right: Eukarya for two replicates of: S/DWNT-COOH (B2) treated samples and SWNT-COOH (A) (30-60% G + C). Bacteria profiles (35-65% G + C) for three replicates with SWNT-COOH (A). Archaea profiles for two replicates with S/DWNT-COOH (B2) (50-70% G + C).

4.4.6 16S MetaVx™ Environmental Sequencing Library Preparation and Illumina MiSeq Sequencing

General sequence information and diversity indices are shown in Table 4.5 for pooled replicate microcosm subsamples of five different nanotube treatments, as well as the untreated reference set. Total sequence counts are the sum of 16s sequences at the Kingdom level: Bacteria, Archaea, and Unclassified. The percentage of sequences that remained unclassified at the Kingdom level is low, ranging from 0.044 to 0.179 in these samples. A few virus sequences were identified in some but not all samples, and these are included in the total. Calculated sequences were identified at the taxonomic level of Species. The fraction classified is this number divided by the total number of sequences. Species identified is the count of sequences identified down to the species level. Shannon diversity indices range from 3.47 to 3.76, with the nanotube-treated samples all being higher than the untreated reference. Evenness distributions range from 0.55 to 0.6. These numbers are all slightly higher in the treated samples than the untreated reference.

Table 4.5. Number of sequences and diversity indices for 16s DNA from rumen microcosms

Treatment	Total sequences	Calculated Sequences	Fraction Classified	Species Identified	Shannon Diversity Index	Shannon Evenness
Untreated reference	278,419	155,009	0.56	544	3.47	0.55
SWNT (A)	274,244	115,279	0.42	543	3.76	0.60
MWNT (B)	258,602	125447	0.49	524	3.58	0.57
MWNT-COOH (B)	238,761	123,502	0.52	517	3.59	0.57
SWNT-COOH (A)	247,767	120,482	0.49	507	3.69	0.59
S/DWNT-COOH (B2)	185,794	110,707	0.60	548	3.72	0.59

Relative abundances at the phylum level are shown in Figure 4.15. Sequences at less than 1% are pooled and shown as white space above each sample. In the three samples at the right of the figure, sequences classified as phylum Crenarchaeota are still present, but with relative abundances < 1%. This decrease was seen with all three types of functionalized nanotubes. Although relative abundances of Crenarchaeota remained above 1% in SWNT (A) and MWNT (B) – treated samples, both were slightly lower than the untreated reference. Relative increases in Euryarchaeota are seen with nanotubes from Manufacturer B but not from Manufacturer A. Firmicutes and Bacteroidetes were the most abundant two phyla. Their relative abundances shifted somewhat with no apparent consistency in nanotube manufacturer, length, or degree of functionalization as shown in Table 3. No apparent pattern was seen with the small shifts in relative abundance of Proteobacteria. Small decreases in Synergistetes were seen with all treated samples. Unclassified sequences were identified as belonging to Bacteria, Archaea, or Virus kingdoms, but could not be further classified. These comprised a relatively small fraction (~2.3-5.4%) of all sequences.

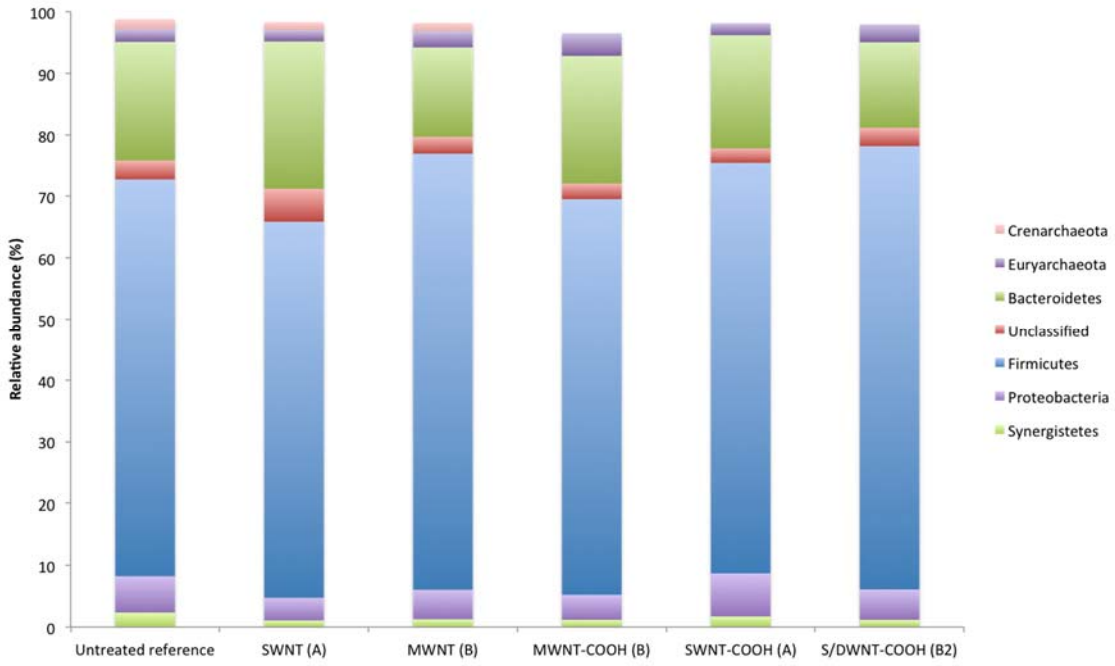

Figure 4.15. Comparison of 16s Phylum level at 1% relative abundance or higher. White space is pooled "other" groups at <1% relative abundance.

At the Class level (Fig. 4.16), all three types of functionalized nanotubes (samples at right) showed increases in Methanomicrobia, a major class of methanogens. A corresponding decrease in Thermoprotei, the dominant class of Crenarchaeota in these samples, also occurred. As with the previous figure, Synergistia (the most abundant class of phylum Synergistetes) decreases with treatment of all types of nanotubes shown.

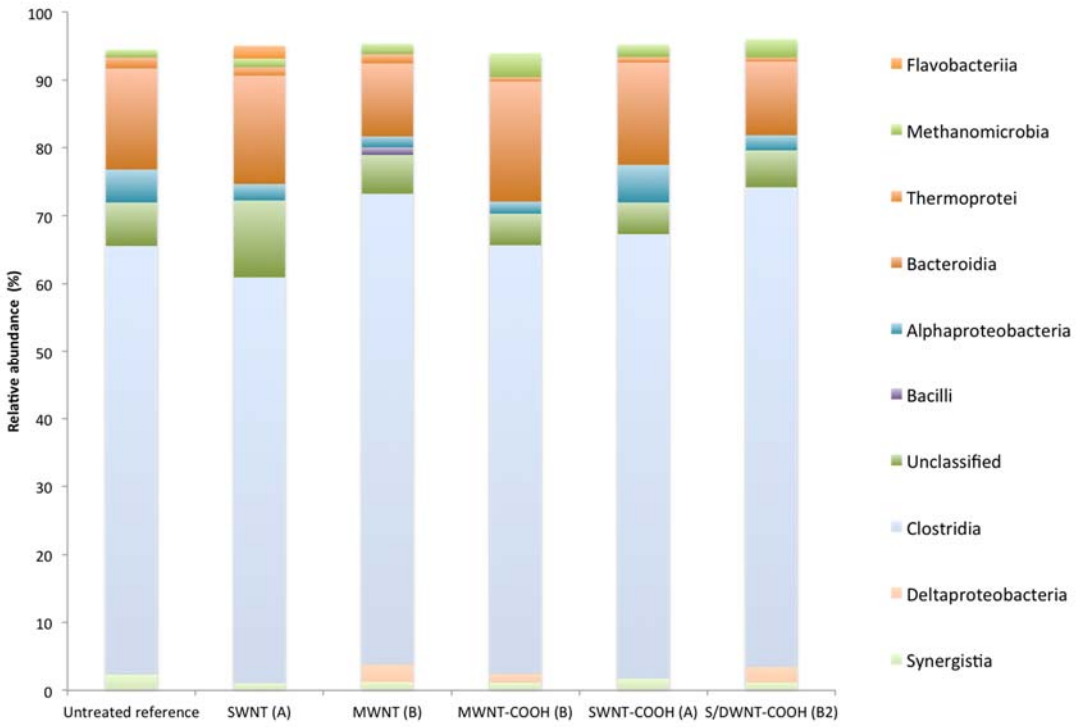

Figure 4.16. Comparison of 16s Class level at 1% relative abundance or higher. White space is pooled "other" groups at <1% relative abundance.

Class Clostridia was by far the most abundant class in all the samples. Figure 4.17 shows a distribution of families in this class. Many are in the order Clostridiales. Relative abundance of *Peptococcaceae* and *Clostridiaceae* increase with nanotubes from Manufacturer B but not Manufacturer A.

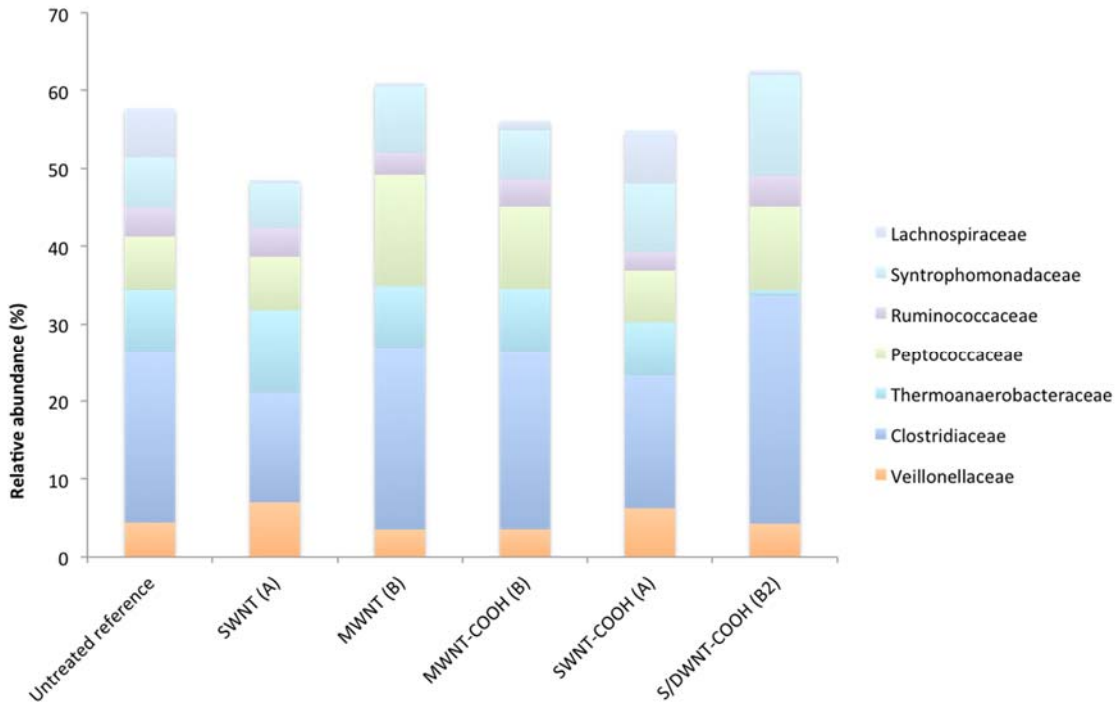

Figure 4.17. Relative abundance of bacterial families in Class Clostridia.

Figure 4.18 focuses on sequences in the Kingdom Archaea, which are functionally very important in methanogenic environments. Relative abundance of this kingdom increased with MWNT and MWNT-COOH from Manufacturer B. Treatments with other types of nanotubes revealed a lower relative abundance of Archaea than the untreated reference. As noted previously, Class Methanomicrobia increased in samples with functionalized nanotubes, with corresponding decreases in Class Methanobacteria as well as Class Thermoprotei, which comprises the majority of Crenarchaeota sequences in the samples. A small increase in Methanomicrobia is seen with MWNT (B). Two orders in Class Methanomicrobia are Methanomicrobiales and Methanosarcinales. Methanosarcinales were not detected in the untreated reference or the SWNT (A) – treated samples. In the

SWNT-COOH (A) – treated samples, their relative abundance was < 0.001%. For MWNT (B) and MWNT-COOH (B) their relative abundance was ~ 0.34-0.35%. For S/DWNT-COOH (B2) samples, it increased to 1.63 %.

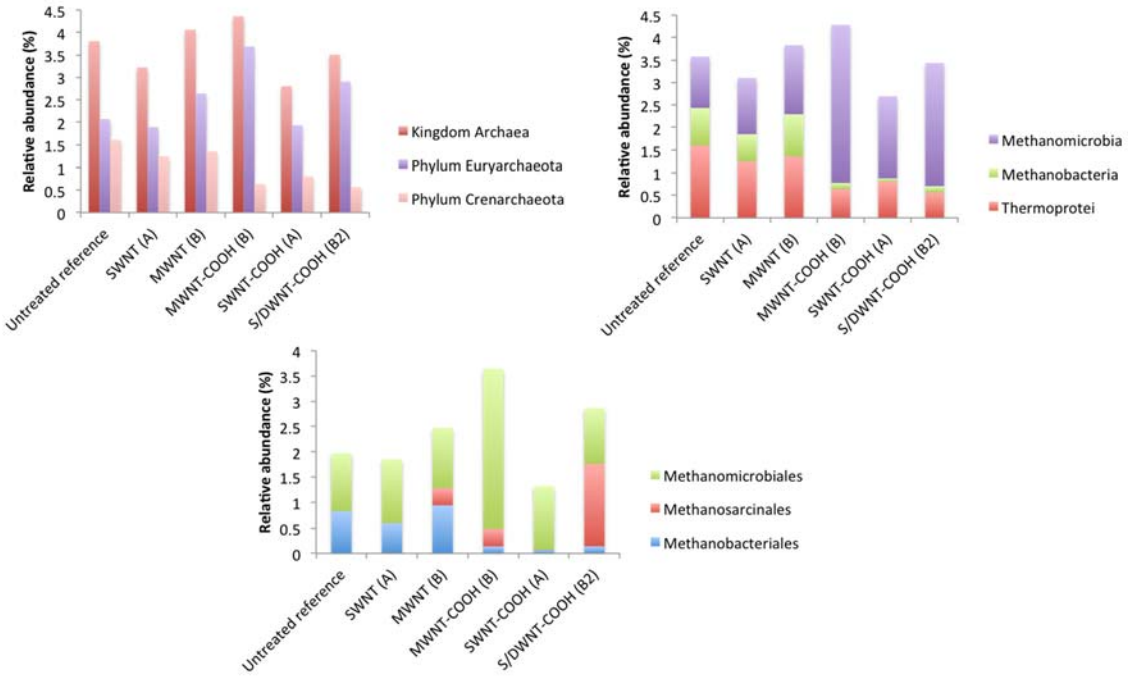

Figure 4.18. Relative abundances for: Kingdom Archaea and two major phyla (top left). Euryarchaeota is dominated by methanogens. Two methanogen classes identified and Thermoprotei, the most abundant class in phylum Crenarchaeota (top right). Thaumarchaeota, not shown, were < 0.001%. Three methanogen orders (bottom) from two classes above right.

Fig. 4.19 shows relative abundance of taxonomic groups with evidence of participation in direct interspecies electron transfer, as described in section 4.1. Relative abundance of genus *Clostridium* is high in all samples, but increased with treatment of MWNT-COOH

and S/DWNT-COOH, both from Manufacturer B. Family *Anaerolinaceae*, and the genera *Geobacter* and *Methanosaeta* are increased in all three samples treated with nanotubes from Manufacturer B (the two with increased *Clostridium* and also with neat MWNT.)

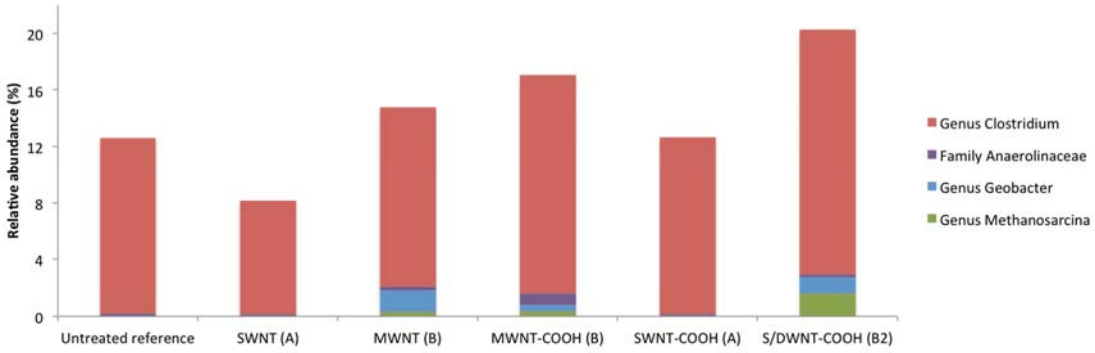

Fig. 4.19. Relative abundances of Family Anaerolinaceae and various genera in the present rumen experiment. These groups show evidence of association with direct interspecies electron transfer (DIET), as found by other studies.

4.4.7 Nickel and Yttrium Concentrations Measured by ICP-MS

After the end of the Biomethane Potential (BMP) Assay, metals concentrations were measured in both solid and aqueous phases, in microcosms treated with SWNT-COOH from Manufacturer A, as well as untreated reference microcosms. Data are shown in Table 4.6. As expected, nearly all of the nickel and yttrium in treated microcosms partitioned to the solid phase. Ratio of nickel to yttrium calculated by solid phase measurements is close to the expected ratio of 7.16 for SWNT-COOH (A) calculated from measurements in row 1 of Table 4.3 (4.37 wt. % for nickel/0.61 wt. % for yttrium).

Row 2 of Table 4.3 shows EDX results for SWNT-CO(NH_2) from the same manufacturer (1.37 wt. % for nickel/0.23 wt. % for yttrium = 5.96). A similar Ni/Y ratio was expected for this product as for SWNT-COOH (A), and 5.96 is actually closer to ICP-MS results for microcosms treated with SWNT-COOH (A). Due to variability in background levels measured in untreated reference samples, the average of these was not subtracted from measurements in treated samples before calculating the ratio of nickel to yttrium in the solid phase.

Table 4.6. Metals concentrations in replicate samples. Microcosms treated with SWNT-COOH from Manufacturer A are compared with untreated reference samples. Deviations from expected concentrations may reflect heterogeneous distribution of nanotubes in the solid phase of microcosms. Ratio of Ni/Y in nanotube-treated samples is consistent with EDX results.

Sample	Nickel Solid phase (ppm)	Nickel Aqueous phase (ppm)	Yttrium Solid phase (ppm)	Yttrium Aqueous phase (ppm)	Expected Nickel solid phase (ppm)	Expected Yttrium solid phase (ppm)	Nickel/Yttrium ratio Solid phase
SWNT-COOH (A)	134	0.55	22	0.04	5,650	785	6.09
SWNT-COOH (A)	364	0.512	61	0.0183	5,650	785	5.97
SWNT-COOH (A)	438	0.353	74	0.0138	5,650	785	5.92
Untreated reference	18	0.02	2.2	0.00031	n/a	n/a	8.18
Untreated reference	1.4	0.018	bdl	0.00037	n/a	n/a	n/a

4.5 Discussion

The biomethane potential (BMP) assay of microbial community function clearly showed that none of the materials studied were toxic even at high concentrations. However, community function and structure were each affected by several different types of carbon nanotubes, both functionalized and non-functionalized.

Treatment with most of the nanotube products substantially accelerated anaerobic gas production. However, the difference in average cumulative gas volumes at the end of the experiment was not significantly different from the untreated reference microcosms. Barring biotransformation of the exogenous nanomaterials, this would be expected from only a single addition of endogenous rumen contents at the beginning of the experiment. However, an overall trend of higher gas production in the nanotube-treated samples was noted. Headspace analysis showed a significant methane fraction decrease in some sets of these nanotube-treated microcosms, which provides evidence for enhanced oxidation of organic matter. The overall trend was lower methane in nanotube-treated microcosms that had shown accelerated gas production months before.

No toxicity was observed with either of the two cellulose nanomaterials. Gas production was enhanced in microcosms treated with freeze-dried nanocellulose and slightly lower in microcosms treated with CN film, but these differences were not significant due to variability between replicates. Headspace methane fraction increased in microcosms

treated with microcrystalline cellulose, but did not change significantly with either of the two cellulose nanomaterials.

Even taking into account pH instability in the startup phase, the effect of nanotubes on gas production was significant through much of the experiment. The two exceptions were SWNT-O^+ (B) and SWNT-$CO(NH_2)$. In the first case, variability between replicates remained high. Effect of pH was likely a contributing factor, as these bottles were not among those that stabilized and recovered methanogenic function most quickly (see red and orange areas of Fig. 4.8 indicating low pH). The same depletion of biomass and loss of color and particulate matter after 730 days was seen in these microcosms (Fig. 8) as for other microcosms, e.g. the S/DWNT-COOH (B2) treated ones that produced the highest gas volumes. Therefore, it is possible that the SWNT-O^+ (B) bottles started out with slightly lower masses of biodegradable rumen contents. In the second case, only 30 mg of amide-functionalized nanotubes were added to each bottle in this set, due to their relatively high cost. Masses three to ten times higher were used for other nanomaterial treatments. It is possible that the amidated tubes would also have had a similar effect at a high enough concentration. However, involvement of the amide group in mitigating any possible effect of the nanotube carbon cannot be excluded.

Metals measurement by ICP-MS contributed to interpretation of biological data for SWNT-COOH (A) and to some extent for SWNT (A) and SWNT-$CO(NH_2)$ (A) treatments. This is due to the fact that Manufacturer A uses nickel and yttrium as catalyst

in synthesizing all these nanotube products[85]. First, the average aqueous phase concentration of nickel was approximately 25 times higher in SWNT-COOH (A)-treated samples than in untreated microcosms with only background levels of nickel. The average aqueous concentration of yttrium in treated samples was approximately 70 times higher than background. Aqueous concentrations of nickel and yttrium in untreated samples were consistent with levels previously measured in surface waters. Safavi et al[86] found. 10.4-12.2 ppb nickel in river water and sea water, respectively. In another study[87], the average yttrium concentration detected by ICP-MS in reference river water SLRS- 4 was 0.1374 ppb.

Further, ICP-MS data showed that almost all of the metals partitioned to the solid phase, as expected. A mass balance could not be achieved for the solid phase because subsamples were taken from microcosms and nanotubes were heterogeneously distributed in the biomass blanket. This is the most likely explanation for why the measured levels are substantially lower than the expected maximum concentrations. Finally, Ni/Y ratio calculated from these measurements is within range of manufacturer's specifications as well as the EDX results presented in this study.

Another possible mechanism of effect considered was amorphous carbon content of the nanotubes. The S/DWNT-COOH (B2 and B1, respectively)-treated microcosms that produced the highest and next-highest volumes of gas, as well as had the most accelerated gas production, have less than 3% (by wt.) reported amorphous carbon

content[88]. Based on the masses of nanotubes added to the microcosms, amorphous carbon mass was estimated. Theoretical gas calculations showed that less than 10 ml of average gas production compared with the untreated reference microcosms would be expected if amorphous carbon biodegradation was the only mechanism of the effect. Instead, approximately 100 ml higher gas production was seen in these nanotube-treated microcosms, even though it was not statistically significant by the end of the experiment.

For community structure assessment, variability in start-up pH stability is a possible explanation for differences between replicates in genetic fingerprints generated by PCR-DGGE. Replicates were pooled for Illumina sequencing and Metagenomic analysis, which revealed increases in community diversity and evenness of nanotube-treated samples in the roughly half of all sequences that could be classified down to the species level. One limitation of this technique is that profiles were limited to 16s sequences. Eukaryotic small fragments (V8 region of the 18s rRNA gene) were amplified in the rumen samples, although relatively high volumes of template DNA were needed in the reaction, possibly due to low relative abundance of these sequences compared with non-target Bacterial and Archaeal genomic DNA. It should be noted that 18s fragments amplified would include plant DNA from the cow's diet. However, microcosms were sampled for DNA extraction quite late in the experiment when rumen dietary contents were somewhat depleted. Of interest for future work would be in-depth assessment of fungal and protist communities. These are overall underrepresented in the literature about the metagenome of cow rumen[89, 90] Also of note for future study is that rumen DNA

yields and resulting community structure can be affected by rumen sampling technique, and to a lesser extent by the choice of DNA extraction procedure[91].

Metagenomic assessment of these samples showed an increase in relative abundance of members of the order Methanosarcinales, as well as two major families in Class Clostridia. Methanosarcinales are generally associated with acetoclastic methanogenesis[92], which is not the predominant pathway in rumen. Mayumi et al.[93] found a shift in favor of acetoclastic methanogenic over hydrogenotrophic with increasing CO_2 concentrations in oil reservoirs. For the data in this rumen study, species identified within order Methanosarcinales are among those capable of splitting acetate to methane and carbon dioxide, but it was not possible to conclusively determine whether a similar metabolic shift occurred as in the oil reservoir study. First, the methanogenic pathway of choice can differ between strains of the same species. Second, many Methanosarcinales are known to be capable of using either pathway. Finally, in the rumen experiment, acetate concentrations were not measured and microcosm headspace measurements were not taken throughout the BMP assay. In revisiting the direct interspecies electron transfer (DIET) hypothesis for explaining the mechanism of conductive carbon effects on anaerobic reactors, the importance of Methanosarcinales is again highlighted[94].

Although multiple publications provide compelling evidence that direct interspecies electron transfer (DIET) does occur, it is not a fully satisfactory explanation for the results of this rumen study. The dramatic decolorization and biomass blanket depletion seen over time in nanotube-treated samples would not be explained by this phenomenon.

Other work has illustrated the capability of carbon nanotubes to produce reactive oxygen species (ROS), even in the absence of light[95]. By this mechanism, surface catalytic oxidation of biological molecules was demonstrated. Taken along with the data presented here, another possible mechanism of effect of carbon nanotubes should be further explored; that is that multiple types of nanotubes have surface catalytic properties enabling biodegradation of endogenous plant material, including humic acids, chlorophyll derivatives, and other recalcitrant compounds. Images presented in this study also support assertions of other researchers that the nanotubes could enhance community function by a physical mechanism of scaffolding to support biofilm formation[96].

In summary, these results from methanogenic communities enriched from cow rumen inoculum show that enhancement of community function and increases in community diversity cannot be fully explained by functional groups or residual metals, at least not for the materials tested. Multi-walled nanotube treatment without –COOH groups actually showed slightly accelerated gas production compared with its MWNT-COOH counterpart from the same manufacturer. Both carboxylated and non-carboxylated single-walled tubes from Manufacturer A also had a similar but less pronounced effect on gas production and also affected microbial community structure. Interestingly, these were shorter nanotubes compared with those from Manufacturer B. In general, a stronger effect on community function and structure was associated with increasing nanotube length, which makes sense given the higher surface area compared with shorter tubes.

Recent publications on the effect of carbon nanotubes on anaerobic microbial communities present an exciting new direction for further study. Any enhancing effects on anaerobic digestion are currently of great interest in order to take full advantage of this environmentally preferable treatment strategy for a sustainable energy future. A note of caution is suggested in the likelihood of poorly managed release of carbon nanomaterials to the environment. Multiple lines of evidence suggest that they are not purely benign under all conditions. For example, accelerated methanogenesis would not be desirable in cow rumen. Anaerobic microbial communities are clearly affected in terms of both their structure and function, by interaction of likely multiple factors that require further study in order to fully explain. However, it is clear that carbon nanomaterials very substantially accelerate methanogenic activity, and may in fact facilitate biotransformation of recalcitrant biopolymeric material.

CHAPTER 5. ASSESSING THE IMPACT OF CONDUCTIVE CARBON NANOMATERIALS ON ANAEROBIC MICROORGANISMS IN ENGINEERED SYSTEMS

5.1 Abstract

Carbon nanotubes are among a suite of conductive carbon materials of recent interest for facilitating direct interspecies electron transfer (DIET) between microorganisms. Addition of these materials for optimization of anaerobic digestion technologies is being explored. The long-term environmental impact of carbon-based nanomaterials remains unclear, with most available studies being of short duration or with pure cultures in a laboratory. Furthermore, conflicting evidence leaves unresolved questions about the mechanisms of any effects observed. In the current study, a biomethane potential (BMP) assay lasting 730 days with anaerobic sludge inoculum was carried out to assess the effects of carbon nanotubes from two different manufacturers and their associated metal residue on the microbial community. Analysis of community structure with PCR-DGGE was compared with Metagenomic data from 16s Illumina sequencing. Sodium 2-bromoethanesulfonate (BES) was used as a toxic reference because it is a known inhibitor of methanogenesis. Effect of nanotubes and metals on the anaerobic microcosms was influenced by acclimation to one of two different substrate mixtures. The choice of substrate affected community structure independently of the nanotubes or metals.

Nanotube treatments and metals were associated with a small but significant acceleration of gas production for the microcosms receiving glucose, methanol, and ethanol, while headspace methane was generally unaffected. For the microcosms fed with PEG-600, and intermittently with ethanol and methanol as a substrate challenge, mild inhibition by nanotubes was observed with concurrent effects on community structure. Overall, the nanotubes and metals did not affect community structure or function to the degree that BES did at the concentrations tested (up to 85,000 mg/kg for nanotubes, 30,000 mg/kg for a nickel/yttrium mixture, and 50 μmol/ml for BES). However, some community shifts did occur, with enrichment of some taxonomic groups associated with DIET in other studies.

5.2 Introduction

Carbon nanotubes have long been known to have electricity conducting properties[97], which make them of interest for a variety of industrial applications, but also of concern for environmental impacts due to their unique chemical and physical properties. The anaerobic digester at a wastewater treatment plant is a receptor for waste streams from manufacturing of carbon nanotubes, as well as from their industrial, household and biomedical end use. Land application of sludge biosolids is a likely route of exposure for both organic and inorganic nanomaterials and of concern to ecotoxicologists[98, 99]. A potentially beneficial effect of nanotubes and other forms of conductive carbon is that they may facilitate interactions between microorganisms that would enhance their community function and possibly increase diversity of community structure. Direct

interspecies electron transfer (DIET)[100] has recently been described as one such effect and has become a focus of intense interest in the scientific community.

The anaerobic microcosm assay with rumen inoculum described in Chapter 4 exhibited substantial acceleration of gas production with most types of nanotubes tested; both single- and multi-walled, -COOH functionalized, or neat. More acceleration was associated with longer nanotubes (3-30 μm), whereas a smaller effect was seen with shorter nanotubes (0.5 - 3 μm). These nanotubes of different length ranges came from two different manufacturers. Manufacturer A produces the shorter nanotubes with nickel/yttrium catalyst. The effect of this combination of metals apart from carbon nanotubes was explored in the present study.

Another recent study found acceleration of anaerobic gas production by granular sludge in response to single-walled carbon nanotubes[67]. On a dry mass basis, their nanotube concentration was about 20x higher than those used in the rumen study or the highest final concentration used in the sludge assay described here. Also of note, their nanotubes were 5-20 μm in length. Furthermore, the manufacturer of these nanotubes used cobalt as a catalyst[101].

The effect of metals addressed in this study has focused on the nickel/yttrium catalyst found in a relatively high concentration (5-7% by wt.) in nanotubes from Manufacturer A. However, nanotubes from Manufacturer B used in the rumen and sludge studies are also reported to contain residual cobalt catalyst at ~1% by weight[88]. In the EDX data for these

materials, cobalt was detected at 0.35% (wt.) in only one of two nanotube products tests from this company. These were the multi-walled carboxylated nanotubes (MWNT-COOH), also used in the sludge microcosm study described here. Previous work has shown low bioavailability and lack of toxicity of residual metals in nanotubes of both low and high purity, with and without functional groups[102]. Although other recent studies indicate some effect of the conductive carbon structure of nanotubes on anaerobic microbial structure and function, the possible contribution of these metals to any enhancing effect needs to be better characterized.

5.3 Experimental Design

Nanotubes from two different manufacturers (Carbon Solutions, Inc. and Cheap Tubes, Inc., designated as A and B, respectively, for brevity in tables and figures) were included in the experimental design. For Manufacturer A, the ratio of semiconducting to metallic nanotubes produced by arc discharge is 2 to 1[85]. For Manufacturer B, this ratio is about 1.5 to 1 with the catalytic chemical vapor deposition production method[103]. Single-walled carboxylated nanotubes (SWNT-COOH), amide-functionalized single-walled nanotubes (SWNT-CO(NH_2), neat multi-walled nanotubes (MWNT), carboxylated multi-walled nanotubes (MWNT-COOH), and two different batches (B1 and B2) of single- and double-walled carboxylated nanotubes (S/DWNT-COOH) were used as treatments. Due to the presence of nickel/yttrium catalyst remaining in the SWNT-COOH (A) at non-negligible concentrations (5-7 wt.%), one set of microcosms was designated as a reference for the effect of these alone, apart from the nanotubes. The reported ratio of

Ni/Y in the nanotube product is ~ 6.5:1. Nickel (5-20 nm) and yttrium (40 mesh, smallest size commercially available at the time) (both from Alfa-Aesar) were combined in this ratio and used as the metals reference.

The experimental design for each of two substrate mixtures is shown in Table 5.1 and Table 5.2. A series of challenges was carried out during the BMP assay in order to better characterize some of the effects seen early in the experiment. These challenges are described in the footnotes for Table 5.1 and Table 5.2. First, microcosms fed with PEG-600 also received methanol and ethanol at alternate feedings to test the hypothesis that changing substrates would enhance any inhibitory effects of the nanotubes on the microbial community. Microcosms that showed mild, non-significant ($p \geq 0.05$) inhibition by nanotubes were given some extra substrate and additional nanotubes, with addition of substrate also to all relevant reference microcosms. Finally, for microcosms fed with a different substrate mixture (glucose, methanol, and ethanol) that showed enhanced gas production in response to nanotubes or metals, these materials were added one or more times later in the experiment without concurrent substrate addition. This was accomplished in order to test the hypothesis that some biotransformation of the nanotubes was occurring, or alternatively that enhancement of degradation of endogenous bioavailable substrates in the case of the metals reference set would explain the increased gas production. Nanotube treatments for SWNT-COOH (A) are designated as “low” and “high” due an order of magnitude difference between them at T0. None of the nanotube products from Manufacturer B were added or increased after T0, therefore the final

concentrations when the BMP assay ended at day 730 were the same as at T0, assuming no biotransformation of the nanotubes occurred.

Sodium 2-bromoethanesulfonate (Aldrich) was used as a toxic reference, added to one set of nanotube-treated microcosms at the second substrate feeding, after methanogenesis had already been established. The BES concentration was 50 μmol/ml, the level reported to completely inhibit methanogenesis[104].

Table 5.1. Experimental Design for Microcosms with PEG-600 (1.9 mM) as substrate. At alternate feedings starting with the second feeding, microcosms also received methanol (25.4 mM) and ethanol (16.9 mM), abbreviated "ME". This experimental group is referred to as PEG (ME) (+ any other treatments). A substrate-only reference set is also included. Except where otherwise noted, there were three replicates in each set.

Treatment at T0	Nanotube Concentration (mg/kg biomass (dw))
PEG (ME) reference[a,b2]	n/a
PEG (ME) + low SWNT-COOH (A)[b3]	1,700
PEG (ME) + high SWNT-COOH (A)[a,b1]	17,000
PEG (ME) + S/DWNT-COOH (B1)[b3]	50,000
PEG (ME) + high-SWNT-COOH (A) + BES[a,b3,c]	17,000
PEG + Ni/Y[a,b2,,d]	n/a

[a] One DNA sample from day 131 from a single microcosm in each set indicated was sent for Illumina sequencing.
[b1]These microcosms received additional nanotubes at 17,000 mg/kg each on day 265 only, for a final concentration of 34,000 mg/kg, along with additional PEG (1.9 mM) the same day.
[b2]These microcosms received additional PEG (1.9 mM) on day 265.
[b3]These microcosms did not receive PEG on day 265.
[C]BES added at second feeding with PEG(ME), day 65, at 50 μmol/ml.
[d] Metals reference samples received a 6.5:1 mixture of Ni to Y, at ~ 10,000 mg/kg and a subsequent metals treatment at 20,000 mg/kg on day 131, for a final concentration of 30,000 mg/kg.

Table 5.2. Experimental Design for Microcosms with Glucose (8.36 mM), methanol (25.4 mM) and ethanol (16.9 mM) as substrate. This experimental group is referred to as GME (+ any other treatments). A substrate-only reference set is also included. Except where otherwise noted, there were three replicates in each set.

Treatment at T0	Nanotube Concentration (mg/kg biomass (dw))
GME reference[a]	n/a
GME + low SWNT-COOH (A)[b1]	1,700
GME + high SWNT-COOH (A)[a,b2]	17,000
GME + SWNT-CO(NH_2) (A)	20,000
GME + MWNT-COOH (B)	50,000
GME + MWNT (B)	50,000
GME + S/DWNT-COOH (B1)	50,000
GME + S/DWNT-COOH (B2)	50,000
GME + Ni/Y[a,c]	n/a

[a] One DNA sample from day 131 from a single microcosm in each set indicated was sent for Illumina sequencing.
[b1]These microcosms received additional nanotubes at 17,000 mg/kg each on two subsequent days (day 265 and day 278), for a final concentration of 35,700 mg/kg.
[b2]These microcosms received additional nanotubes at 34,000 mg/kg each on days 265 and day 278, for a final concentration of 85,000 mg/kg. There were six replicates in this set.
[c] Metals reference samples received a 6.5:1 mixture of Ni to Y, at ~ 10,000 mg/kg and a subsequent metals treatment at 20,000 mg/kg on day 131, for a final concentration of 30,000 mg/kg.

5.4 Results

5.4.1 Biomethane Potential (BMP) Assay

Average cumulative gas production over time for microcosms with GME substrate is shown in Fig. 5.1. None of the nanotubes or metal treatments were associated with inhibition of gas production in this group. The highest gas volume at the end of the experiment occurred in microcosms receiving GME + high SWNT-COOH (A) with almost 1.3 L of biogas produced over 730 days (about 50 ml higher than the GME

reference). This increase was not significant ($p \geq 0.05$) by the end of the experiment, but was significant ($p < 0.05$) through day 623, when the average difference between the treated set and the reference was 967 ml compared with 908 ml, respectively.

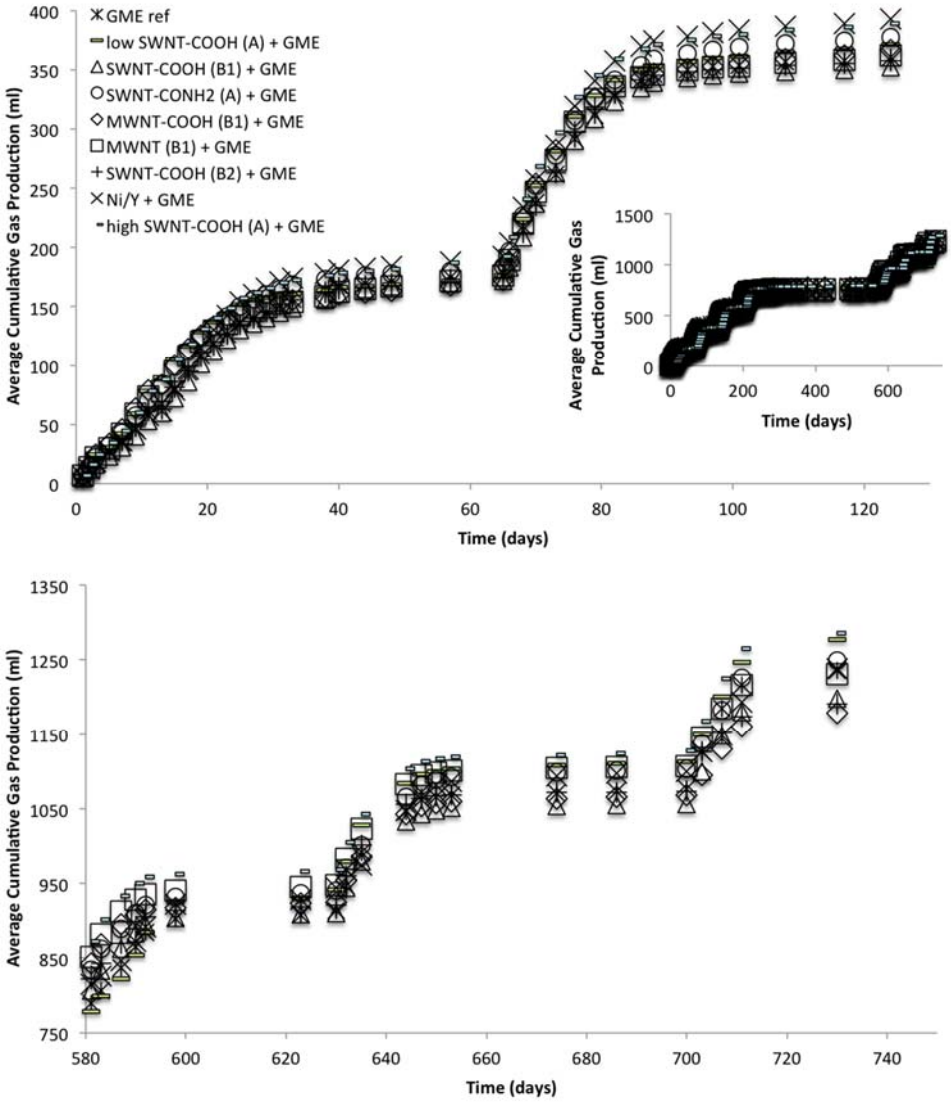

Figure 5.1. Average cumulative gas production over time for microcosms fed with glucose, methanol, and ethanol (GME). Detail is shown for day 1 through day 130 (top), and again for day 580 through day 730 (bottom). The complete time plot with eight feedings is shown (top, inset). Microcosms with the high concentration of SWNT-COOH (A) (short dashes) had significantly higher gas production ($p < 0.05$) than the GME reference through day 623.

Average cumulative gas production normalized to the GME reference for this substrate group at three different time points is shown in Fig. 5.2. Experimental error for each reference or treatment set is shown in Table 5.3.

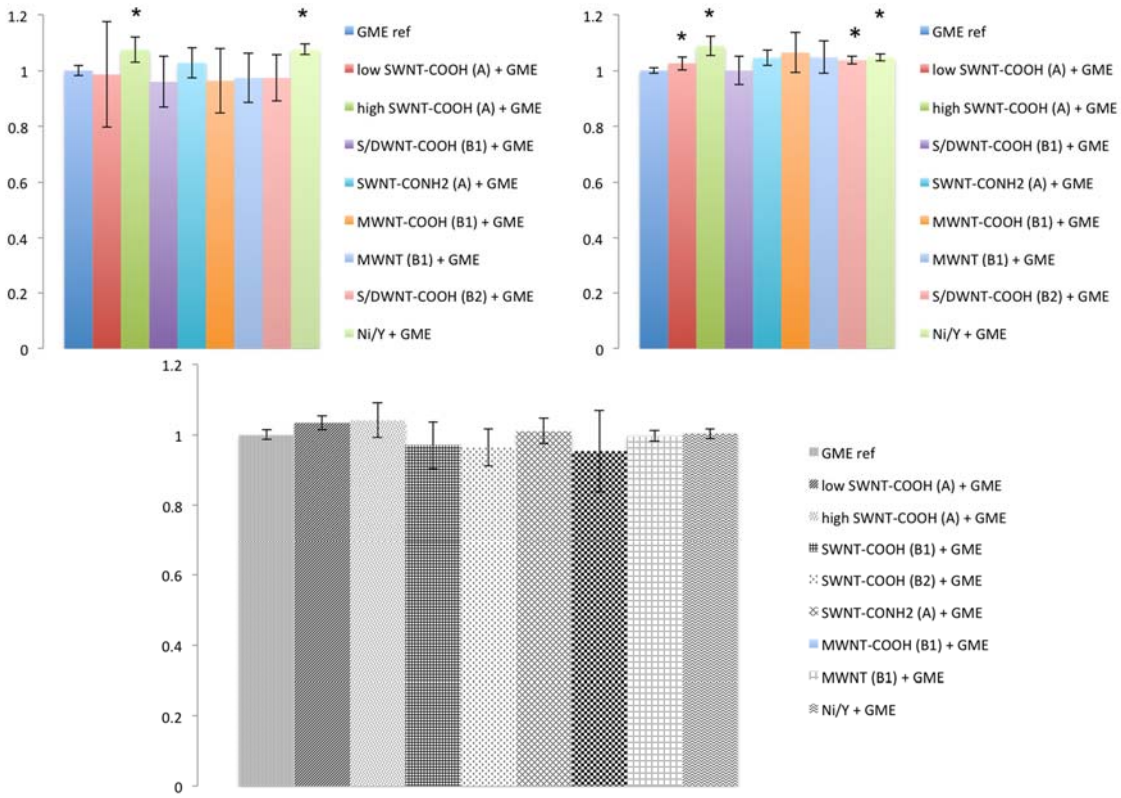

Figure 5.2. Average cumulative gas production normalized to the GME reference at day 65 (top left), day 296 (top right), and day 730 (bottom). Low SWNT-COOH (A) was significantly higher ($p < 0.05$) for days 201, 202, and 282-296. High SWNT-COOH (A) treatment was significantly higher than the GME reference from day 1 through day 623. S/DWNT-COOH (B2) was significantly higher from day 1, and 267- 425. Ni/Y + GME was significantly higher from day 23 – 68, 76-132, 142-144, 169-200, and 221 to day 445. Not shown, MWNT treatment was significantly higher on day 583 only, and SWNT-$CO(NH_2)$ (A) on days 33-38. For all treatments and reference sets, n=3. Error bars are omitted for clarity.

Table 5.3. Average % error for sludge experiment

Treatment	avg % error day 3 to day 730
PEG (ME) ref	**10.48**
GME ref	**1.52**
low SWNT-COOH (A) + PEG (ME)	**6.76**
high SWNT-COOH (A) + PEG (ME)	**7.98**
low SWNT-COOH (A) + GME	**5.77**
high SWNT-COOH (A) + GME	**1.28**
S/DWNT-COOH (B1) + PEG (ME)	**3.81**
S/DWNT-COOH (B1) + GME	**7.37**
high SWNT-COOH (A) + GME	**5.67**
SWNT-$CONH_2$ (A) + GME	**4.86**
MWNT-COOH (B1) + GME	**8.09**
MWNT (B1) + GME	**7.13**
S/DWNT-COOH (B2) + GME	**3.69**
Ni/Y + PEG(ME)	**2.54**
Ni/Y + GME	**3.01**
high SWNT-COOH (A) + PEG (ME) + BES 2nd feeding	**2.13**
high SWNT-COOH (A) + GME	**4.35**

Average cumulative gas production over time for microcosms with PEG (ME) substrate is shown in Fig. 5.3. Complete inhibition of methanogenesis occurred in BES-treated microcosms shortly after BES addition at day 65. These microcosms never recovered gas production, and were noted to have a pH of ~5 after addition of sodium 2-bromoethanesulfonate. A slight inhibition of gas production with some nanotube and metal treatments compared with the substrate reference was seen that was not significant ($p \geq 0.05$) except for the PEG + Ni/Y treatment from days 205-219. Some of them received additional nanotubes, metals, and PEG as described in Table 5.1. No apparent

further effect of the treatments was seen after these additions. Minor differences in gas production around this time are accounted for by some treatment sets not having been included in this extra substrate feeding.

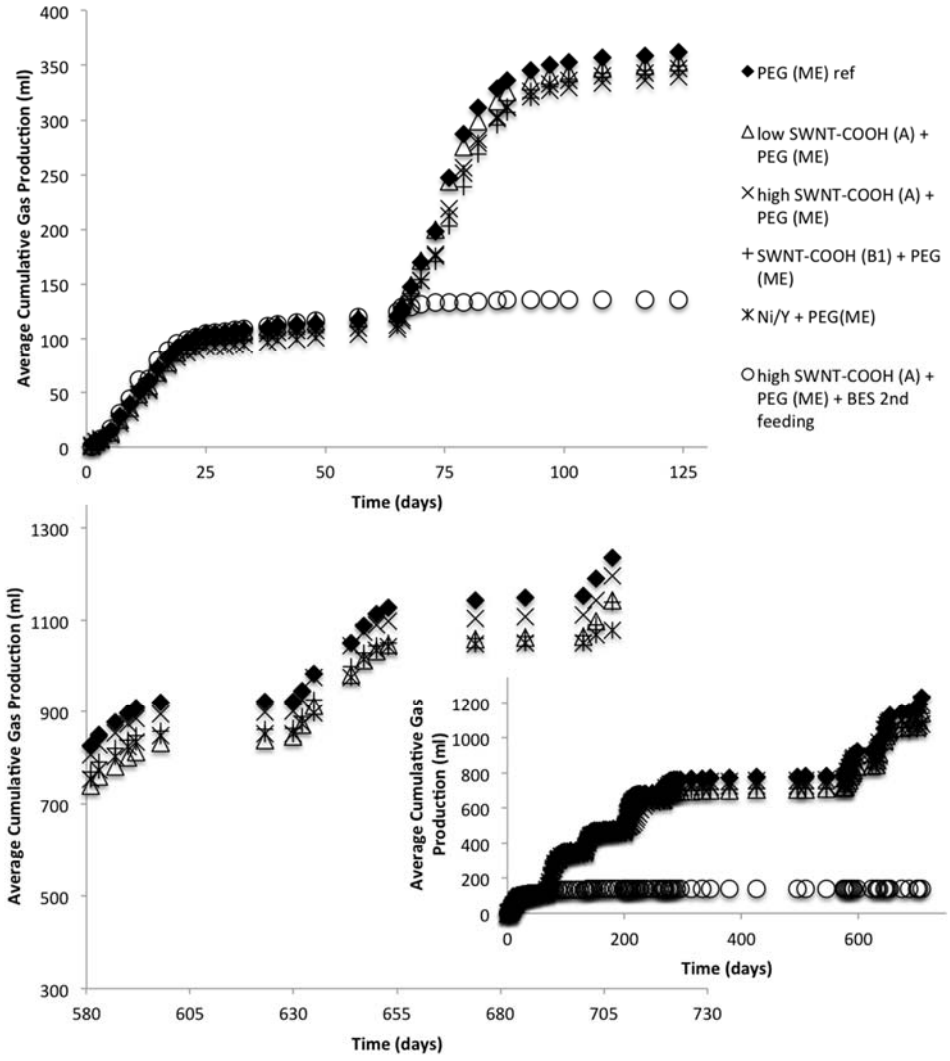

Figure 5.3. Average cumulative gas production over time for microcosms fed with PEG and also with methanol and ethanol (ME) at every alternate feeding beginning with the second feeding. Detail is shown for day 1 through day 130 (top), and again for day 580 through day 730 (bottom). The complete time plot with eight feedings is shown (bottom, inset). Microcosms treated with BES at the second feeding stopped producing gas and never recovered. For all treatments and reference sets, n=3. Error bars are omitted for clarity.

Average cumulative gas production normalized to the PEG (ME) reference for this group is shown (Fig. 5.4) at the same three time points as in Fig. 5.2.

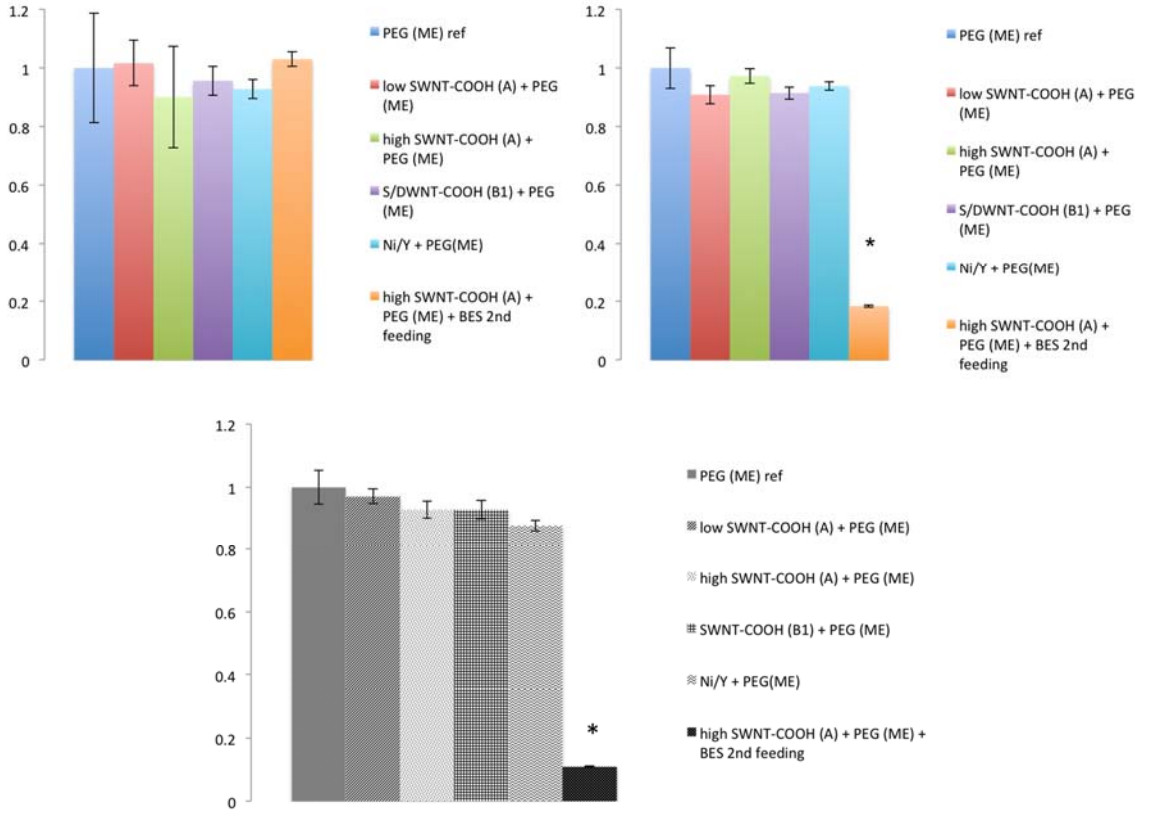

Figure 5.4. Average cumulative gas production normalized to the PEG (ME) reference, at day 65 (top left), day 296 (top right), and day 730 (bottom). Ni/Y + PEG (ME) treatment was significantly lower than the reference from days 205-219. Otherwise, only the BES treatment added to half the replicate set (three microcosms) with the higher concentration of SWNT-COOH (A) was significantly different ($p < 0.05$) than the reference, with essentially complete inhibition of methanogenesis after addition on day 65.

Figure 5.5 shows methane normalized to the substrate reference in both groups of microcosms at day 635. A small methane peak was detected in microcosms with BES

treatment. It should be noted that these microcosms were not under positive pressure as were all other samples taken for headspace analysis. Pre-BES treatment, average methane for these microcosms was similar to that of the PEG (ME) reference set.

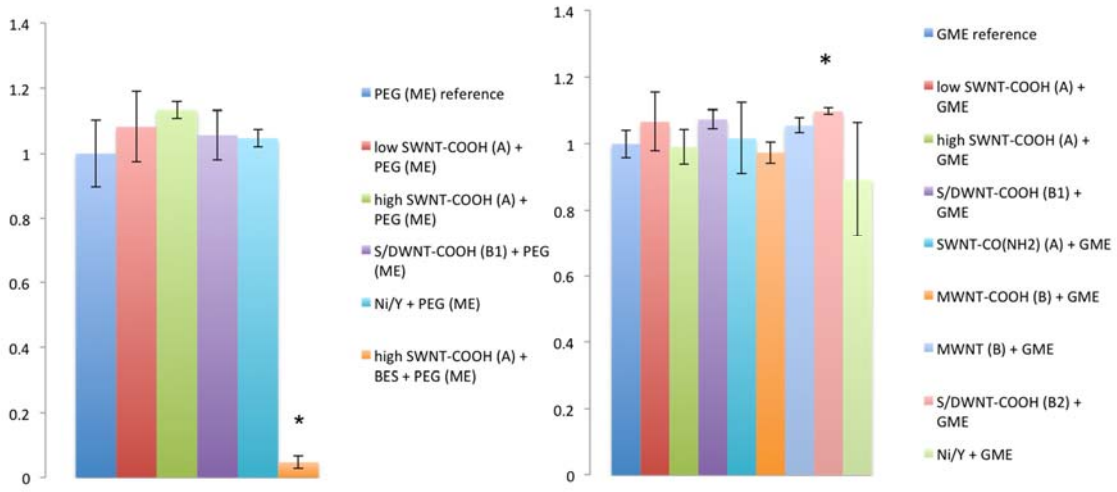

Figure 5.5. Microcosm headspace analysis from day 635, a representative data set. Addition of BES at day 65 almost completely inhibited methanogenesis through the end of the experiment. Methane was generally not significantly different from the substrate reference, with one exception shown here, at right (S/DWNT-COOH (B2)).

Microcosm photos were taken after all nanotube and metal additions had been completed. These are shown in Fig. 5.6 (SWNT-COOH (A)) and Fig. 5.7 (S/DWNT-COOH (B1 and B2)), compared with a GME reference microcosm. In Fig. 5.7, some de-colorization of aqueous phase is seen, similar to, but less pronounced than the effect described in rumen microcosms in Chapter 4.

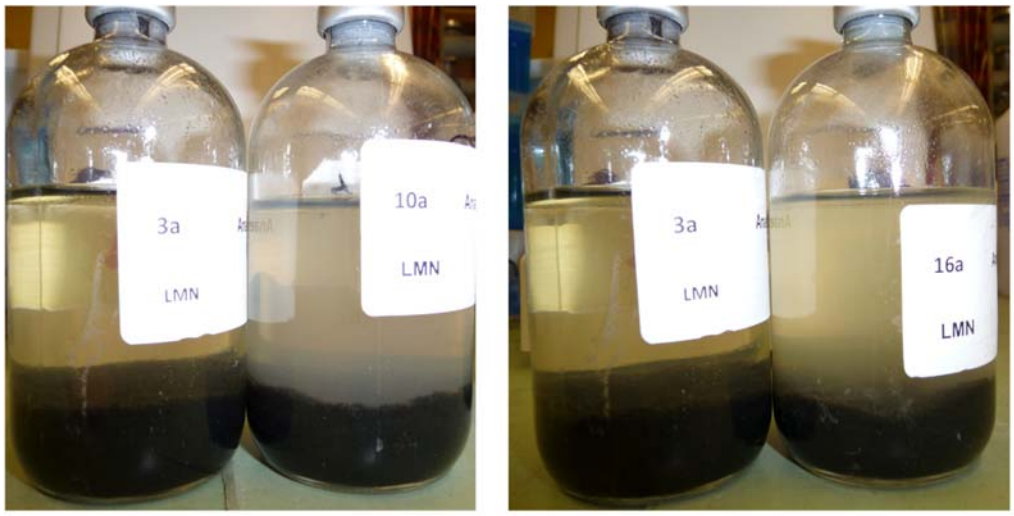

Figure 5.6. Day 296 of the BMP assay, Comparison of a GME reference microcosm (Bottle #3a in each photo) with a treated microcosm. Left: GME-fed microcosm also treated with SWNT-COOH (A) (Bottle #10a in first photo). Image was taken after three nanotube additions with a final concentration of 85,000 mg/kg. Right: GME-fed microcosm with metals reference mixture. Final concentration was 30,000 mg/kg metals with a 6.5:1 mixture of nickel/yttrium.

Figure 5.7. Day 296 of the BMP assay. A GME reference microcosm, bottle #3a, is shown at far left in each photo. Left: Bottles #9a, 9b, 9c are fed with GME and also treated with 50,000 mg/kg S/DWNT-COOH (B1). Right: Bottles #14a, 14b, 14c are fed with GME and also treated with 50,000 mg/kg S/DWNT-COOH (B2). There were no subsequent nanotube additions after T0. Some de-colorization of the aqueous phase can be seen in microcosms with nanotubes from Manufacturer B.

5.4.2 Microbial Community Analysis

DGGE profiles using 16s primers for Bacteria are shown in Fig. 5.8. Gradient is 35-65% denaturant, with increasing concentration from top to bottom of the gel. This sampling date was the second to last. Subsamples were taken for DNA extraction when gas production was very active, in the middle of a feeding pulse. Some differences are visible between samples with different treatments, or treated samples and the substrate references, but minor differences are also found between two replicates of GME + high SWNT-COOH (A) shown on the same gel. It is difficult to discern whether or not apparently missing bands are truly absent or merely reduced in intensity. For most bands on this gel, it appears to be the latter.

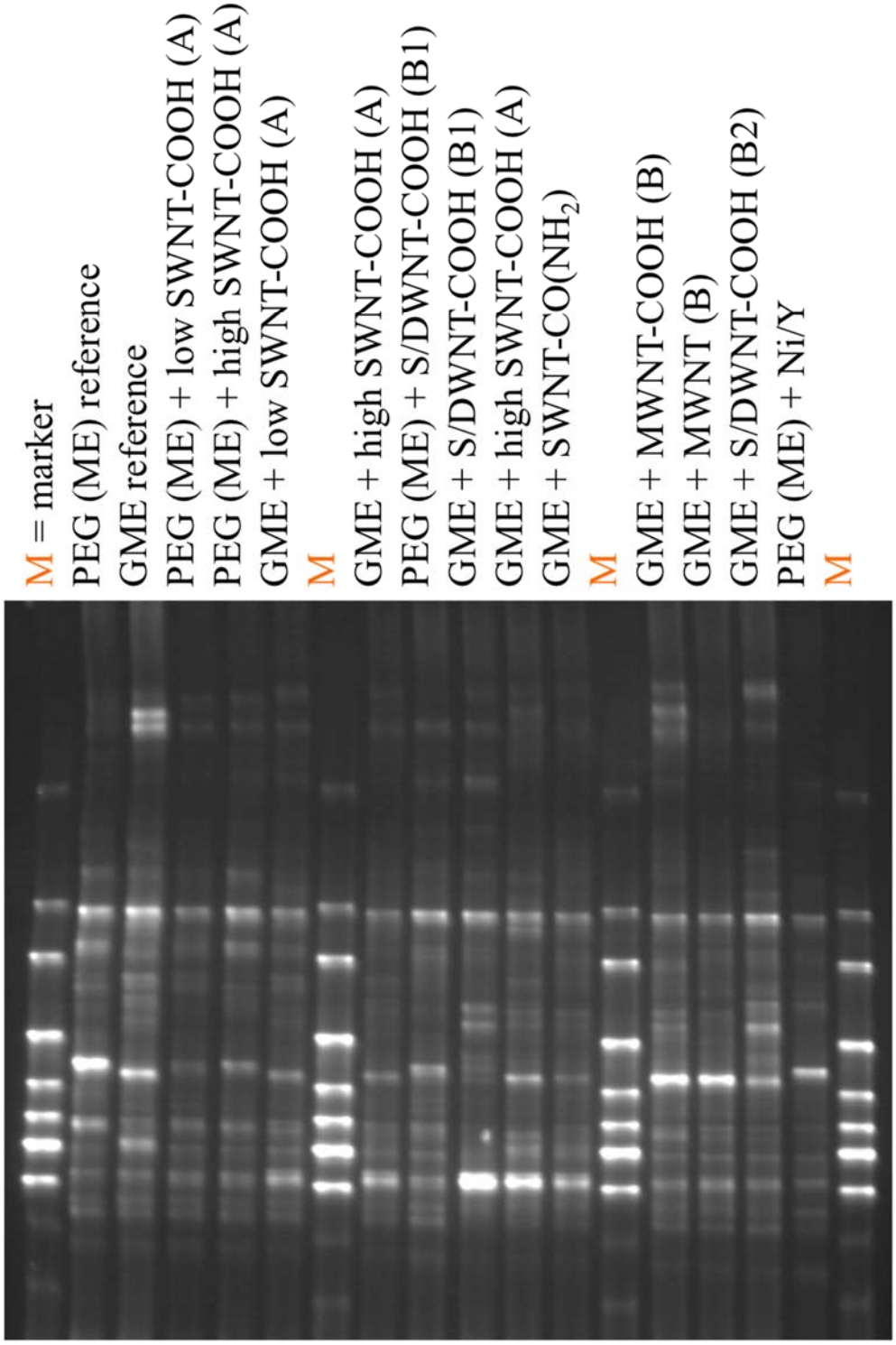

Figure 5.8. DGGE profiles for Bacteria, run on a 35-65% gradient, day 592 during active gas production after feeding. All nanotube and metals additions had been completed by this point. Two replicates of GME + high SWNT-COOH (A) are shown.

Figure 5.9 shows Archaea community profiles for BES treatment compared with the PEG (ME) reference, both before and a few months after treatment. Some nanotube-treated and metals reference samples are shown for comparison. In the BES post-treatment sample (red arrow), one bright band and appears to be missing, compared with the pre-treated replicates and the PEG (ME) references. The PEG + Ni/Y sample (second from right), appears to show enrichment of a band that is higher G+C than the profile found in the PEG (ME) reference at the same time point.

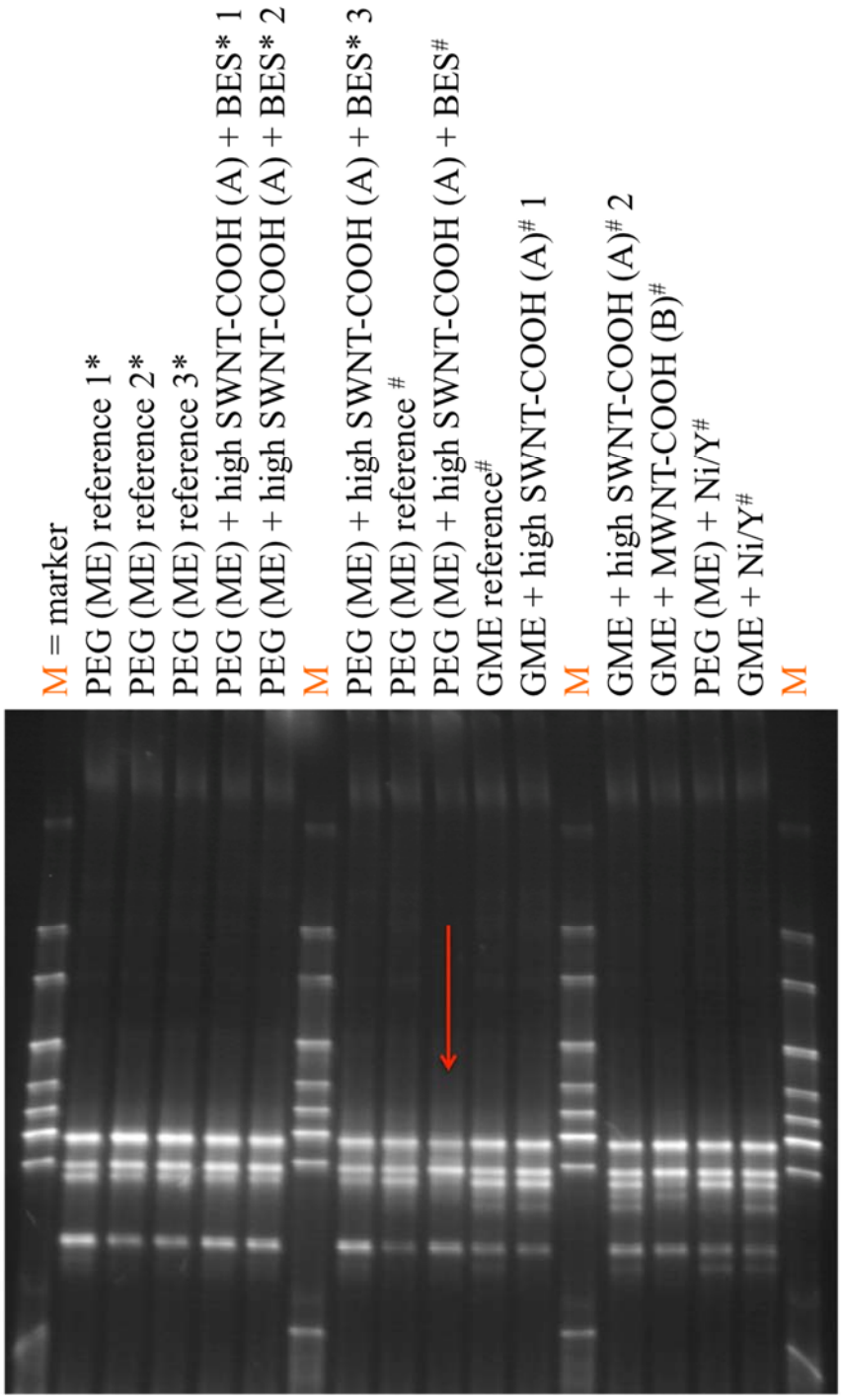

Figure 5.9. DGGE profiles for Archaea, run on a 40-70% gradient. Numbers listed after samples are replicates. First six sample lanes from far left are from day 65, *before addition of BES. The "#" symbol is for day 198, post-BES addition to that set of microcosms. BES-treated sample is indicated with a red arrow. Substrate references and some nanotube-treated samples are shown from the same sampling day for comparison. All these sampling days are before any further additions of nanotubes or metals after T0.

In samples from the GME group shown on this gel, that high-GC band is apparent in the GME reference, and one of the GME + high SWNT-COOH (A) replicates, but it is not seen in the other replicate for that treatment. It is also not present in the GME + MWNT-COOH (A) treated sample. At least one other band is missing from the MWNT-COOH (A) treated sample compared with the GME reference.

Figure 5.10 shows 18s Eukarya profiles from day 131, the same sampling day for which genomic DNA samples were sent for 16s Illumina sequencing. Again, some differences are seen between two replicates of the same treatment. This was typical of Eukarya DGGE fingerprints throughout the experiment, regardless of sample treatment.

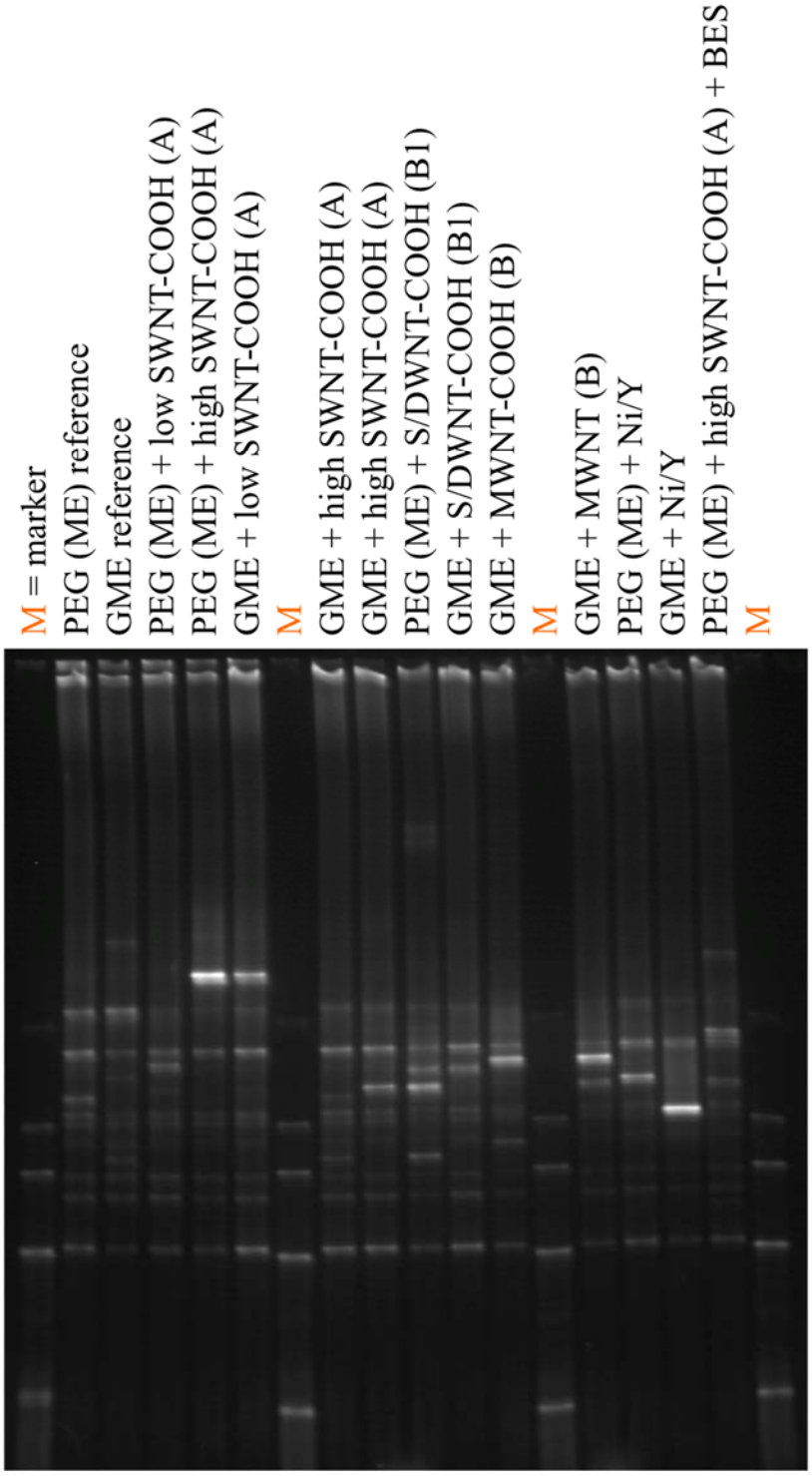

Figure 5.10. DGGE profiles for Eukarya from day 131, run on a 30-60% gradient. Two replicates of GME + high SWNT-COOH (A) are shown.

Sequence and species counts, along with diversity indices were calculated from 16s Illumina sequencing and Metagenomic data. These are shown in Table 5.4. The highest Shannon diversity index and evenness distributions were for the BES-treated sample (fed PEG (ME)) and also treated with SWNT-COOH (A). The lowest values were for the GME reference. Metals (Ni/Y) treatment for both substrate groups was associated with higher diversity index and slightly increased evenness. A smaller increase of diversity and evenness was seen with GME + SWNT-COOH (A) compared with the GME reference. For the PEG (ME) group, the SWNT-COOH (A) treated sample had the same evenness distribution and slightly lower diversity index.

Table 5.4. General sequence information and diversity indices for 16s DNA from sludge microcosms.

Treatment	Total sequences	Calculated Sequences	Fraction Classified	Species Identified	Shannon Diversity Index	Shannon Evenness
PEG (ME) reference	242,442	95,663	0.39	1,120	4.47	0.64
PEG (ME) + high SWNT-COOH (A)	203,010	77,179	0.38	1,031	4.41	0.64
PEG (ME) + high SWNT-COOH (A) + BES	221,503	90,013	0.41	1,187	4.74	0.67
PEG (ME) + Ni/Y	215,524	75,647	0.35	1,129	4.60	0.65
GME reference	241,966	115,010	0.48	1,055	4.26	0.61
GME + high SWNT-COOH (A)	273,405	118,579	0.43	1,155	4.41	0.63
GME + Ni/Y	182,656	79,955	0.44	1,045	4.46	0.64

At the Phylum level (Fig. 5.11, showing 1% or higher relative abundance), the most apparent differences were with BES treatment. The two substrate groups (GME vs. PEG (ME)) are also clearly different.

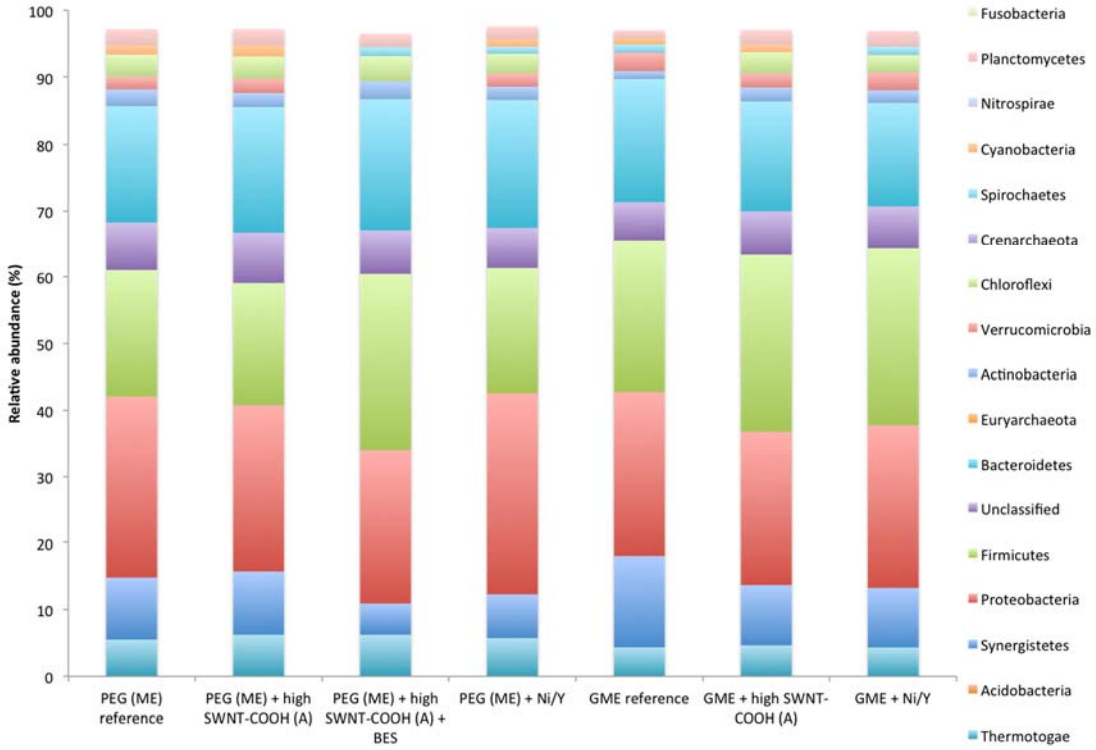

Figure 5.11. Comparison of 16s Phylum level at 1% relative abundance or higher. White space is pooled "other" groups at <1% relative abundance.

These differences between substrate groups can be examined with finer resolution by comparing samples at species level. The GME group is shown in Fig. 5.12. Any species at 1% relative abundance or higher in any of the seven samples from the sludge experiment is shown at its relative abundance in each sample in the figure. Even those sequences with n= 1-3 detected are visible as very thin colored lines. GME-fed samples with SWNT-COOH (A) and Ni/Y treatments appear similar to one another, and both different from the GME reference.

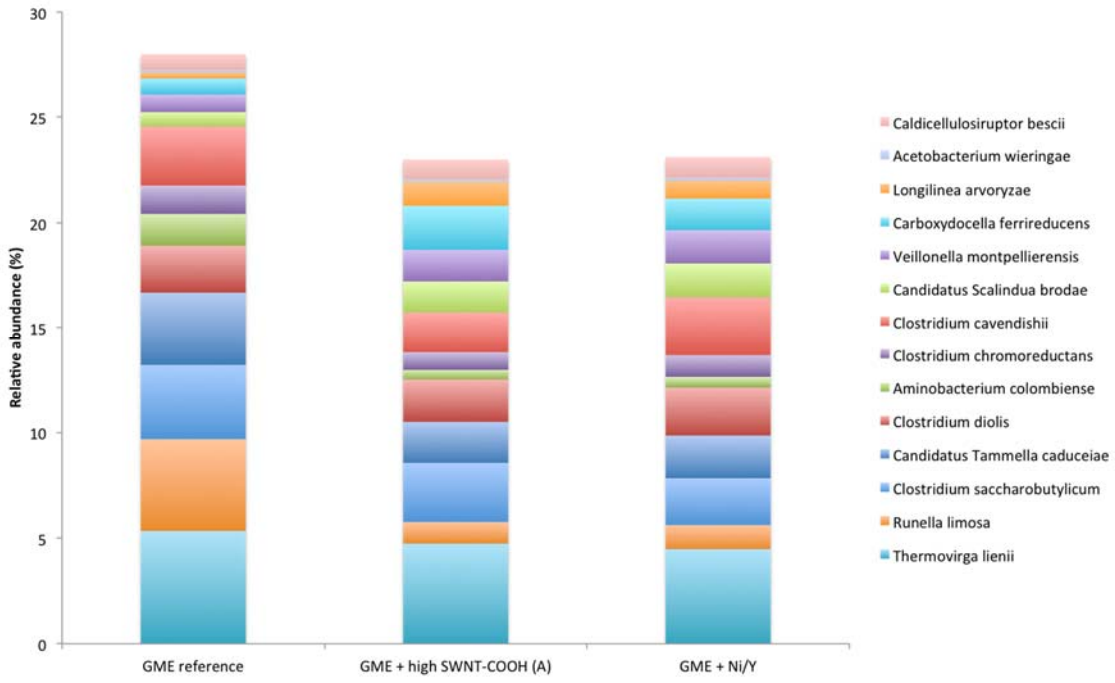

Figure 5.12. Species comparisons for GME microcosms. Relative abundances for all species with at least 1% relative abundance in one of these samples are shown.

Species comparison for the PEG (ME) group is shown in Fig. 5.13. The PEG (ME) + SWNT-COOH (A) treated sample is most similar to the reference sample. More differences visible in relative abundances are seen with BES and Ni/Y treatment, although the overall profile of species is the same.

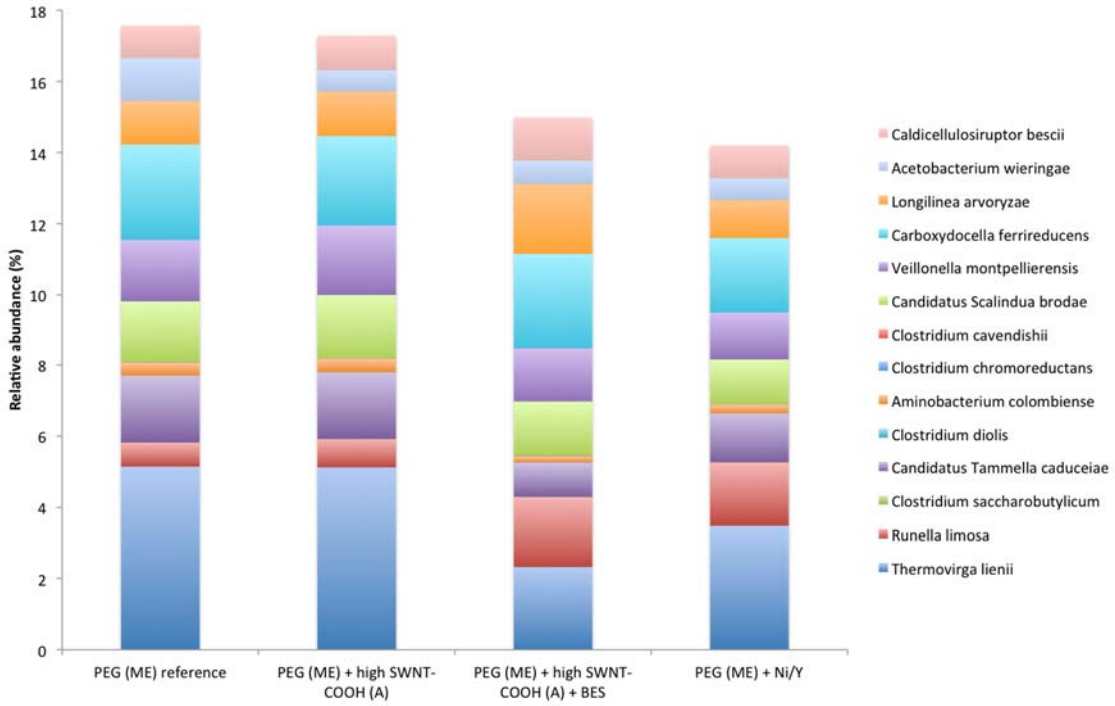

Figure 5.13. Species comparisons for PEG (ME) microcosms. Relative abundances for all species with at least 1% relative abundance in one of these samples are shown.

A comparison of methanogens at the genus level is shown for all seven samples in Fig. 5.14. No minimum relative abundance is indicated in this figure, as the total for methanogens is less than 0.7%. Overall relative abundance for this taxonomic group is highest in the PEG (ME) + Ni/Y sample, and lowest with BES treatment.

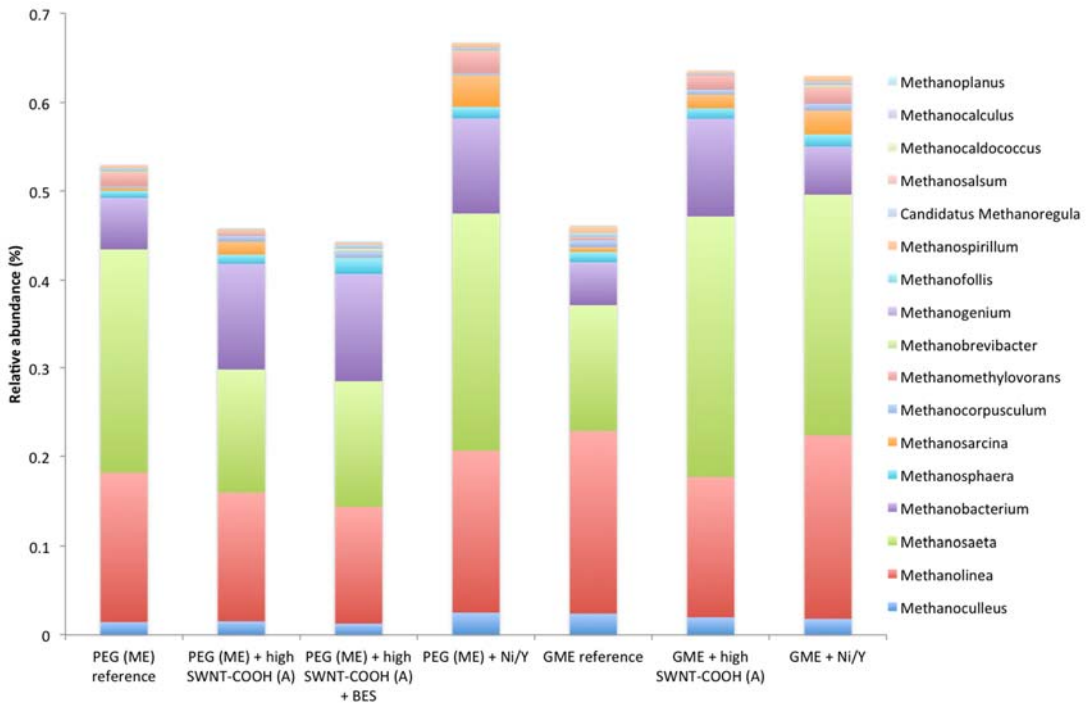

Figure 5.14. Relative abundances of methanogen genera.

Other members of Archaea are shown in Fig. 5.15. It appears that Thermoprotei relative abundances were slightly decreased with BES treatment and slightly enhanced with nanotube and metals treatment. Thaumarchaeota[105] were the least abundant Archaeal group detected, but they were present in all samples even with BES treatment. Their relative abundance decreased with all treatments in the PEG (ME) set, but increased in the GME substrate group. Their response follows the pattern seen with many other microbial groups in this study.

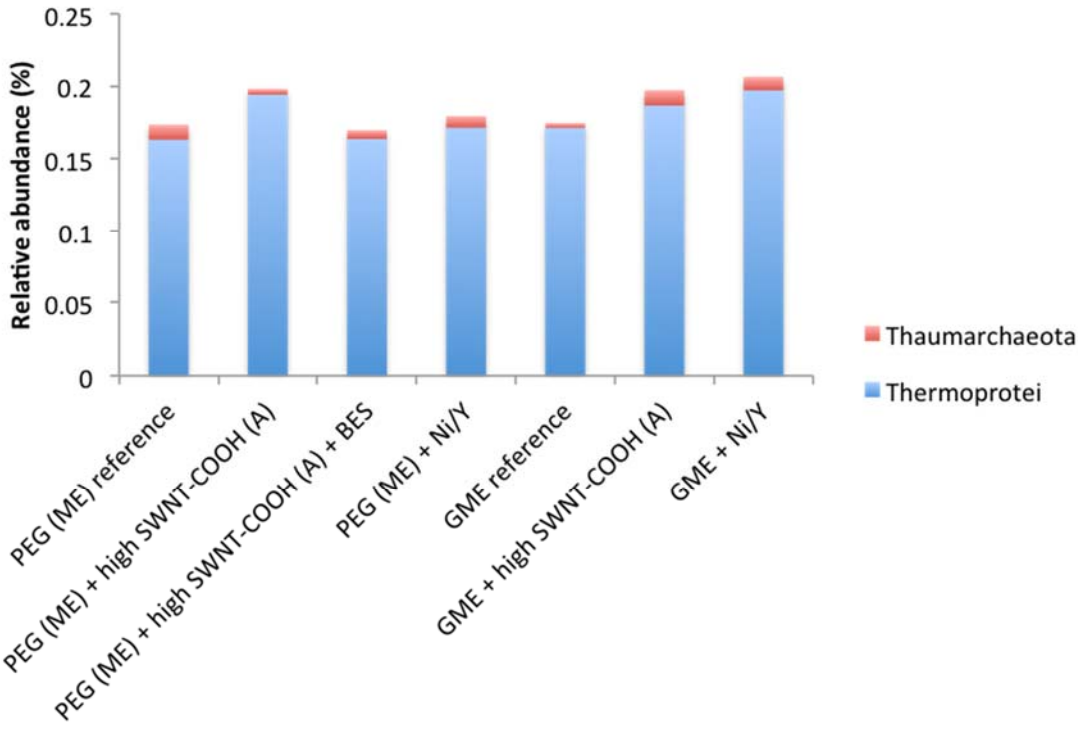

Figure 5.15. Phylum Crenarchaeota (Class Thermoprotei) and Thaumarchaeota, which recently became established as its own phylum[105].

Figure 5.16 shows relative abundance of taxonomic groups with evidence of involvement in direct interspecies electron transfer (DIET). Genus *Clostridium* is much higher in the GME substrate group. Its relative abundance increases with Ni/Y but remains unchanged with SWNT-COOH (A). Some increase is seen with both treatments and GME for family Anaerolinaceae, but the genus *Geobacter* decreases with both nanotube and metals treatment. As previously indicated, methanogens overall increased in the GME group, with *Methanosaeta* and *Methanosarcina* also shown here but with their relative abundances dwarfed by the high numbers for Bacteria.

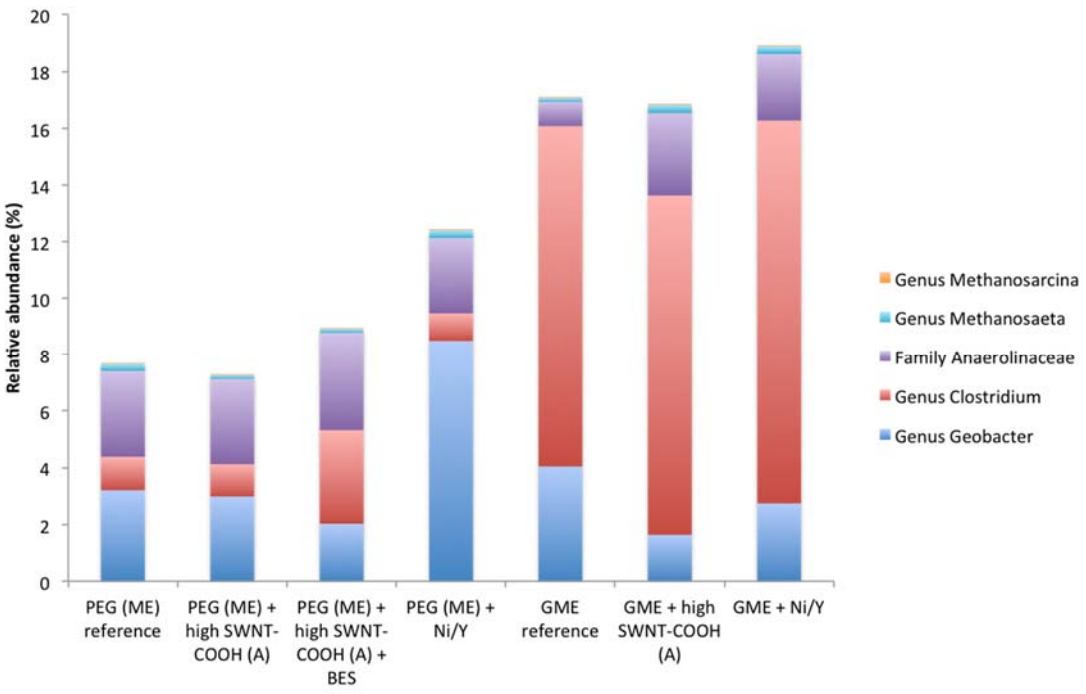

Figure 5.16. Relative abundances of Family *Anaerolinaceae* and various genera in the present digester sludge experiment. These groups show evidence of association with direct interspecies electron transfer (DIET), as found by other studies.

For the PEG (ME) group, *Geobacter* increases with metals treatment but decreases with nanotubes and BES. *Clostridium* is overall much lower than for the GME group, and highest with BES treatment. *Anaerolinaceae* decreases slightly with metals and is essentially the same as the substrate reference for the other two treatments. *Methanosaeta* and *Methanosarcina* both increase with metals treatment. With nanotubes and PEG (ME), *Methanosarcina* increase, but with a corresponding decrease in *Methanosaeta*.

5.5 ICP-MS Measurement of Nickel and Yttrium

Both solid and aqueous phase concentrations of nickel and yttrium from microcosm subsamples are shown in Table 5.5. Samples were analyzed after all nanotube or metals additions had been completed, as reflected by the final concentrations indicated with the treatments. Expected background concentrations in reference microcosms are mean values reported elsewhere for sewage sludge[106]

Table 5.5. Metals concentrations in replicate samples. Microcosms treated with SWNT-COOH from Manufacturer A are compared with untreated reference samples. Deviations from expected concentrations may reflect heterogeneous distribution of nanotubes and metals in the solid phase of microcosms. Ratio of Ni/Y in nanotube-treated samples is consistent with EDX results. Expected concentrations are based on one to three additions of nanotubes or metals and resulting final concentrations in the microcosms. Bdl = below detection limit

Sample	Nickel Solid phase (ppm)	Nickel Aqueous phase (ppm)	Ytrrium Solid phase (ppm)	Yttrium Aqueous phase (ppm)	Expected Nickel solid phase (ppm)	Expected Yttrium solid phase (ppm)	Nickel/Yttrium ratio Solid phase
SWNT-COOH (A) 1,700 mg/kg	10.7	0.0194	1.33	bdl	72	10	8.05
SWNT-COOH (A) 34,000 mg/kg	85	0.0203	13	0.000428	1440	200	6.54
SWNT-COOH (A) 35,700 mg/kg	298	0.0204	45.8	0.000619	1512	210	6.51
SWNT-COOH (A) 85,000 mg/kg	173	0.0242	26	0.000785	3,650	500	6.65
SWNT-COOH (A) 85,000 mg/kg	74	0.027	11	0.0011	3,650	500	6.73
Ni/Y reference 30,000 mg/kg	1580	1	527	0.027	25,500	4,500	3.00
Ni/Y reference 30,000 mg/kg	611	4.6	67	0.025	25,500	4,500	9.12
Ni/Y reference 30,000 mg/kg	1660	0.74	183	0.0013	25,500	4,500	9.07
Untreated reference	3.5	0.018	0.3	Bdl	20*	11*	11.7
Untreated reference	2.8	0.012	0.27	Bdl	20*	11*	10.4

*Mean values in sewage sludge reported by Swedish EPA, 2001.

5.6 Discussion

Overall results of this study show that none of the nanotube or metal treatments inhibited microbial community function or shifted community structure to anywhere near the extent of a known methanogen inhibitor such as BES. This chemical provided a useful benchmark for toxicity by completely inhibiting community function. Surprisingly, the effect on community structure was relatively subtle, although other researchers[107] have recently made a similar observation with community profiles from a short-term BES experiment. This group found increased activity and relative abundance of some bacterial groups (e.g. cellulose degraders and others more typical of a rumen environment) with corresponding inhibition of especially acetoclastic methanogens and syntrophic bacteria. This result is consistent with the increased diversity seen with BES treatment in this long-term BMP assay. Certainly, BES exerted the strongest effect on community structure of any treatment shown here. Future studies would include 18s sequencing of Eukarya in addition to 16s Bacteria and Archaea, as ciliate protozoa and methanogens have a functionally important symbiotic relationship in anaerobic ecosystems[108].

For the PEG (ME) substrate group, a small, generally non-significant decrease in gas production resulted for microcosms treated with the higher concentration of SWNT-COOH (A) and also with Ni/Y ($p < 0.05$ for a few days). This trend did not change for the rest of the experiment even with one more addition of nanotubes or metals and an additional feeding of PEG. For the GME group, a significant increase in gas production occurred for GME + SWNT-COOH (A) microcosms, as well as those with GME and the

Ni/Y mixture. Other nanotube treatments were associated with either no effect or increases in gas production compared with the GME reference that were significant for shorter periods of time. By day 730, the end of the BMP assay, the average gas volumes were not significantly different. Therefore, these increases reflect an acceleration of gas production rather than an absolute increase. A similar but more pronounced phenomenon was also seen in a microcosm study with rumen inoculum, as described in Chapter 4.

Important differences between the digester sludge experiment and the rumen experiment were as follows. First, hydrogenotrophic methanogenesis is predominant in the rumen, whereas acetoclastic methanogenesis is dominant in anaerobic sludge digestion. Some methanogen groups of both types, many with metabolic versatility, can be detected in both anaerobic ecosystems. However, the metagenomic data from both studies confirm the relative abundance of different taxonomic groups depending on which methanogenesis pathway takes precedence.

Second, the concentration of nanotubes used in the rumen experiment was overall higher than in the digester sludge assay. Only the highest concentration of SWNT-COOH (A) after three total nanotube additions at 85,000 mg/kg was in the same range as concentrations used with rumen microcosms. Third, the sludge microcosms were fed periodically with either GME or PEG (ME). Rumen microcosms started with a defined wet mass of endogenous rumen contents and were not given any other substrate throughout the experiment.

In the sludge experiment, the substrate to which the microbial community becomes acclimated and establishes methanogenesis clearly affects community structure. Differences between the two substrate groups in gas production in response to treatments were relatively subtle. However, these are reflected somewhat in DGGE profiles and to an even greater extent with Illumina sequencing and metagenomic analysis.

The effect of BES on methanogen relative abundance is clearly detectable by DGGE, as shown in the Archaea profile of Fig. 9. However, differences between replicates of other samples make the overall DGGE data set difficult to interpret. In some cases, even a very intense band such as the one that is absent in the BES-treated sample, would be present in one or more replicates of the same treatment but not in the others. Crenarchaeota, in particular Class Thermoprotei, relative abundance also decreased with BES exposure.

Illumina sequencing was done with samples taken from relatively early in the experiment, with only the nanotube and metal additions from T0. Differences between community profiles are more easily appreciated at the species level than comparisons of different phyla, with the possible exception of BES treatment. In general, for both substrate groups, metals affected community structure more than nanotube treatment that included residual metals. This is consistent with the higher concentration (about an order of magnitude) of the metals treatment compared with the concentration of residual metal catalyst in the nanotube treatment.

These data indicate that any effect of nanotubes seen is enhanced by an effect of residual metals. For anaerobic digestion, both nickel and cobalt can be either beneficial or highly inhibitory depending on the concentration, at least in part because they are important components of different enzymes involved in methanogenesis[109]. Given that both metals are present in different forms of carbon nanotubes as residual catalyst, this interaction cannot be ignored. For this study, yttrium was also a factor. A paucity of data exists on the effect of this element on anaerobic microorganisms. However, lanthanum, another rare earth element, has been shown to decrease relative abundance of methanogens and associated protozoa in cow rumen[110]. A decrease in methane production was reported in the same study with an increase in total gas production. These elements are of interest to either optimize anaerobic wastewater treatment in the first case or secondly, to manipulate the rumen ecosystem for control of livestock digestion and resulting greenhouse gas emissions.

The results of this digester sludge experiment and the rumen nanomaterial experiment, along with other recent studies, indicate at least four potential factors involved in a synergistic effect of carbon nanotubes on anaerobic microbial communities. First, a physical scaffolding effect of nanotubes may augment biofilm formation in granular sludge and rumen. Second, evidence exists that direct interspecies electron transfer (DIET) may be facilitated by nanotubes and other conductive carbon materials[70,94, 111]. Thirdly, an additional effect of, essentially, advanced oxidation of biological materials may occur as a result of surface catalytic ROS production by carbon nanotubes. This hypothesis is supported by visual evidence of de-colorization and disappearance of some

likely recalcitrant material in the rumen nanomaterial study. This de-colorization effect was seen to a lesser extent in the sludge experiment described here. For the suspended particulate matter, the possibility of sorption to the nanotubes cannot be ruled out. As with the rumen experiment, the effect in sludge microcosms is more visible with longer nanotubes from Manufacturer B. The concentration of nanotubes used here was lower than in either the rumen assay or the nanotube experiment with granular sludge previously cited. The latter experiment[67] showed increased excretion of extracellular polymeric substances (EPS) in response to nanotubes, which would protect microorganisms from oxidation.

Finally, this study with digester sludge highlights the importance of residual metals found in commercial nanotube preparations. Even under conditions in which toxicity is not observed and bioavailability is assumed to be low, metals may contribute a great deal to any enhancing effects on anaerobic microbial communities. These properties could be better understood for development of improved anaerobic digestion technologies, to degrade resistant waste materials and produce sustainable energy. However, the effect of these metals continues to present an additional variable of concern in the event of a large-scale release of carbon nanotubes to the environment. De-stabilization and inhibition of microbial ecosystems in response to metals would likely occur in a concentration-dependent manner.

CHAPTER 6. ANAEROBIC MICROBIAL COMMUNITY STRUCTURE AND FUNCTION CHANGES IN RESPONSE TO NONYLPHENOL ETHOXYLATE (NPEO) SURFACTANT TERGITOL® NP-9 AND ITS 4-NONYLPHENOL (4-NP) MOIETY IN WETLAND SEDIMENT

6.1 Abstract

Alkylphenol ethoxylate surfactants, specifically nonylphenol ethoxylate (NPEOx) detergents are widely used in industrial, pharmaceutical, and personal care products. The alkylphenol moiety is known to persist in sediments, with toxic effects on aquatic life and recognized endocrine-disrupting properties. Their ethoxylate chains are readily biodegradable, increasing potential for accumulation of relatively insoluble alkylphenols in the environment. The effect of Tergitol® NP-9 on an anaerobic microbial community from freshwater wetland sediment was investigated. Community function was assessed using a Biomethane potential (BMP) assay with microcosm headspace analysis. Tergitol® NP-9 increased gas production compared with reference samples in a BMP assay that lasted 473 days, after a brief period of inhibition. However, gas production was only about 12% of the expected theoretical value if the ethoxylate chain was completely biodegraded at 60 mM Tergitol® NP-9. A BMP assay lasting 35 days confirmed the short-term inhibitory effect of this surfactant on gas production, with a measured decrease in the fraction of headspace methane. Treatment with 4-NP, the Tergitol® NP-9 daughter product after removal of the ethoxylate chain, at 1.1 ppm was associated with

mild inhibition of gas production. Microbial community structure was characterized with polymerase chain reaction and denaturing gradient gel electrophoresis, and also by 16s Illumina sequencing and metagenomics. Treatment with Tergitol® NP-9 in the long-term experiment resulted in substantial enrichment of *Geothrix fermentans* and *Desulfovibrio burkinensis*. An increase in relative abundance of genus *Methanospirillum* was also observed in the same experiment. Relatively subtle community shifts occurred with phenol and also with 4-NP treatment, but some important differences were noted especially considering the low concentrations used in the experiment. Within three days of a second BMP assay, *Tolumonas auensis* and *Prevotella paludivivens* increased significantly with Tergitol® NP-9 treatment. These results highlight the need for further research into the mechanisms of effects of anthropogenic chemicals, in particular those that reduce microbial community diversity. Moreover, they provide further evidence that those chemicals that completely biodegrade anaerobically as well as aerobically would be an environmentally preferable alternative.

6.2 Introduction

Nonylphenol ethoxylate (NPEOx) detergents are widely used as industrial surfactants and also in pharmaceutical and personal care products[112]. However, a great deal of evidence exists that biodegradation products of these compounds are toxic and persistent in the environment. The U.S. Environmental Protection Agency has proposed a Significant New Use Rule[113] for 15 NPE and NP compounds, and this class of chemicals has been banned in the EU[114]. The basic structure of this class of compounds is shown in Fig. 6.1.

Aqueous solubility of the nonylphenol moiety (NP) has been reported to be quite low at approximately 5 mg/L[115, 116]. In general, experimental studies have found a linear relationship between increasing ethoxylate chain length and solubility.

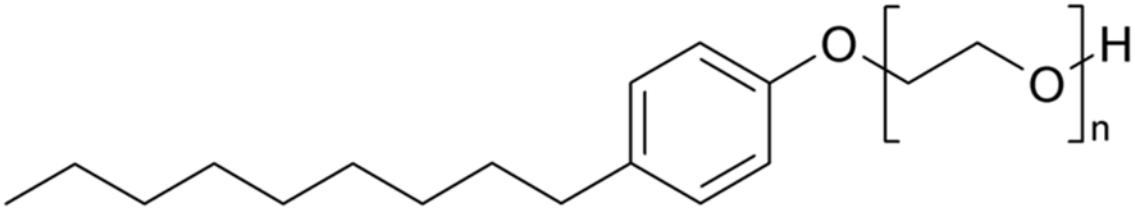

Figure 6.1. Structure of a Nonylphenol ethoxylate detergent. Source: Nonylphenol and Nonylphenol Ethoxylates. Lead author: Katarina Lah. Topic Editor: Maria M. Williams. Updated by: Maria Mergel. Licensed under Creative Commons. Accessed July 27, 2016. http://www.toxipedia.org/display/toxipedia/Nonylphenol+and+Nonylphenol+Ethoxylates

Biodegradation of NPEOx occurs both aerobically and anaerobically. A few different *Pseudomonas* and *Xanthomonas* spp. from activated sludge have been identified as NPEO degraders[117]. It is generally agreed that NPEO(x) degrade anaerobically to nonylphenol, leading to accumulation of NP in sludge[118] and sediments[119]. Anaerobic biodegradation of NP has been reported in river sediment samples, with an intermediate rate of transformation seen under methanogenic conditions (lower than sulfate reducing and higher than nitrate reducing)[120]. However, simple disappearance of a compound is not sufficient to establish that biodegradation occurs, and thus far, NP metabolites have not been measured in anaerobic systems[121]. The prevailing scientific view is that NPs are recalcitrant under strictly methanogenic conditions, although some new evidence supports previous assertions that biodegradation occurs with sulfate and nitrate respiration[122].

Ejlertsson et al. found that the shorter chain nonylphenol ethoxylates (a mixture of NPEO 1-2) were further degraded to NP in anaerobic sludge microcosms.[123] They observed temporary inhibition of methanogenesis at 60 and 308 mg/L. Another study found that nonylphenol diethoxylate (NPEO 2) degraded further to NPEO 1 and NP in anaerobic microcosms, but observed no further degradation attacking the aromatic ring[124]. Therefore, NP concentrations increased with disappearance of NPEO2. Anaerobic gas production was not inhibited at either 1 or 30 mg/L NPEO 2.

Gejlsbjerg et al.[125] found an EC50 of 754 mg/kg (soil/sludge mixture dry wt.) for nonylphenol with respect to CH_4 production in soil amended with land-applied sewage sludge. In the same study, it was found that anaerobic CO_2 production was less sensitive with only 20% inhibition at the highest concentration. This suggests that methanogenic function is more affected than that of fermenting bacteria, since both groups produce CO_2.

Most of these studies reporting relatively high inhibitory concentrations of NP for microorganisms compared with generally ppb levels for endocrine disruption and toxicity to model aquatic organisms[114]. However, the vast majority of concentrations tested have been done with sewage sludge, which is a very different environment than sediment. Theoretically, it is possible that lower concentrations would also affect microorganisms under the right conditions, possibly through analogous endocrine-disrupting mechanisms. That mammalian polypeptide and steroid hormones have been found in microorganisms, in addition to the well-known, likely ubiquitous presence of insulin[126], makes this an important consideration. A wide range of concentrations for nonylphenol in sediments

has been reported, summarized by Soares et al. (<0.01-3,000 mg/kg sediment), with a frequently reported value of about 1 mg/kg[114].

Few studies have addressed the effect of nonylphenol ethoxylate surfactants and NP moiety on microbial community composition. A few studies have examined the effect of nonylphenol degradation on community structure using terminal restriction fragment length polymorphism (TRFLP) analysis[127] or next-generation Illumina sequencing[122, 128]. The TRFLP study found an overall reduction in diversity with greater response by ammonia-oxidizing Archaea than by ammonia-oxidizing Bacteria. Changes in functional gene relative abundance were found to occur in a concentration dependent manner with nonylphenol in aerobic river sediment[128]. With regard to anaerobic degradation, it has been found that bacterial diversity increased with nitrate-respiring degradation of nonylphenol, while diversity was slightly reduced under sulfate-respiring conditions[122].

Effect of NPEO(x) and NP on microbial community structure has not only environmental relevance but is also pertinent to human health considerations for exposure to these compounds through normal use. Schreiber et al.[129] found an increase in anaerobic gram-negative rods in vaginal microflora associated with higher dose and frequent use of spermicides containing nonoxynol-9. They also cited conflicting evidence related to nonoxynol-9 use and risk of STIs. This compound, also known as Tergitol® NP-9, is a useful model NPEO compound due to its prevalence in consumer products.

To assess the impact of Tergitol® NP-9 and its chemical constituents on anaerobic sediment community function, a Biomethane potential assay was used, along with microcosm headspace measurements of methane. Effect of the surfactant as well as 4-NP, phenol, and PEG-400 was studied. Polymerase chain reaction with denaturing gradient gel electrophoresis was used to screen for effects of any of these treatments on microbial community structure in each of the three domains Bacteria, Archaea, and Eukarya. Next-generation sequencing of the 16s rRNA gene with the Illumina platform and metagenomics were used for in-depth analysis of community structure for Bacteria and Archaea.

As a result of substantial community shifts seen with Tergitol® NP-9 treatment in preliminary DGGE data from the first experiment (Experiment A), a second microcosm study (Experiment B) was initiated. The first objective of this follow-up experiment was to assess the effect of Tergitol® NP-9 on the DNA extraction procedure by taking both treated and untreated samples at time-zero. The hypothesis that this nonionic surfactant would shift community profiles through selective lysis of cell membranes of certain microbial groups was overall not supported by PCR-DGGE or next-generation sequencing data. The second objective of this assay was to detect how early the community shifts would start after Tergitol® NP-9 exposure and with which taxonomic groups.

6.3 Experimental Design

For each of two experiments, sediment was collected from Celery Bog nature area in West Lafayette, IN. Twigs, roots, and other large materials were removed by hand. For Experiment A, approximately 20 g of sediment (wet wt.) was transferred to 50 ml glass serum bottles (Wheaton), along with phosphate buffer (pH ~7.2) at a working volume of 35 ml to allow some remaining headspace in the bottles. Three replicate microcosms were air-dried for weeks and the average sediment dry weight was found to be 7 g. This measurement showing that wet sediment was 65% water was used to calculate sediment dry weight for Experiment B. Two replicates for each treatment were used, for a total of twelve experimental microcosms. Two replicate microcosms had no substrate or treatment added to serve as a reference of baseline function. The purpose of this set was to account for background gas production in the sediment during the BMP assay. One pair of microcosms received only glucose, methanol, and ethanol (GME) as a positive reference for gas production. All other microcosms (4-pairs) received GME as substrate in addition to the treatment. Treatments for Experiment A and their concentrations are listed in Table 6.1 (PEG-400, phenol, 4-nonylphenol, and Tergitol® NP-9 all from Sigma-Aldrich). All treatments for Experiment A were applied once at the beginning of the experiment and repeated at day 312.

About four years into Experiment A, after the BMP assay was finished at 473 days, one of the two Tergitol® NP-9 + GME microcosms burst. Therefore, only one bottle form this treatment remained for DNA subsampling.

Table 6.1. Design for Sediment Experiment A. Two replicates were used for each set. All treatments were added a second time at day 312. All microcosms were also fed both times with a mixture of glucose (8.6 mM), methanol (28.2 mM), and ethanol (14.7 mM), abbreviated GME throughout the text. A GME reference set and an untreated reference set were also included (two replicates each).

Treatment	Tergitol® NP-9 moiety equivalents	Concentration
PEG 400	0.065	3.92 mM
Phenol	0.15	9.1 mM
4-nonylphenol	1.6×10^{-5}	1.1 µg/g*
Tergitol® NP-9	1	60 mM

*This concentration is reported on a mass basis due to low solubility in water.

For Experiment B, 100 ml glass serum bottles (Wheaton) were used. Sediment wet weight was ~ 32 g, with a working volume of 85 ml phosphate buffer. Treatment is shown in Table 6.2. Only the effect of Tergitol® NP-9 was assessed in this experiment, at about half the concentration used in Experiment A. Seven replicates of GME reference microcosms were used, along with 21 replicates with Tergitol® NP-9 + GME. In Experiment B, some pH adjustment was necessary in the first 20 days of the experiment. This was accomplished with small volumes of 100x phosphate buffer or sodium

carbonate ($NaHCO_3$). Each time point that a microcosm was subsampled for DNA extraction, it was sacrificed and no longer included on gas production plots shown in the Results section.

Table 6.2. Design for Sediment Experiment B. Seven replicates were used for the GME reference set and 21 replicates for the Tergitol NP-9 treated set. Microcosms were sacrificed for DNA isolation at each of four time points including time-zero. Glucose was 7.1 mM, methanol was 21.6 mM, and ethanol was 14.4 mM.

Treatment	Tergitol® NP-9 Concentration
GME reference	n/a
GME + Tergitol® NP-9	25.3 mM

6.4 Results

Treatment with Tergitol® NP-9 significantly affects anaerobic gas production and headspace methane measurement, with early inhibition and then later increased average cumulative gas production compared with the GME reference. However, the gas production was much less than the expected value if biotransformation of all the

ethoxylate chains on the surfactant molecule were biotransformed. The low, but environmentally relevant concentration of 4-NP could not contribute measurably to gas formation. This treatment did show an inhibitory effect with less gas production than the GME reference, even though it was not statistically significant. Phenol and PEG-400 did contribute to gas production as substrates, although at less than the expected value.

Tergitol® NP-9 very substantially shifts the microbial community with a different effect seen over time. Significant enrichment of just a few species occurred with remarkably increased relative abundance compared with the reference samples. Less pronounced community shifts were also seen with phenol and with 4-NP treatment.

6.4.1 Biomethane Potential (BMP) Assay

6.4.1.1 Experiment A

Average cumulative gas production over time for Experiment A is shown for two replicates in each set (Fig. 6.2). Feeding with GME and all treatments were repeated on day 312. A duplicate set of untreated microcosms (data not shown) had average background gas production of 17 ml at day 312 and 21 ml at day 473. Figure 1 shows that 4-nonylphenol microcosms had less average gas production than the GME reference. The concentration of 4-nonylphenol was too low to have contributed more than negligible (12 µl) theoretical gas volume if it were completely biodegraded. This compound appeared to inhibit gas production compared with the GME reference even though it was not

statistically significant ($p < 0.05$). As expected, gas production was increased with phenol, PEG-400, and Tergitol® NP-9 additions compared with the GME reference.

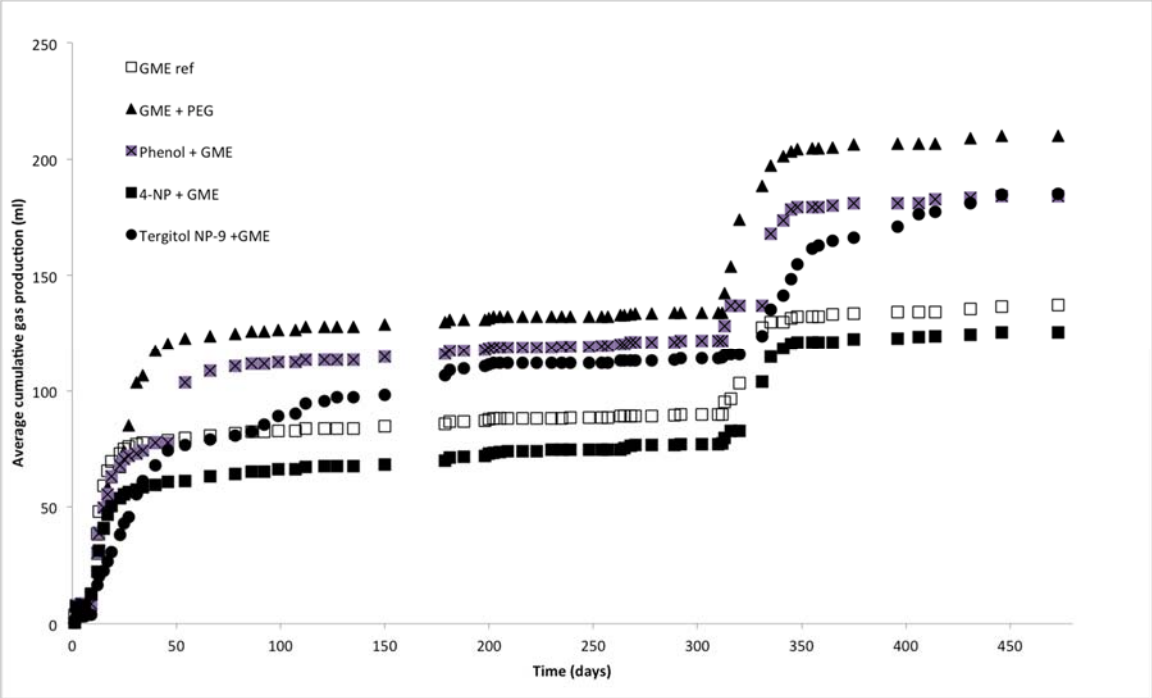

Fig. 6.2. Average cumulative gas production over time for Experiment A. At second feeding on day 312, all treatments were added again at same concentrations. All samples for genomic DNA isolation were collected after this phase of the experiment ended. For all treatments and reference samples, n=2. Error bars are omitted for clarity. Average % error throughout this experiment was 3.9% for the GME reference, 6.9% for the PEG-400 + GME treatment, 3.4% for phenol + GME, 32.8% for 4-nonylphenol + GME, and 8.7% for Tergitol® NP-9 + GME.

Figure 6.3 shows average cumulative gas production normalized to the GME reference for Experiment A, at day 34 and day 312. An asterix (*) indicates the difference is significant at $p < 0.05$. For the GME reference, the average cumulative gas volume at day 312 was 78% of the theoretical maximum. Expected values for the other treatments, if

used as substrate, were normalized to the GME reference. Average background gas production (not shown) in the untreated reference set was subtracted from the totals for day 312. Phenol treatment + GME had 91% of expected gas formation if phenol were completely biodegraded. PEG-400 + GME had 93% of the expected value. 4-nonylphenol + GME microcosms had the same expected average value as the GME reference, given that the concentration of 4-nonylphenol was too low to contribute appreciably to gas production if it were completely biodegraded. However, these microcosms reached only 76% of the expected gas production. Tergitol® NP-9 + GME had only 12.3% of the expected gas production even though the average volume was higher than the GME reference set. A relatively high concentration of Tergitol® NP-9 was used, and the expected gas production assumes that only the ethoxylate chain moiety would be biodegraded.

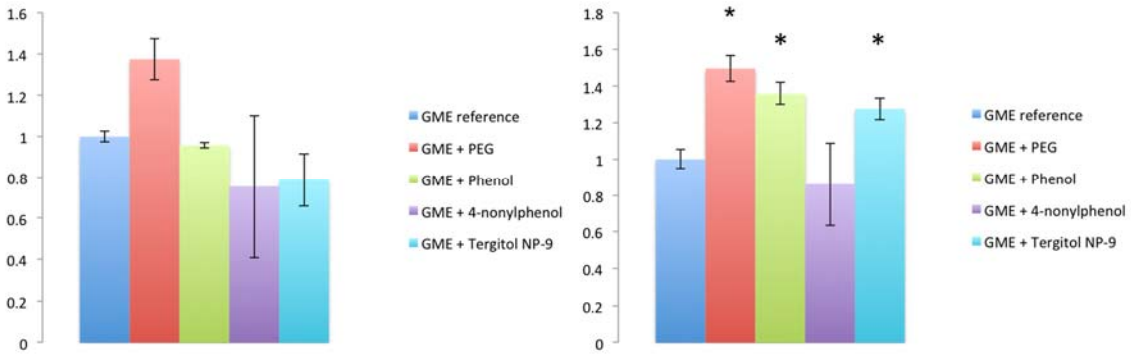

Fig. 6.3. Average cumulative gas production normalized to the GME substrate reference for day 34 (left) and day 312 (right).

6.4.1.2 Experiment B

Average cumulative gas production over time is shown in Fig. 6.4 for Experiment B, which lasted for 35 days. Gas production in the Tergitol® NP-9 treated microcosms started higher than the GME reference. This difference is significant ($p < 0.05$), although small. At day 21, gas production shifted as the GME reference set increased with some apparent inhibition in the Tergitol® NP-9 microcosms. Slightly less than half the concentration of this surfactant was used in Experiment B as in Experiment A.

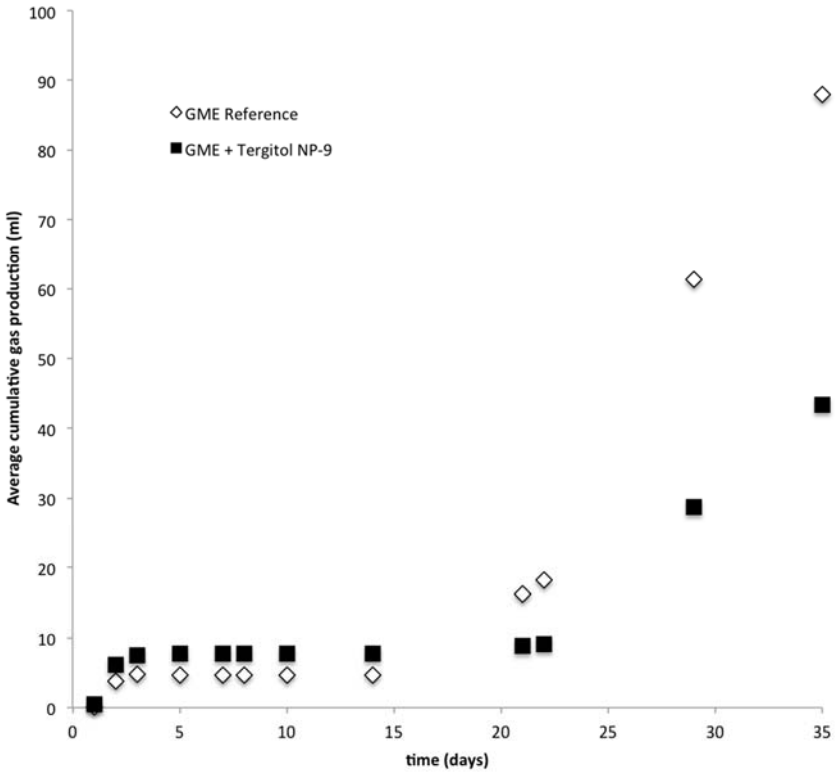

Fig. 6.4. Average cumulative gas production over time for Experiment B. Differences are significant ($p < 0.05$) for all 35 days, with Tergitol® NP-9 treated samples having higher gas production than the GME reference set until day 21, when the GME reference gas production increased. For the GME reference set, n=7. For the Tergitol® treated set, n=21. Error bars are omitted for clarity. Average % error for the GME reference set was 32.6%, and 33.5% for the Tergitol® treated set.

Differences in gas production are significant ($p < 0.05$) throughout Experiment B. Average cumulative gas production normalized to the GME reference at day 35 is shown in Fig. 6.5.

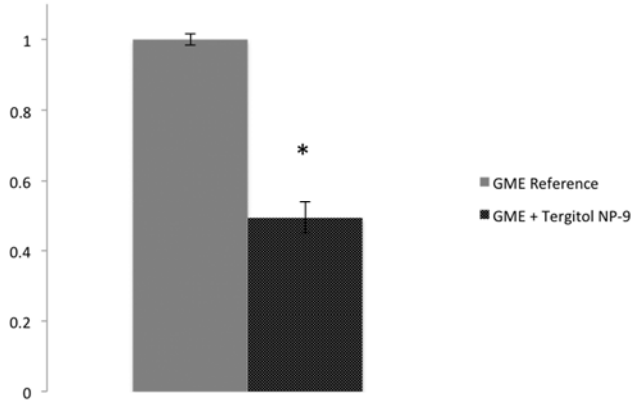

Fig. 6.5. Average cumulative gas production at 35 days normalized to the GME substrate reference for Experiment B. Microcosms treated with Tergitol® NP-9 have significantly lower ($p < 0.05$) gas production than GME reference microcosms.

A representative microcosm, exhibiting substantial coloration of the buffer medium from Experiment B is shown in Fig. 6.6.

Fig. 6.6. A Tergitol® NP-9 treated microcosm from Experiment B.

6.4.2 Microcosm Headspace Analysis

Results of microcosm headspace analysis for Experiment B are shown in Fig. 6.7. For both sampling days, methane is decreased compared with the GME reference set. This difference is significant at day 28.

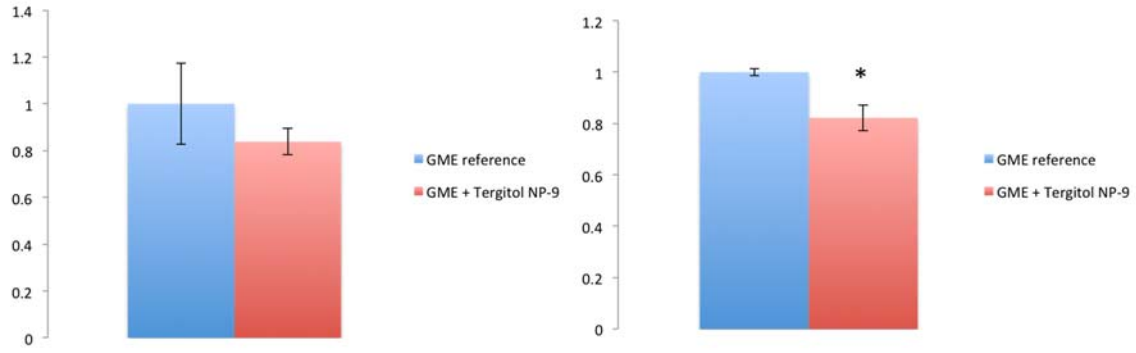

Fig. 6.7. Microcosm headspace analysis for Experiment B on day 21 (left) and day 28 (right). Methane is normalized to the GME reference, and is the average of three replicate measurements on each day. Tergitol® NP-9 microcosms have significantly lower methane ($p < 0.05$) than the GME reference set on day 28.

6.4.3 Polymerase Chain Reaction and Denaturing Gradient Gel Electrophoresis

Differences in microbial community structure are shown in the 16s Bacteria profiles early in Experiment B (Fig. 6.8), comparing GME reference and Tergitol® NP-9 treated samples at T0 and T=3 days. Little to no effect of the surfactant is seen on T0 community profiles, although an artifact of Tergitol® treatment in the DNA extraction procedure is theoretically possible. Bacteria community profiles in Experiment A (not shown) showed differences in just a few bands for all treatments except Tergitol® NP-9. The surfactant-treated sample had almost no resemblance in band pattern with the duplicate GME reference samples. The Tergitol®-treated sample bands had higher G+C content and ran off the 40-55% gradient used to best visualize band separation in the other samples.

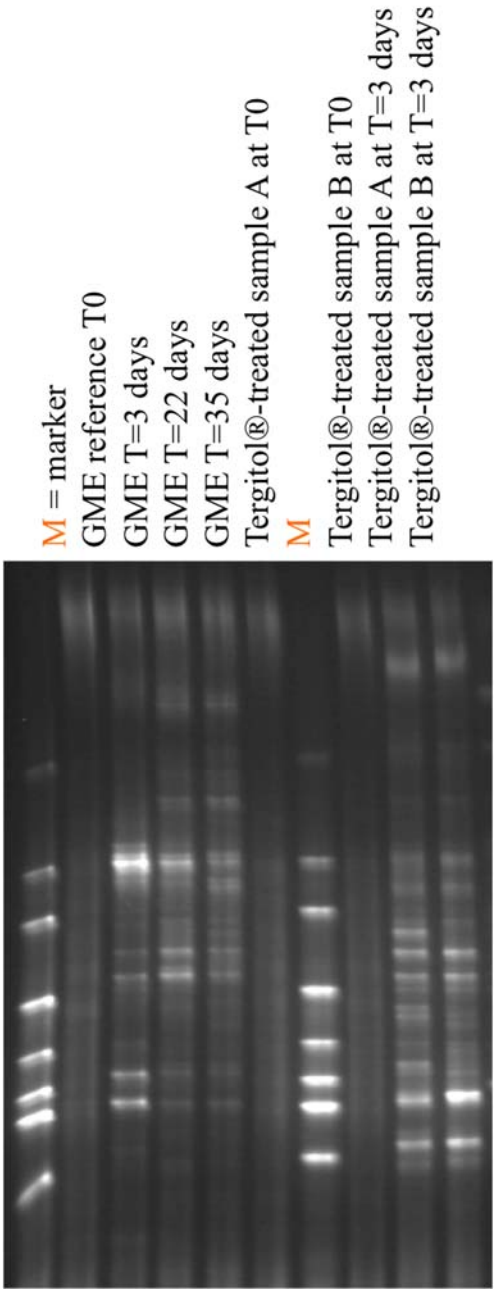

Figure 6.8. Bacteria 16s profile for Experiment B on a 35-65% gradient. Left to right: marker, GME reference T0, GME T=3 days, GME T=22 days, GME T=35 days, Tergitol®-treated sample A at T0, marker, Tergitol®-treated sample B at T0, Tergitol®-treated samples A and B at T=3 days. Marked differences over time are seen in all four GME reference samples. Profiles appear similar in T0 sediment, with little to no effect of Tergitol® addition before subsampling for DNA extraction. Differences are visible with shifts in multiple bands between the GME reference at T=3 days and the duplicate Tergitol®-treated samples.

Archaeal 16s profiles for both Experiment A and B are shown in Fig. 6.9. Community shifts are seen with Tergitol® NP-9 treatment over a period of a few years as well as after just 3 days. Subtler shifts are seen with other treatments in Experiment A. Clearly, differences in Archaea community composition occur over time in these microcosms, with greater prevalence of high G+C sequences found in the long-term BMP assay.

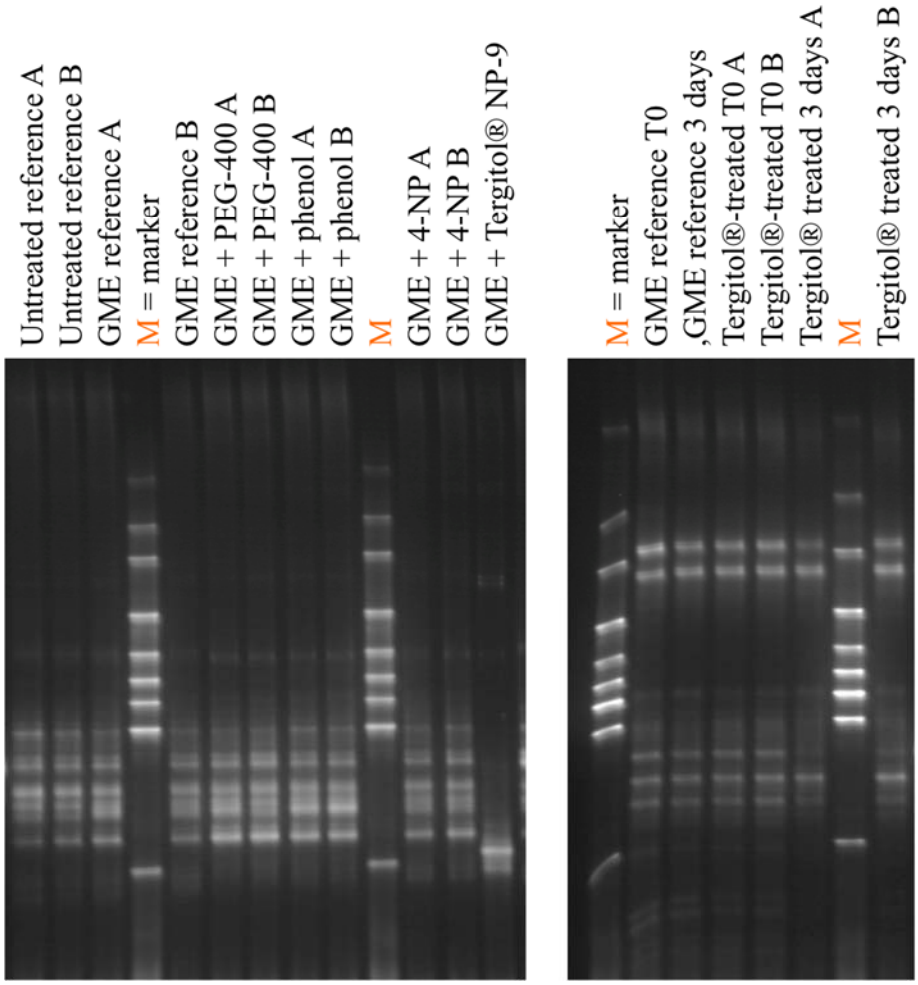

Figure 6.9. At left: Sediment Archaea profiles for Experiment A, T2, on a 40-70% gradient. Duplicate samples are shown except for Tergitol® treatment. Left to right: untreated reference A, untreated reference B, GME reference A, marker, GME reference B, GME + PEG-400 A, GME + PEG-400 B, GME + phenol A, GME + phenol B, marker, GME + 4-NP A, GME + 4-NP B, and GME + Tergitol® NP-9 (from a single microcosm). There appears to be enrichment of a single band with phenol, and loss of a slightly higher G+C band with 4-NP, but the Tergitol® NP-9 sample shows a remarkable shift in the Archaeal community with one dominant band that does not appear in any other sample. At right. 40-70% Archaeal profiles for T0 and T = 3 days in Experiment B. Left to right: marker, GME reference T0, GME reference T = 3 days, Tergitol®-treated replicates A and B at T0, Tergitol® treated replicate A and T=3 days, marker, and Tergitol® treated replicate B at T=3 days. At least two Archaeal bands are absent or have greatly reduced intensity in the treated samples after 3 days.

Sediment 18s Eukarya profiles for all time points in Experiment B are shown in Fig. 6.10. Minor differences between GME reference and Tergitol® treated profiles are visible even at T0. However, a prominent band appears only in treated samples after 3 days that is slightly lower on the gel than any bands in the T0 profiles, indicating its higher G+C content. It is difficult to tell if this band is lost in the ~ 2.5 weeks intervening between this sampling point and the next, or if it is merely reduced in intensity. Results for Experiment A are not shown for the Eukarya domain because differences between duplicate samples were so prevalent that it was impossible to determine the effect of any treatment in these samples.

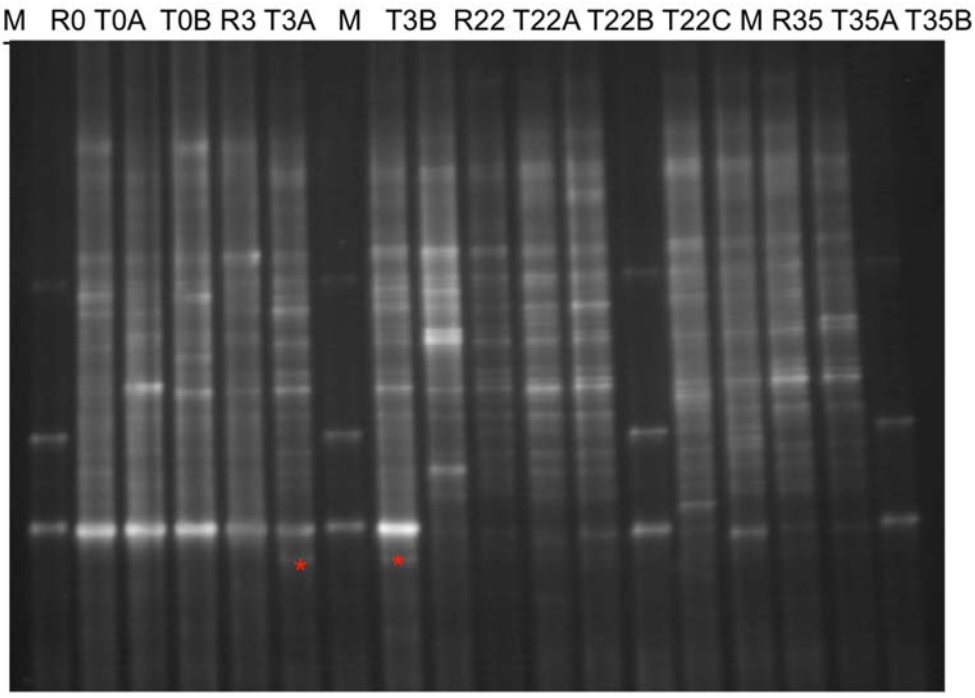

Figure 6.10. Sediment 18s Eukarya DGGE profiles for Experiment B, run on a 35-55% gradient. M = marker. R = GME reference at each time point of 0, 3, 22, and 35 days. T = Tergitol® NP-9 treated samples at each time point, with A, B, and C being replicates. Some differences are visible at T0, however enrichment of a higher G+C band is visible in treated samples after 3 days.

6.4.4 16S MetaVx™ Environmental Sequencing Library Preparation and Illumina MiSeq Sequencing

Sequence information and diversity indices for Experiment A are shown in Table 6.3. Treatment with Tergitol® NP-9 resulted in lower diversity and evenness at all three time points. Diversity and evenness are also decreased (albeit a smaller effect) with phenol treatment and 4-NP treatment, compared with the GME reference.

Table 6.3. Number of sequences and diversity indices for 16s DNA from sediment microcosms, Experiment A.

Treatment	Total sequences	Calculated Sequences	Fraction Classified	Species Identified	Shannon Diversity Index	Shannon Evenness
GME reference (T1)	225,819	98,477	0.44	1,241	4.97	0.70
GME + Tergitol® NP-9 (T1)	246,505	144,722	0.59	977	2.64	0.38
GME reference (T2)	239,354	106,164	0.44	1,197	4.83	0.68
GME + Tergitol® NP-9 (T2)	225,439	143,954	0.64	716	1.81	0.28
GME reference (T3)	173,837	81,546	0.47	975	4.59	0.67
GME + Tergitol® NP-9 (T3)	201,126	135,169	0.67	755	2.13	0.32
GME + Phenol (T3)	218,917	86,960	0.40	1,025	4.45	0.64
GME + 4-nonylphenol (T3)	215,783	91,068	0.42	1,054	4.40	0.63

Kingdom level comparisons for Experiment A are shown in Fig. 6.11. Virus relative abundance is extremely low (< 5 sequences detected of ~ 200,000 total). Unclassified percentage are other 16s sequences that could not be classified at the Kingdom level.

Overall relative abundance of Archaea is low, as expected. Treatment with Tergitol® NP-9 decreased Archaea. This effect is less pronounced at the third GME feeding, when methanogenesis would have recommenced. A slight decrease in Archaea is seen with 4-NP treatment.

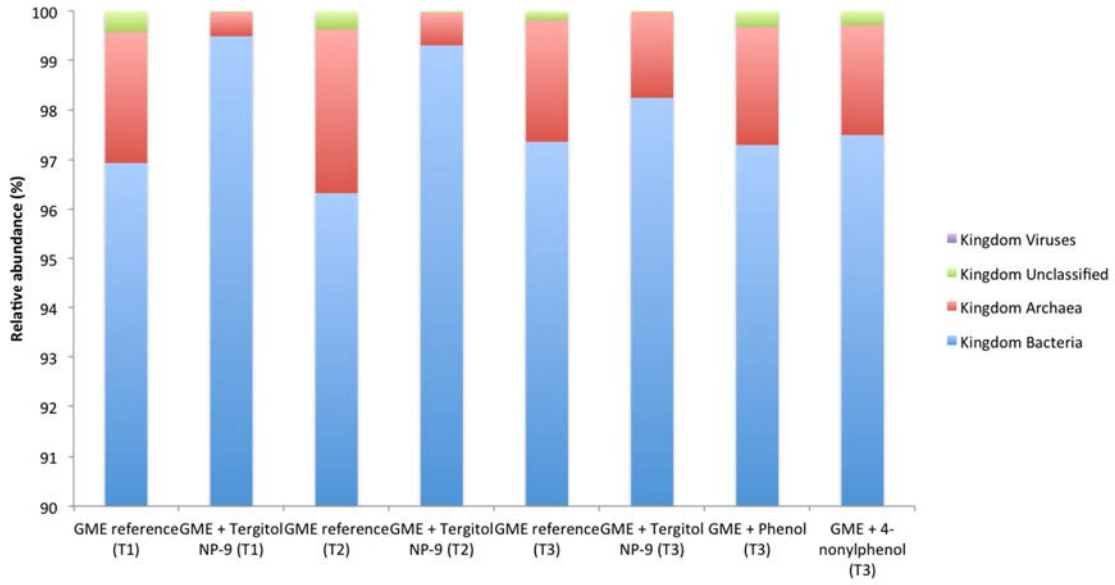

Figure 6.11. Relative abundances at the Kingdom level for Experiment A. A decrease in Archaea is seen with Tergitol® NP-9 exposure. Archaea increase somewhat in the Tergitol® NP-9 microcosm at T3 compared with T1 and T2. At T3, microcosms were fed GME again.

Phylum-level comparisons for Experiment A are shown in Fig. 6.12. The Tergitol® NP-9 treated microcosm has increased Proteobacteria and Acidobacteria sequence abundance compared with the GME reference. At T3, phenol and 4-NP treatments have increased Bacteroidetes and decreased Firmicutes compared with the GME reference at the same time point. A small relative increase in Proteobacteria is also seen with both these treatments.

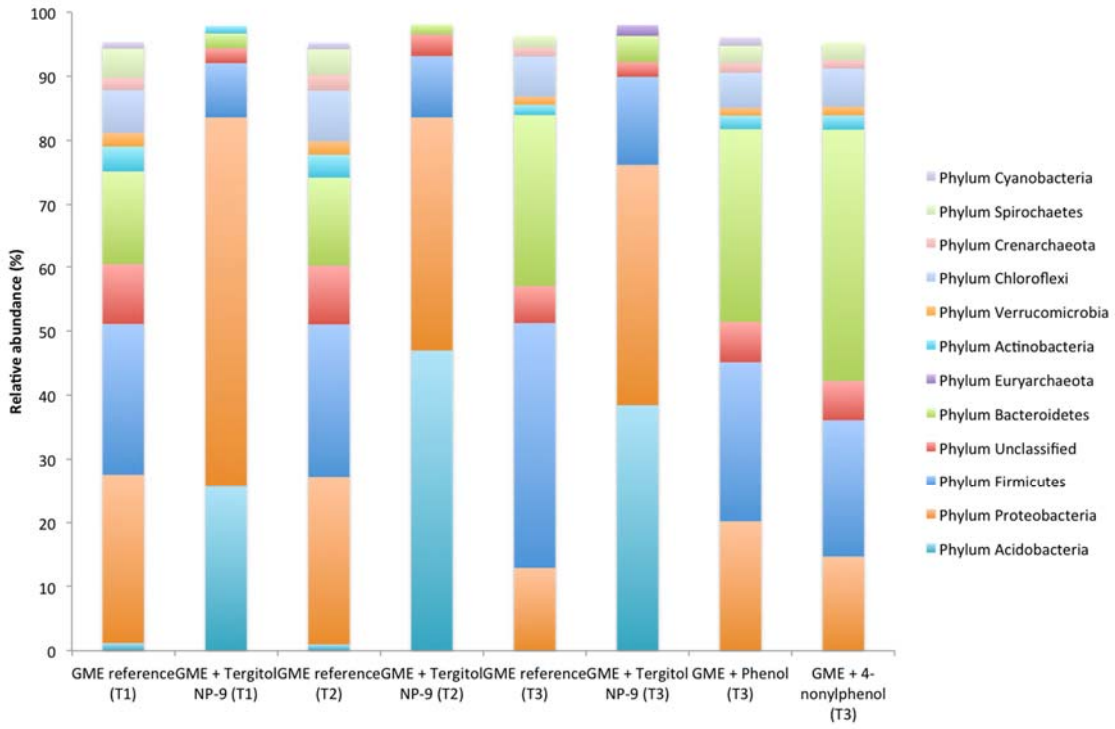

Figure 6.12. Comparison of 16s Phylum level at 1% relative abundance or higher, for Experiment A. White space is pooled "other" groups at < 1% relative abundance.

Figure 6.13 shows Class-level community shifts within the Kingdom Archaea. Thermoprotei is the most abundant class of Phylum Crenarchaeota in the sediment. Both this group and the Thaumarchaeota are substantially decreased with Tergitol® NP-9 treatment. Most of the decrease in Kingdom Archaea is attributable to the loss of these Crenarchaeota. However, a shift in methanogen community composition is also seen. Class Methanococci already had very low relative abundance in this sediment, but a slight decrease occurred with Tergitol® NP-9 treatment. More striking is the almost complete loss of Methanobacteria sequences in the Tergitol® NP-9 treated microcosm. Methanomicrobia relative abundance increased over time compared with the GME reference. A slight decrease in this class is seen at T3 with phenol and 4-NP treatment.

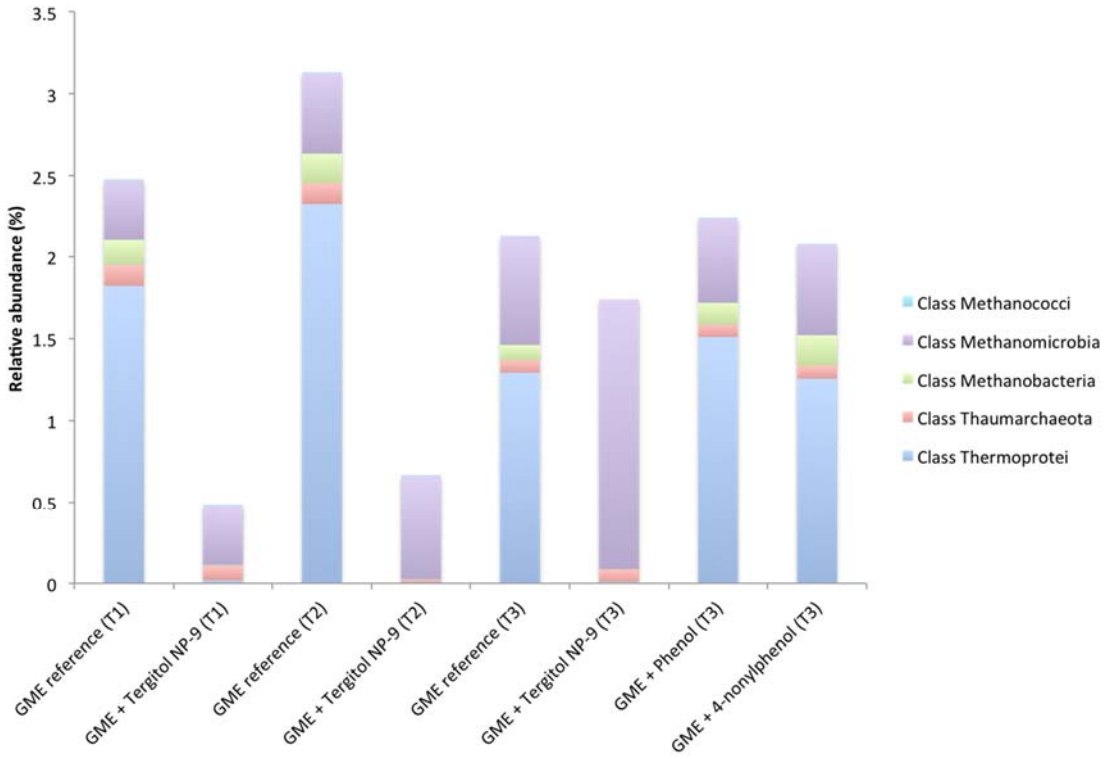

Figure 6.13. Relative abundance of Classes within Kingdom Archaea for Experiment A. Methanococci and Methanomicrobia belong to Phylum Euryarchaeota. There are substantial shifts in Archaeal sequence relative abundance with Tergitol® NP-9 exposure.

Species comparisons for Experiment A are shown in Fig. 6.14. Any species with relative abundance of at least 1% in one of these samples is shown in the figure, even though very low relative abundances cannot be easily seen. At T2 when microcosms had been maintained anaerobically but not fed any additional substrate for approximately 4.5 years, *Geothrix fermentans* had increased to 41.9% relative abundance among all species present in the Tergitol® NP-9 microcosm. *Desulfovibrio burkinensis* was 7.2% relative abundance at T2 in the same microcosm.

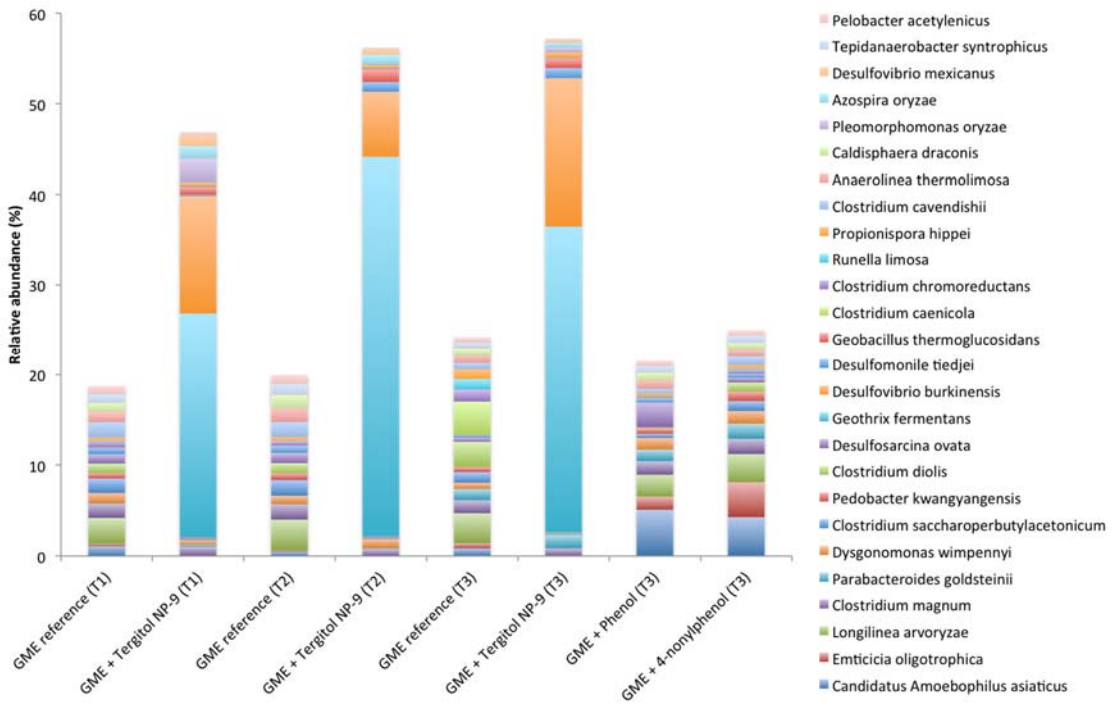

Figure 6.14. Species comparisons for Experiment A. Relative abundances for all species with at least 1% relative abundance in one of these samples are shown. *Geothrix fermentans* and *Desulfovibrio burkinensis* have a marked increase of relative abundance in the Tergitol® NP-9 treated sample. Some community shifts are also seen with phenol and also 4-NP treatment.

Considering that the high relative abundance of these species in Tergitol® NP-9 treated microcosm dwarfs the other species relative abundances in Fig. 13, some detail is shown by changing the scale in Fig. 6.15, comparing the GME reference, GME + phenol, and GME + 4-NP treatments at T3. Treatment with phenol and with 4-NP increased *Candidatus Amoebophilus asiaticus* and *Emticicia oligotrophica* compared with the GME reference. Some Clostridium species (*C. diolis* and *C. caenicola*) are decreased with each of these treatments.

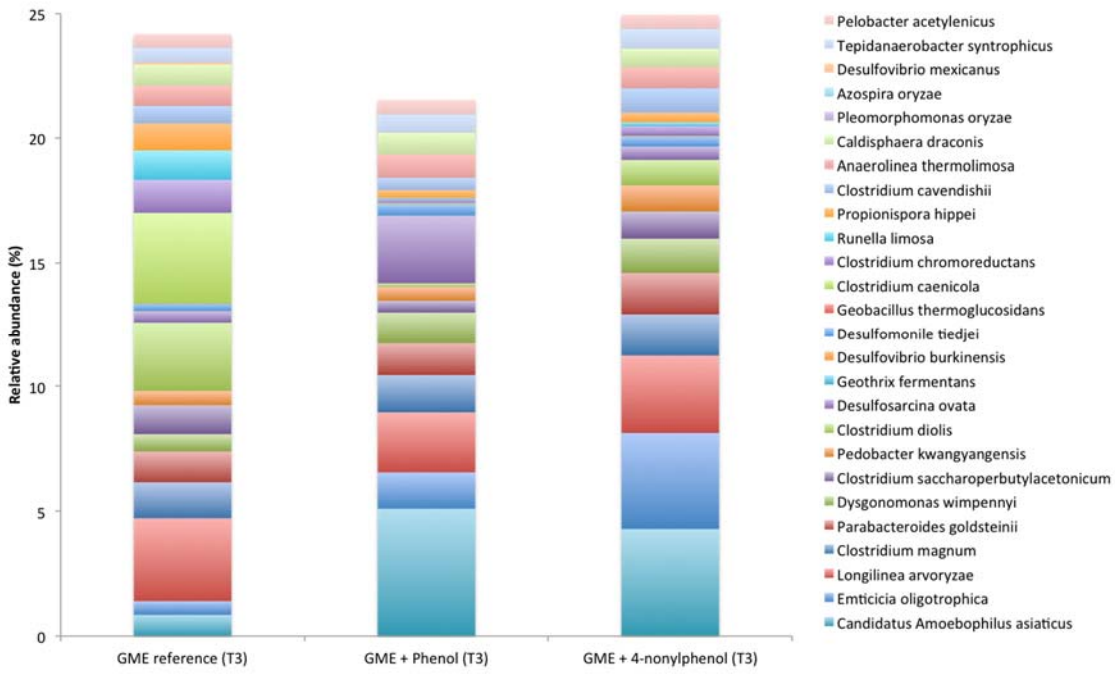

Figure 6.15. Detail of species comparisons for T3 of Experiment A, as shown in Fig. 13.

Finally, for Experiment A, methanogen relative abundances are compared at the genus level in Fig. 6.16. Treatment with Tergitol® NP-9 substantially decreased methanogen diversity. Methanogen relative abundance did increase substantially in the Tergitol® NP-9 microcosm at T3. Some difference in methanogen community composition also occurred over time in the GME reference microcosms. Again, community shifts in the phenol and 4-NP microcosms at T3 were somewhat similar to one another.

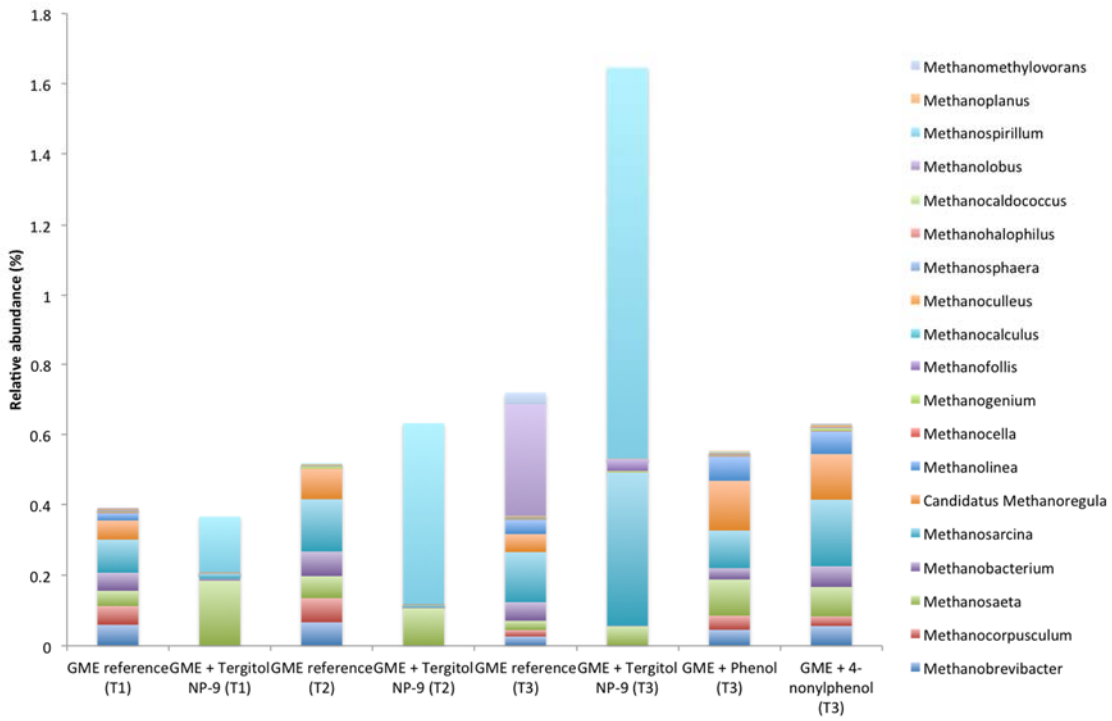

Figure 6.16. Methanogen Genus level comparison for Experiment A. Methanogen sequence diversity decreases with Tergitol® NP-9 exposure. Their relative abundance increases at T3, with a third feeding of GME and no further treatment of Tergitol® NP-9.

Sequence information and diversity indices for Experiment B are shown in Table 6.4. Diversity and evenness for the reference microcosm and the one with Tergitol® addition, both at T0 are fairly close. This suggests little to no effect of Tergitol® NP-9 on the DNA extraction procedure, although a small effect cannot be ruled out. Both diversity and evenness decrease substantially after 3 days as samples became anaerobic, establishing conditions favorable to methanogenesis. This effect is more pronounced in the Tergitol® NP-9 treated microcosms compared with the GME reference.

Table 6.4. Number of sequences and diversity indices for 16s DNA from sediment microcosms, Experiment B.

Treatment	Total sequences	Calculated Sequences	Fraction Classified	Species Identified	Shannon Diversity Index	Shannon Evenness
GME reference (T0)	172,103	71,316	0.41	1,340	5.27	0.73
GME + Tergitol® NP-9 (T0)	192,506	76,234	0.40	1,316	5.31	0.74
GME reference (day 3)	223,420	136,972	0.61	1,114	3.32	0.47
GME + Tergitol® NP-9 (day 3)	272,654	140,418	0.52	963	2.94	0.43

Phylum-level comparisons for Experiment B are shown in Fig. 6.17. Few differences are seen between the GME reference and the microcosms with Tergitol® NP-9 addition at T0. Some small differences could represent some effect of the surfactant on DNA extraction or could merely represent an effect of subsampling. The GME reference and Tergitol® NP-9 microcosms at day 3 are very different from time-zero and also from one another. One apparent temporal difference that is Acidobacteria are decreased after 3 days. In the GME reference, Fusobacteria and Firmicutes are more relatively abundant after three days. This does not occur with Tergitol® NP-9 treatment. Instead, a large increase of Proteobacteria is seen with the surfactant treatment.

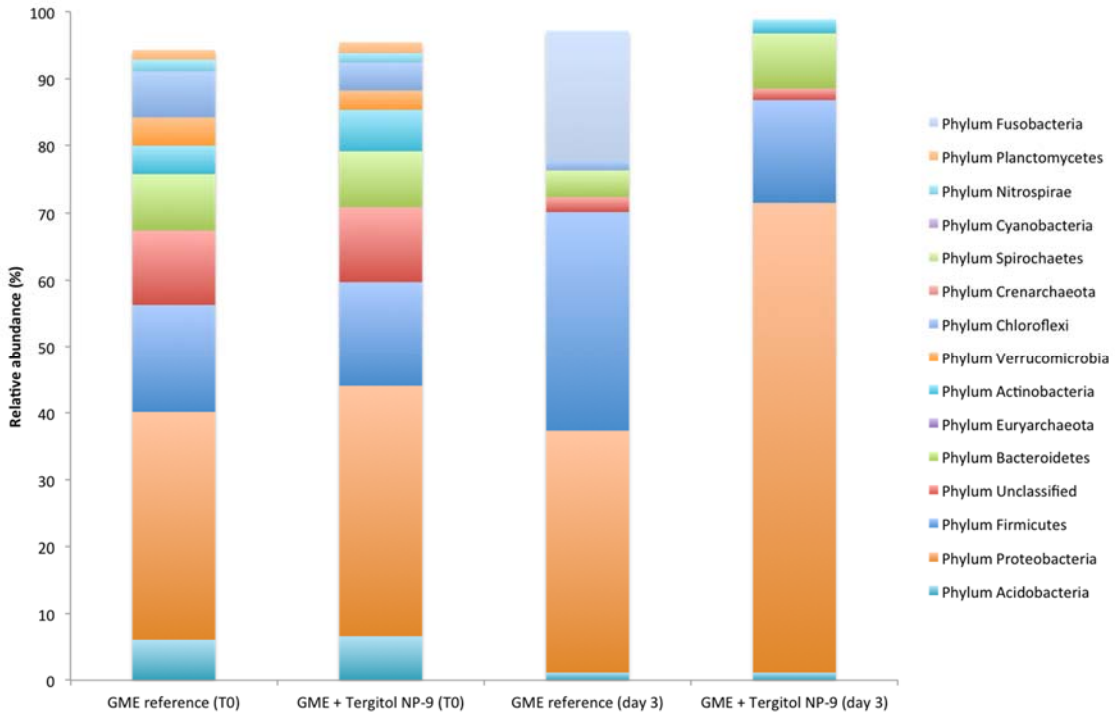

Figure 6.17. Phylum level comparison for Experiment B, at 1% or higher relative abundance. Samples collected at time-zero have similar profiles, showing likely little if any effect of Tergitol® NP-9 on the DNA extraction procedure. Notable differences are seen at day 3 in the GME reference and also with Tergitol® NP-9 treatment after 3 days.

As for Experiment A, it is useful to compare relative abundances at the species level. In Fig. 6.18, all species with relative abundance greater than or equal to 1% in one of these samples is shown. Very thin lines represent low relative abundances, and some species cannot be seen in one sample or another if their relative abundances are very low (sometimes < 10 sequences detected while being relatively abundant in a different sample). After 3 days in the GME reference, a marked increase of *Sebaldella termitidis* is apparent. To a lesser extent, increases in *Tolumonas auensis* and two *Clostridium* species

are seen. In contrast, Tergitol® NP-9 treatment is associated with a further increase in *T. auensis* and also higher relative abundance of *Prevotella paludivivens*.

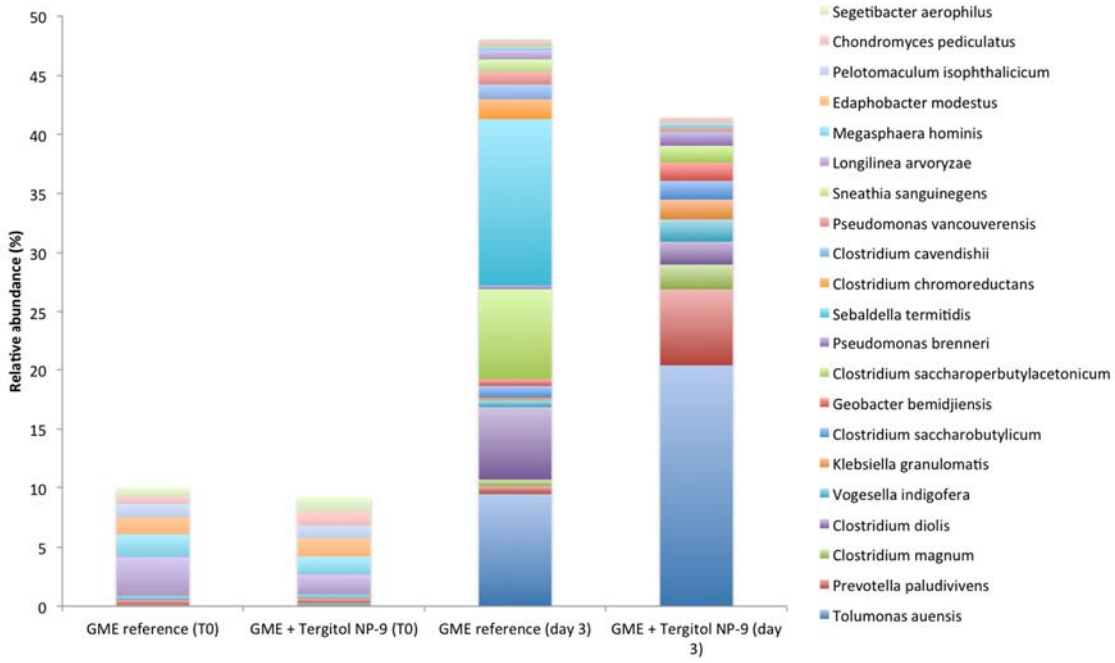

Figure 6.18. Species comparisons for Experiment B. Relative abundances for all species with at least 1% relative abundance in one of these samples are shown. *Tolumonas auensis* and *Prevotella paludivivens* have a marked increase of relative abundance in the Tergitol® NP-9 treated sample at day 3. *Tolumonas auensis* has somewhat increased relative abundance also in the GME reference at day 3, with increases also seen in *Sebaldella termitidis* and some *Clostridium* species.

In Figure 6.19, some decrease in relative abundance of Archaea is shown between T0 and 3 days. Crenarchaeota (and its two major classes present in the sediment) decrease substantially, but the same effect is seen with the methanogens. This effect over time is slightly more apparent with Tergitol® NP-9 treatment.

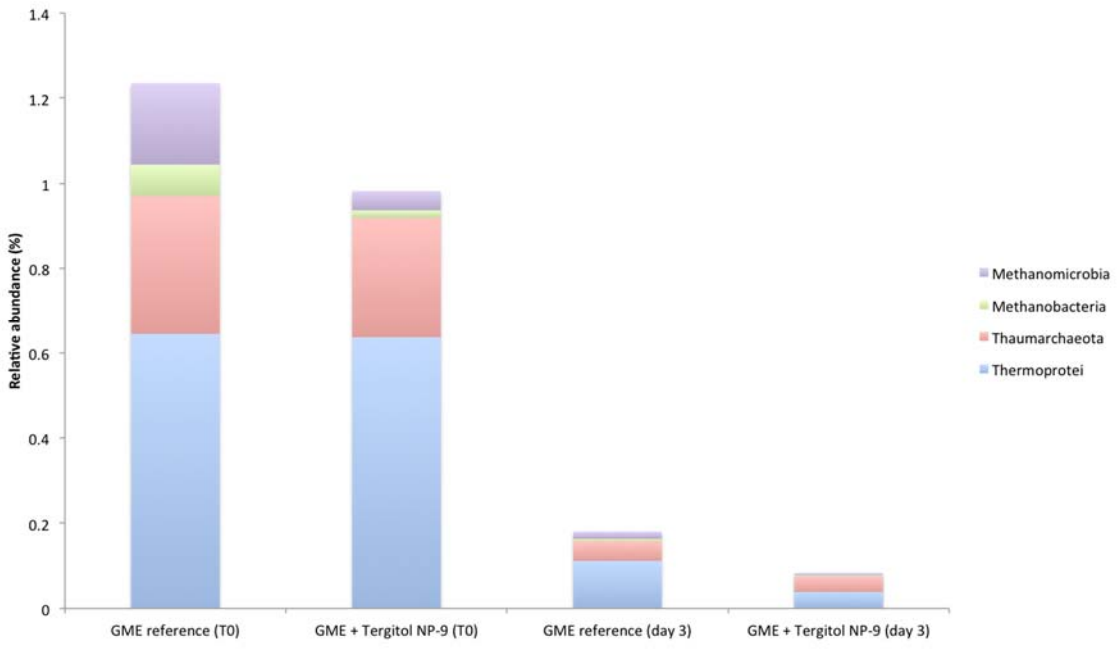

Figure 6.19. Decreases in relative abundance of different Archaea classes seen between time-zero and day 3 after microcosm set-up. This effect is somewhat more pronounced with Tergitol® NP-9 exposure. A slight decrease in overall Archaea is seen with Tergitol® NP-9 addition at T0, although the Archaea community composition remains similar.

6.5 Discussion

The BMP assays of anaerobic microbial community function clearly shows an effect of both Tergitol® NP-9 and its 4-nonylphenol moiety on gas production, compared with the GME reference. Both phenol and PEG-400 increased gas production in Experiment A, as was expected since they are known to biodegrade under anaerobic conditions. Gas production for neither treatment reached the expected value, but both reached more than 90% of this value. Gas production for 4-NP + GME was almost 25% less than the expected value, which suggests toxicity of this treatment at 1.1mg/kg sediment (dw),

even though the difference was not statistically significant with two replicates in each set. This experimental concentration is in the range of reported values in the literature[114].

Tergitol® NP-9 clearly increased gas production in the longer Experiment A compared with the GME reference, but only reached a small fraction of the expected value if all the ethoxylate chains were biotransformed. It is possible that the toxic 4-NP concentration increased in these microcosms as the ethoxylate chains were degraded.

In Experiment B, some pH inhibition early in the BMP assay may have altered microbial function in response to Tergitol® NP-9. Reference (GME) microcosms were slightly but significantly more inhibited than those with the surfactant treatment for the first 20 days of the experiment. Afterward, the gas production trend reversed, with GME reference microcosms producing approximately twice as much gas in 35 days. Headspace methane also decreased in Tergitol® NP-9 treated microcosms.

In both experiments, microbial community structure was drastically altered by Tergitol® NP-9 treatment, and to a lesser extent by phenol and 4-nonylphenol. Data obtained with PCR-DGGE suggested that the magnitude of community shifts seen with especially long-term treatment and the higher concentration of the surfactant would be high. Early differences in Eukarya 18s DGGE profiles suggest that next-generation sequencing of this domain would be advantageous for future studies of the effects of these chemicals in sediment. This is especially relevant given the preponderance of evidence for NP toxicity at generally lower levels in eukaryotic species than for the prokaryotes. Illumina 16s

sequencing and metagenomics showed dramatic increase in relative abundance of just a few species, with temporal differences between the two experiments. To the author's knowledge, an enrichment of these few microorganisms by this surfactant has never been reported in the literature. Further, some notable enrichment of a few species occurred in the GME reference of Experiment B just 3 days after microcosm setup.

In Experiment A, the most striking shift in community composition occurred with *Geothrix fermentans*[130] in Tergitol® NP-9 treated samples. Relative abundances ranged from 24.7 % (T1), to 41.9% (T2), with 33.8% relative abundance at T3, after a third feeding with GME that led to a restoration of methanogenesis. In GME reference samples, phenol, and 4-NP treated samples, relative abundances ranged from ~0.01%-0.04%. In time-zero sediment of Experiment B, relative abundance is about 0.2%. In the 3-day samples, *G. fermentans* relative abundance is 0.06% and about 0.1% with Tergitol® NP-9. Therefore, the dramatic increase in relative abundance of this species would likely need much more time to develop.

This microorganism is of interest because it can use Fe (III) as an electron acceptor[130] in addition to a wide variety of organic compounds and a poised electrode[131]. Evidence exists that it can employ an electron shuttle to reduce metal oxides without direct contact[132] and also to transfer electrons using an electrode as the sole electron acceptor[133]. For this reason, *G. fermentans* is of great interest to researchers investigating microbial fuel cell technology. Notwithstanding its adaptability regarding surfactant fermentation, *Geothrix fermentans* may also have the ability to degrade the 4-NP moiety under optimal

syntrophic conditions. Zemb *et al.*[134] identified a *Geothrix* species in activated sludge as a putative degrader of 4-nonylphenol, based on assimilation of ^{13}C from the labeled aromatic ring of 4-NP into its rRNA. This technique, called RNA-SIP (rRNA- based stable isotope probing), in combination with pyrosequencing, identified 18 other phylotypes in addition to the unidentified *Geothrix*.

In the same experiment, *Desulfovibrio burkinensis*[135] relative abundance was also greatly affected. This microorganism has been shown to use a wide array of organic compounds as electron acceptors[135]. In GME reference samples from all three time points, and for phenol and 4-NP treatments, relative abundance is very low ($n < 10$). However, with Tergitol® NP-9 treatment, relative abundance increased remarkably for this species (13%, 7.2% and 16.4% at T1, T2, and T3, respectively). In Experiment B, this species sequence was detected at n=0-5. Differences between samples are likely not meaningful in such low numbers. Many other species of sulfate reducers are present in these samples, with no apparent enrichment of any species. Surprisingly, the community profiles of Phenol + GME and 4-NP + GME were quite similar. The concentration of phenol used in the experiment was considerably higher than that for 4-NP, which has very low water solubility in contrast with phenol. However, phenol is a naturally occurring compound, whereas a major source of 4-NP is via biotransformation of APEO(x).

Tolumonas auensis[136] has been identified as an anaerobic freshwater sediment bacterium. It has the unusual capability to produce toluene from aromatic amino acids and other compounds with a phenyl ring. This species was greatly enriched between T0 and 3 days

in Experiment B for both GME and Tergitol® NP-9 + GME samples. However, its relative abundance in the Tergitol® sample was more than double that found in the reference sample (20.4% vs. 9.47% with ~ 0.01% at T0). In long-term Experiment A, this 16s sequence is detected in very low numbers in all samples ($n \leq 15$). *S. termitidis* is a fermenting obligate anaerobe member of the Phylum Fusobacteria[137] that was found to be enriched (~14% relative abundance) in the GME reference sample of Experiment B after 3 days. It presumably found a competitive advantage in the sediment microcosms with abundant substrate. Within three days, oxygen would have been depleted with inhibition of other microorganisms associated with surface sediment, as well as non-fermenters. Its relative abundance in T0 sediment was < 0.5%, and with Tergitol® NP-9 treatment at 3 days, this dropped almost an order of magnitude. Originally found in termite hindgut[138] and more recently in beetle *Poecilus chalcites* [139], reports of this microorganism are relatively rare in the literature[137]. Eisenberg at al.[140] recently identified it as a tooth root pathogen in the lesser dwarf lemur *Cheirogaleus medius*. An identical 16s sequence has also been found in anaerobic digester sludge[141]. This 16s sequence was also found in Experiment A (0.1-0.3% in GME references at all three time points, much less in all three Tergitol® NP-9 + GME samples (n=3-10 sequences), ~0.2% with both Phenol + GME and 4-NP + GME. Therefore, it appears that only Tergitol® NP-9 treatment affected its relative abundance, along with an apparent temporal effect.

Finally, *Prevotella paludivivens* was also enriched by treatment with Tergitol® NP-9 after 3 days (6.52% vs. 0.67% in the 3-day GME reference). At T0, the relative abundance of this microorganism was ~ 0.01%. This is another strictly anaerobic

fermenting bacterium, again first isolated from rice fields, that is known to degrade hemicellulose[142]. It was not detected (n=0) in any samples from Experiment A, which had been enriched for methanogenesis over several years.

In Experiment A, the main community shift with methanogens was seen with enrichment of Genus *Methanospirillum* with Tergitol® NP-9 treatment. Most of these sequences were not characterized at the species level. However, one detected species, *M. hungatei* GP1, has been found to have two unusual polar lipids, which make up a majority of its lipid composition (64% by weight)[143]. Possibly, this species and others of its genus have cell membranes that are particularly resistant to disruption by the surfactant even at high concentrations. Some enrichment of *Methanosaeta* and *Methanosarcina* also occurred to a lesser extent.

The amount of time that passed between setup of Experiments A and B presents a challenge for interpreting the results of Experiment B as representative of the start-up phase of Experiment A. After all, local development could have affected the Celery Bog sediment community in the intervening years. However, it also seems likely that these results capture some of the complex and shifting community dynamics that would occur over time with commencement and maintenance of strictly anaerobic conditions. Of note for future studies would be the potential contribution of the ethoxylate chain of the surfactant to community structural shifts favoring acetogenesis and acetoclastic methanogenesis. Many of the species enriched by the Tergitol® treatment are associated

with these metabolic functions. However, known acetogens[144] such as *Pelobacter* and *Clostridium spp.*, were also well-represented in the GME reference microcosms.

Tergitol® NP-9 clearly enriches for some intriguing, little-known, and metabolically versatile species. Basic research on the physiology, genetics, and ecology of these microorganisms could lead to important developments for sustainable energy production and other beneficial innovations. The surfactant concentrations used in this study were relatively high, but illustrate the potential for substantial community shifts in just a few days, comparable to the magnitude of change undergone when the microbial community becomes strictly anaerobic. However, the associated reductions in community diversity and evenness are cause for concern.

Overall, the Tergitol® NP-9 significantly diminished microbial community diversity. As ethoxylate groups are biodegraded their solubilizing function will decrease and the molecule will eventually adsorb to sediment particles or microbial cells. The properties of biodegradation intermediates are not well known. Complete removal of the ethoxylate chain produces 4-NP as a daughter product. These alkylphenols are known to be toxic and harmful. APEO(x), such as Tergitol® NP-9 are found in household consumer products and released to sewage systems and the environment through normal use. Anthropogenic chemicals that reduce microbial community diversity place ecosystems at risk. More research into the mechanisms of their effects is needed; however, using alternative chemicals that undergo complete biodegradation aerobically and anaerobically might be a prudent strategy for environmental protection.

CHAPTER 7. CONCLUSIONS AND FUTURE WORK

The primary findings of the studies described here include significant effects of emerging contaminants on anaerobic microbial community structure and function. A substantial acceleration of gas production occurred with exposure to several types of carbon nanotubes. Furthermore, treatment with longer nanotubes (3-30 μm) was associated with increased relative abundance of taxonomic groups known or thought to be involved in direct interspecies electron transfer (DIET) and also a possible shift toward acetoclastic methanogenesis in rumen microcosms. In the sludge experiment, a similar but less pronounced effect was observed, with the choice of substrate at the beginning of the experiment strongly influencing microbial community structural and functional response to nanotube exposure. Treatment with a nonylphenol ethoxylate surfactant showed both inhibition and enhancement of gas production at different times, with major community shifts occurring over time but starting almost immediately after exposure.

Emerging contaminants and their metabolites are often strongly hydrophobic and transported to anaerobic environments where they may affect microbial community structure and function. Anaerobic ecosystems are critical to life on Earth, particularly through their essential role in the carbon cycle. The work described in this thesis contributed to filling the knowledge gap with respect to the complex relationship between

microbial community structural and functional changes in response to these chemicals of concern. The diverse anaerobic communities studied in cow rumen, anaerobic digester sludge, and wetland sediments provide further evidence that industrial and domestic products exert profound impacts on the environment.

Results of these studies may be applied to benefit the environment and human health in numerous ways, in addition to their intended purpose, which is to inform responsible management and disposal of the materials assessed. First, development of non-conducting "electron sinks" that would be safe for animal consumption could potentially help to control methanogenesis in ruminants. On the other hand, as described in several recent papers cited here, conductive carbon materials could enhance functioning of anaerobic digesters, which could provide for increased energy recovery. Accelerated kinetics in these systems would allow for smaller reactors and reduced capital costs.

Thus, a long-term objective for future work would be to develop ecologically safe materials to both enhance and inhibit methanogenesis. In the short to medium term, the insights gained from metagenomics profiles could be enhanced by including the sequences that remained unclassified at the species level (approximately half across all the experiments). A significant fraction of these were classified at the genus level (~65-85% total depending on the experiment, or anywhere from 20-40% additional sequences beyond those already identified at species level). Future work would include further exploration of the biological relevance of differences found between metagenomic profiles, using analytical tools such as STAMP software[145]. This analysis would likely

contribute to understanding long-term implications of microbial community shifts induced by exposure to emerging contaminants. These data also raise further questions about how microbial community shifts cascade through ecosystems. Given that anaerobic microbes are foundational organisms functioning in tightly coupled systems, these larger potential ecosystem impacts could potentially be significant.

LIST OF REFERENCES

LIST OF REFERENCES

1. Koelmans, A. A.; Nowack, B.; Wiesner, M. R., Comparison of manufactured and black carbon nanoparticle concentrations in aquatic sediments. *Environmental Pollution* **2009,** *157* (4), 1110-1116.

2. Colvin, V. L., The potential environmental impact of engineered nanomaterials. *Nature Biotechnology* **2003,** *21* (10), 1166-1170.

3. de Heer, W. A., Nanotubes and the pursuit of applications. *Mrs Bulletin* **2004,** *29* (4), 281-285.

4. Yang, X.; Zhang, Z.; Liu, Z.; Ma, Y.; Yang, R.; Chen, Y., Multi-functionalized single-walled carbon nanotubes as tumor cell targeting biological transporters. *Journal of Nanoparticle Research* **2008,** *10* (5), 815-822.

5. Helland, A.; Wick, P.; Koehler, A.; Schmid, K.; Som, C., Reviewing the environmental and human health knowledge base of carbon nanotubes. *Environmental Health Perspectives* **2007,** *115* (8), 1125-1131.

6. Ouyang, M.; Huang, J. L.; Lieber, C. M., Fundamental electronic properties and applications of single-walled carbon nanotubes. *Accounts of Chemical Research* **2002,** *35* (12), 1018-1025.

7. Ferguson, P. L.; Chandler, G. T.; Templeton, R. C.; Demarco, A.; Scrivens, W. A.; Englehart, B. A., Influence of sediment-amendment with single-walled carbon nanotubes and diesel soot on bioaccumulation of hydrophobic organic contaminants by benthic invertebrates. *Environmental Science & Technology* **2008,** *42* (10), 3879-3885.

8. Kennedy, A. J.; Hull, M. S.; Steevens, J. A.; Dontsova, K. M.; Chappell, M. A.; Gunter, J. C.; Weiss, C. A., Jr., Factors influencing the partitioning and toxicity of nanotubes in the aquatic environment. *Environmental Toxicology and Chemistry* **2008,** *27* (9), 1932-1941.

9. Allgood, G. S.; McAvoy, D. C.; Woltering, D. M., Environmental assessment of a new food ingredient the fat replacer olestra. *Environmental Toxicology and Chemistry* **1997,** *16* (3), 586-600.

10. Shelton, D. R.; Tiedje, J. M., General method for determining anaerobic biodegradation potential. *Applied and Environmental Microbiology* **1984,** *47* (4), 850-857.

11. Roco, M. C., The long view of nanotechnology development: the National Nanotechnology Initiative at 10 years (vol 13, pg 427, 2011). *Journal of Nanoparticle Research* **2011,** *13* (3), 1335-1335.

12. Owen, R.; Handy, R., Formulating the problems for environmental risk assessment of nanomaterials. *Environmental Science & Technology* **2007,** *41* (16), 5582-5588.

13. Fortner, J. D.; Lyon, D. Y.; Sayes, C. M.; Boyd, A. M.; Falkner, J. C.; Hotze, E. M.; Alemany, L. B.; Tao, Y. J.; Guo, W.; Ausman, K. D.; Colvin, V. L.; Hughes, J. B., C60 in water: nanocrystal formation and microbial response. *Environ Sci Technol* **2005,** *39* (11), 4307-16.

14. Lyon, D. Y.; Fortner, J. D.; Sayes, C. M.; Colvin, V. L.; Hughes, J. B., Bacterial cell association and antimicrobial activity of a C-60 water suspension. *Environmental Toxicology and Chemistry* **2005,** *24* (11), 2757-2762.

15. Tong, Z.; Bischoff, M.; Nies, L.; Applegate, B.; Turco, R. F., Impact of fullerene (C-60) on a soil microbial community. *Environmental Science & Technology* **2007,** *41* (8), 2985-2991.

16. Nyberg, L.; Turco, R.; Nies, L., Assessing the impact of nanomaterials on anaerobic microbial communities. *Environmental Science & Technology* **2008,** *42* (6), 1938-1943.

17. Karakoti, A. S.; Hench, L. L.; Seal, S., The potential toxicity of nanomaterials - The role of surfaces. *Jom* **2006,** *58* (7), 77-82.

18. Jacob, J., The significance of polycyclic aromatic hydrocarbons as environmental carcinogens. *Pure and Applied Chemistry* **1996,** *68* (2), 301-308.

19. Hernadi, K.; Gaspar, A.; Seo, J. W.; Hammida, M.; Demortier, A.; Forro, L.; Nagy, J. B.; Kiricsi, I., Catalytic carbon nanotube and fullerene synthesis under reduced pressure in a batch reactor. *Carbon* **2004,** *42* (8-9), 1599-1607.

20. Petkewich, R., Toxic by-products of nanotubes. *Chemical & Engineering News* **2007,** *85* (35), 12-12.

21. Kang, S.; Mauter, M. S.; Elimelech, M., Physicochemical determinants of multiwalled carbon nanotube bacterial cytotoxicity. *Environmental Science & Technology* **2008,** *42* (19), 7528-7534.

22. Kang, S.; Pinault, M.; Pfefferle, L. D.; Elimelech, M., Single-walled carbon nanotubes exhibit strong antimicrobial activity. *Langmuir* **2007,** *23* (17), 8670-8673.

23. Kang, S.; Herzberg, M.; Rodrigues, D. F.; Elimelech, M., Antibacterial effects of carbon nanotubes: Size does matter. *Langmuir* **2008,** *24* (13), 6409-6413.

24. Kang, S.; Mauter, M. S.; Elimelech, M., Microbial Cytotoxicity of Carbon-Based Nanomaterials: Implications for River Water and Wastewater Effluent. *Environmental Science & Technology* **2009,** *43* (7), 2648-2653.

25. Arias, L. R.; Yang, L., Inactivation of Bacterial Pathogens by Carbon Nanotubes in Suspensions. *Langmuir* **2009,** *25* (5), 3003-3012.

26. Lawrence, J. R.; Swerhone, G. D. W.; Dynes, J. J.; Hitchcock, A. P.; Korber, D. R., Complex organic corona formation on carbon nanotubes reduces microbial toxicity by suppressing reactive oxygen species production. *Environmental Science-Nano* **2016,** *3* (1), 181-189.

27. Woese, C. R.; Kandler, O.; Wheelis, M. L., Towards a natural system of organisms - proposal for the domains Archaea, Bacteria, and Eucarya. *Proceedings of the National Academy of Sciences of the United States of America* **1990,** *87* (12), 4576-4579.

28. **Oremland, R. S.**, The biogeochemistry of methanogenic bacteria. In *The Biology of Anaerobic Microorganisms*, Zehnder, A. J. B., Ed. J. Wiley & Sons: NY, **1988**; pp 405-447.

29. Muyzer, G.; de Waal, E. C.; Uitterlinden, A. G., Profiling of complex microbial populations by denaturing gradient gel electrophoresis analysis of polymerase chain reaction-amplified genes coding for 16S rRNA. *Appl Environ Microbiol* **1993,** *59* (3), 695-700.

30. Ovreas, L.; Forney, L.; Daae, F. L.; Torsvik, V., Distribution of bacterioplankton in meromictic Lake Saelenvannet, as determined by denaturing gradient gel electrophoresis of PCR-amplified gene fragments coding for 16S rRNA. *Applied and Environmental Microbiology* **1997,** *63* (9), 3367-3373.

31. Kowalchuk, G. A.; Gerards, S.; Woldendorp, J. W., Detection and characterization of fungal infections of Ammophila arenaria (marram grass) roots by denaturing gradient gel electrophoresis of specifically amplified 18S rDNA. *Applied and Environmental Microbiology* **1997,** *63* (10), 3858-3865.

32. van Hannen, E. J.; van Agterveld, M. P.; Gons, H. J.; Laanbroek, H. J., Revealing genetic diversity of eukaryotic microorganisms in aquatic environments by denaturing gradient gel electrophoresis. *Journal of Phycology* **1998,** *34* (2), 206-213.

33. Murase, J.; Frenzel, P., A methane-driven microbial food web in a wetland rice soil. *Environmental Microbiology* **2007,** *9* (12), 3025-3034.

34. Hull, M. S.; Kennedy, A. J.; Steevens, J. A.; Bednar, A. J.; Weiss, C. A., Jr.; Vikesland, P. J., Release of Metal Impurities from Carbon Nanomaterials Influences Aquatic Toxicity. *Environmental Science & Technology* **2009,** *43* (11), 4169-4174.

35. Scheller, S.; Goenrich, M.; Boecher, R.; Thauer, R. K.; Jaun, B., The key nickel enzyme of methanogenesis catalyses the anaerobic oxidation of methane. *Nature* **2010,** *465* (7298), 606-U97.

36. Moon, R. J.; Martini, A.; Nairn, J.; Simonsen, J.; Youngblood, J., Cellulose nanomaterials review: structure, properties and nanocomposites. *Chemical Society Reviews* **2011,** *40* (7), 3941-3994.

37. Petersen, N.; Gatenholm, P., Bacterial cellulose-based materials and medical devices: current state and perspectives. *Applied Microbiology and Biotechnology* **2011,** *91* (5), 1277-1286.

38. Harper, B. J.; Clendaniel, A.; Sinche, F.; Way, D.; Hughes, M.; Schardt, J.; Simonsen, J.; Stefaniak, A. B.; Harper, S. L., Impacts of chemical modification on the toxicity of diverse nanocellulose materials to developing zebrafish. *Cellulose* **2016,** *23* (3), 1763-1775.

39. Kovacs, T.; Naish, V.; O'Connor, B.; Blaise, C.; Gagné, F.; Hall, L.; Trudeau, V.; Martel, P., An ecotoxicological characterization of nanocrystalline cellulose (NCC). *Nanotoxicology* **2010,** *4* (3), 255-270.

40. Schwarz, W., The cellulosome and cellulose degradation by anaerobic bacteria. *Applied Microbiology and Biotechnology* **2001,** *56* (5-6), 634-649.

41. Naylor, C. G.; Mieure, J. P.; Adams, W. J.; Weeks, J. A.; Castaldi, F. J.; Ogle, L. D.; Romano, R. R., Alkylphenol ethoxylates in the environment. *Journal of the American Oil Chemists Society* **1992,** *69* (7), 695-703.

42. Li, F.; Tsumori, J.; Suzuki, Y.; Tanaka, H., Vertical distribution of nonylphenol ethoxylates and their derivatives in sediments of a freshwater reservoir. *Water Air and Soil Pollution* **2008,** *189* (1-4), 265-277.

43. Jonkers, N.; Knepper, T. P.; De Voogt, P., Aerobic biodegradation studies of nonylphenol ethoxylates in river water using liquid chromatography-electrospray tandem mass spectrometry. *Environmental Science & Technology* **2001,** *35* (2), 335-340.

44. Shang, D. Y.; Macdonald, R. W.; Ikonomou, M. G., Persistence of nonylphenol ethoxylate surfactants and their primary degradation products in sediments from near a municipal outfall in the strait of Georgia, British Columbia, Canada. *Environmental Science & Technology* **1999,** *33* (9), 1366-1372.

45. Planas, C.; Guadayol, J. M.; Droguet, M.; Escalas, A.; Rivera, J.; Caixach, J., Degradation of polyethoxylated nonylphenols in a sewage treatment plant. Quantitative analysis by isotopic dilution-HRGC/MS. *Water Research* **2002,** *36* (4), 982-988.

46. Schwarzenbach, R. P.; Escher, B. I.; Fenner, K.; Hofstetter, T. B.; Johnson, C. A.; von Gunten, U.; Wehrli, B., The challenge of micropollutants in aquatic systems. *Science* **2006,** *313* (5790), 1072-1077.

47. Lu, J.; Jin, Q.; He, Y.; Wu, J.; Zhang, W.; Zhao, J., Anaerobic degradation behavior of nonylphenol polyethoxylates in sludge. *Chemosphere* **2008,** *71* (2), 345-351.

48. Ying, G. G.; Williams, B.; Kookana, R., Environmental fate of alkylphenols and alkylphenol ethoxylates - a review. *Environment International* **2002,** *28* (3), 215-226.

49. Sherman, D., Method for SEM/EDX characterization and elemental analysis of carbon nanotube preparations. Purdue Life Science Microscopy Facility ed.; 2011.

50. Tarvin, D.; Buswell, A., The methane fermentation of organic acids and carbohydrates. *Journal of the American Chemical Society* **1934,** *56* (7), 1751-1755.

51. Lane, D. J., Nucleic Acid Techniques in Bacterial Systematics. John Wiley & Sons: New York, NY, 1991; pp 115-175.

52. Torsvik, T., V. Torsvik, J. Keswani, and W. B. Whitman, Unpublished results.

53. Brown, P. B.; Wolfe, G. V., Protist genetic diversity in the acidic hydrothermal environments of Lassen Volcanic National Park, USA. *Journal of Eukaryotic Microbiology* **2006,** *53* (6), 420-431.

54. Genewiz LLC personal communication.

55. Shannon, C. E., A mathematical theory of communication. *Bell System Technical Journal* **1948,** *27* (3), 379-423.

56. University of Reading Statistical Services Center Diversity Index Calculator (an add-in for MS-Excel). http://www.reading.ac.uk/ssc/resources/diversity/Diversity.html (accessed July 11, 2016).

57. Bock, R., A Handbook of Decomposition Methods in Analytical Chemistry. T. & A. Constable Ltd.: Edinburgh, **1979**.

58. AOAC International Official Method 990.08. In *"Metals in Solid Waste by ICP-OES". Official Methods of Analysis of AOAC International.*, 16th, 5th revision ed.; **1999**.

59. Skoog, D. A.; West, D. M., Fundamentals of Analytical Chemistry. 4th ed.; Saunders College Publishing: New York, NY, **1986**; p 561.

60. Monteny, G. J.; Bannink, A.; Chadwick, D., Greenhouse gas abatement strategies for animal husbandry. *Agriculture Ecosystems & Environment* **2006,** *112* (2-3), 163-170.

61. Lecoanet, H. F.; Wiesner, M. R., Velocity effects on fullerene and oxide nanoparticle deposition in porous media. *Environmental Science & Technology* **2004,** *38* (16), 4377-4382.

62. Stone, V.; Nowack, B.; Baun, A.; van den Brink, N.; von der Kammer, F.; Dusinska, M.; Handy, R.; Hankin, S.; Hassellov, M.; Joner, E.; Fernandes, T. F., Nanomaterials for environmental studies: Classification, reference material issues, and strategies for physico-chemical characterisation. *Science of the Total Environment* **2010,** *408* (7), 1745-1754.

63. Suri, S. S.; Fenniri, H.; Singh, B., Nanotechnology-based drug delivery systems. *Journal of occupational medicine and toxicology (London, England)* **2007,** *2*, 16-16.

64. Jones-Lepp, T. L.; Stevens, R., Pharmaceuticals and personal care products in biosolids/sewage sludge: the interface between analytical chemistry and regulation. *Analytical and Bioanalytical Chemistry* **2007,** *387* (4), 1173-1183.

65. Tong, Z.-H.; Bischoff, M.; Nies, L. F.; Carroll, N. J.; Applegate, B.; Turco, R. F., Influence of fullerene (C-60) on soil bacterial communities: aqueous aggregate size and solvent co-introduction effects. *Scientific Reports* **2016,** *6*.

66. Yue, Z.-B.; Li, W.-W.; Yu, H.-Q., Application of rumen microorganisms for anaerobic bioconversion of lignocellulosic biomass. *Bioresource Technology* **2013,** *128*, 738-744.

67. Li, L.-L.; Tong, Z.-H.; Fang, C.-Y.; Chu, J.; Yu, H.-Q., Response of anaerobic granular sludge to single-wall carbon nanotube exposure. *Water Research* **2015,** *70*, 1-8.

68. Rotaru, A. E.; Shrestha, P. M.; Liu, F. H.; Shrestha, M.; Shrestha, D.; Embree, M.; Zengler, K.; Wardman, C.; Nevin, K. P.; Lovley, D. R., A new model for electron flow during anaerobic digestion: direct interspecies electron transfer to Methanosaeta for the reduction of carbon dioxide to methane. *Energy & Environmental Science* **2014,** *7* (1), 408-415.

69. Xu, H.; Wang, C.; Yan, K.; Wu, J.; Zuo, J.; Wang, K., Anaerobic granule-based biofilms formation reduces propionate accumulation under high H2 partial pressure using conductive carbon felt particles. *Bioresource Technology* **2016,** *216*, 677-683.

70. Liu, F.; Rotaru, A.-E.; Shrestha, P. M.; Malvankar, N. S.; Nevin, K. P.; Lovley, D. R., Promoting direct interspecies electron transfer with activated carbon. *Energy & Environmental Science* **2012,** *5* (10), 8982-8989.

71. Liu, Z.; Lv, F.; Zheng, H.; Zhang, C.; Wei, F.; Xing, X.-H., Enhanced. hydrogen production in a UASB reactor by retaining microbial consortium onto carbon nanotubes (CNTs). *International Journal of Hydrogen Energy* **2012,** *37* (14), 10619-10626.

72. Yadav, T.; Mungray, A. A.; Mungray, A. K., Effect of multiwalled carbon nanotubes on UASB microbial consortium. *Environmental Science and Pollution Research* **2016,** *23* (5), 4063-4072.

73. Bayane, A.; Guiot, S. R., Animal digestive strategies versus anaerobic digestion bioprocesses for biogas production from lignocellulosic biomass. *Reviews in Environmental Science and Bio-Technology* **2011,** *10* (1), 43-62.

74. Hristov, A. N.; Ahvenjarvi, S.; McAllister, T. A.; Huhtanen, P., Composition and digestive tract retention time of ruminal particles with functional specific gravity greater or less than 1.02. *Journal of Animal Science* **2003,** *81* (10), 2639-2648.

75. Leschine, S. B., Cellulose degradation in anaerobic environments. *Annual Review of Microbiology* **1995,** *49*, 399-426.

76. Eichhorn, S.; Dufresne, A.; Aranguren, M.; Marcovich, N.; Capadona, J.; Rowan, S.; Weder, C.; Thielemans, W.; Roman, M.; Renneckar, S.; Gindl, W.; Veigel, S.; Keckes, J.; Yano, H.; Abe, K.; Nogi, M.; Nakagaito, A.; Mangalam, A.; Simonsen, J.; Benight, A.; Bismarck, A.; Berglund, L.; Peijs, T., Review: current international research into cellulose nanofibres and nanocomposites. *Journal of Materials Science* **2010,** *45* (1), 1-33.

77. Ye, D.; Quensen, J.; Tiedje, J.; Boyd, S., 2-bromoethanesulfonate, sulfate, molybdate, and ethanesulfonate inhibit anaerobic dechlorination of polychlorobiphenyls by pasteurized microorganisms. *Applied and Environmental Microbiology* **1999,** *65* (1), 327-329.

78. Fernandez, A.; Huang, S. Y.; Seston, S.; Xing, J.; Hickey, R.; Criddle, C.; Tiedje, J., How stable is stable? Function versus community composition. *Applied and Environmental Microbiology* **1999,** *65* (8), 3697-3704.

79. Pylro, V. S.; Morais, D. K.; Kalks, K. H. M.; Roesch, L. F. W.; Hirsch, P. R.; Totola, M. R.; Yotoko, K., Misguided phylogenetic comparisons using DGGE excised bands may contaminate public sequence databases. *Journal of microbiological methods* **2016,** *126*, 18-23.

80. Klappenbach, J. A.; Saxman, P. R.; Cole, J. R.; Schmidt, T. M., rrndb: the Ribosomal RNA Operon Copy Number Database. *Nucleic Acids Research* **2001,** *29* (1), 181-184.

81. Stoddard, S. F.; Smith, B. J.; Hein, R.; Roller, B. R. K.; Schmidt, T. M., rrnDB: improved tools for interpreting rRNA gene abundance in bacteria and archaea and a new foundation for future development. *Nucleic Acids Research* **2015,** *43* (D1), D593-D598.

82. Grott, M., Cow dietary information (as-fed, wet weight) from Purdue Dairy.

83. Kessel, J. S. v.; Russell, J. B.; Van Kessel, J. S., The effect of pH on ruminal methanogenesis. *U.S. Dairy Forage Research Center, Research Summaries* **1997,** (March), 83-85.

84. Random.org List Randomizer. https://www.random.org/lists/ (accessed August 31, 2012).

85. Carbon Solutions, Inc. Frequently Asked Questions (FAQ) Page. http://www.carbonsolution.com/faq - Q7 (accessed July 11, 2016).

86. Safavi, A.; Abdollahi, H.; Nezhad, M. R. H.; Kamali, R., Cloud point extraction, preconcentration and simultaneous spectrophotometric determination of nickel and cobalt in water samples. *Spectrochimica Acta Part a-Molecular and Biomolecular Spectroscopy* **2004,** *60* (12), 2897-2901.

87. Lawrence, M. G.; Greig, A.; Collerson, K. D.; Kamber, B. S., Direct quantification of rare earth element concentrations in natural waters by ICP-MS. *Applied Geochemistry* **2006,** *21* (5), 839-848.

88. Cheap Tubes, Inc. Product Page for COOH Functionalized Single Walled-Double Walled Carbon Nanotubes 99%. https://www.cheaptubes.com/product/cooh-functionalized-single-walled-double-walled-carbon-nanotubes-99/ (accessed July 11, 2016).

89. Hess, M.; Sczyrba, A.; Egan, R.; Kim, T.-W.; Chokhawala, H.; Schroth, G.; Luo, S.; Clark, D. S.; Chen, F.; Zhang, T.; Mackie, R. I.; Pennacchio, L. A.; Tringe, S. G.; Visel, A.; Woyke, T.; Wang, Z.; Rubin, E. M., Metagenomic Discovery of Biomass-Degrading Genes and Genomes from Cow Rumen. *Science* **2011,** *331* (6016), 463-467.

90. Kittelmann, S.; Seedorf, H.; Walters, W. A.; Clemente, J. C.; Knight, R.; Gordon, J. I.; Janssen, P. H., Simultaneous Amplicon Sequencing to Explore Co-Occurrence Patterns of Bacterial, Archaeal and Eukaryotic Microorganisms in Rumen Microbial Communities. *Plos One* **2013,** *8* (2).

91. Henderson, G.; Cox, F.; Kittelmann, S.; Miri, V. H.; Zethof, M.; Noel, S. J.; Waghorn, G. C.; Janssen, P. H., Effect of DNA Extraction Methods and Sampling Techniques on the Apparent Structure of Cow and Sheep Rumen Microbial Communities. *Plos One* **2013,** *8* (9).

92. Wilkins, D.; Lu, X.-Y.; Shen, Z.; Chen, J.; Lee, P. K. H., Pyrosequencing of mcrA and Archaeal 16S rRNA Genes Reveals Diversity and Substrate Preferences of Methanogen Communities in Anaerobic Digesters. *Applied and Environmental Microbiology* **2015,** *81* (2), 604-613.

93. Mayumi, D.; Dolfing, J.; Sakata, S.; Maeda, H.; Miyagawa, Y.; Ikarashi, M.; Tamaki, H.; Takeuchi, M.; Nakatsu, C. H.; Kamagata, Y., Carbon dioxide concentration dictates alternative methanogenic pathways in oil reservoirs. *Nature Communications* **2013,** *4*.

94. Chen, S.; Rotaru, A.-E.; Liu, F.; Philips, J.; Woodard, T. L.; Nevin, K. P.; Lovley, D. R., Carbon cloth stimulates direct interspecies electron transfer in syntrophic co-cultures. *Bioresource Technology* **2014,** *173*, 82-86.

95. Hsieh, H.-S.; Wu, R.; Jafvert, C. T., Light-Independent Reactive Oxygen Species (ROS) Formation through Electron Transfer from Carboxylated Single-Walled Carbon Nanotubes in Water. *Environmental Science & Technology* **2014,** *48* (19), 11330-11336.

96. Abbasian, F.; Lockington, R.; Palanisami, T.; Megharaj, M.; Naidu, R., Multiwall carbon nanotubes increase the microbial community in crude oil contaminated fresh water sediments. *Science of the Total Environment* **2016,** *539*, 370-380.

97. Terrones, M., Carbon nanotubes: synthesis and properties, electronic devices and other emerging applications. *International Materials Reviews* **2004,** *49* (6), 325-377.

98. Yang, Y.; Bi, X. Y.; Westerhoff, P.; Hristovski, K.; McLain, J. E., Engineered Nanomaterials Impact Biological Carbon Conversion in Soils. *Environmental Engineering Science* **2014,** *31* (7), 381-392.

99. Wang, D. J.; Su, C. M.; Zhang, W.; Hao, X. Z.; Cang, L.; Wang, Y. J.; Zhou, D. M., Laboratory assessment of the mobility of water-dispersed engineered nanoparticles in a red soil (Ultisol). *Journal of Hydrology* **2014,** *519*, 1677-1687.

100. Lovley, D. R., Reach out and touch someone: potential impact of DIET (direct interspecies energy transfer) on anaerobic biogeochemistry, bioremediation, and bioenergy. *Reviews in Environmental Science and Bio-Technology* **2011,** *10* (2), 101-105.

101. Alpha Nano Technology Products: Single-walled carbon nanotube. http://www.nanotubes.cn/pro-s.htm (accessed August 1, 2016).

102. Tong, Z. H.; Bischoff, M.; Nies, L. F.; Myer, P.; Applegate, B.; Turco, R. F., Response of Soil Microorganisms to As-Produced and Functionalized Single-Wall Carbon Nanotubes (SWNTs). *Environmental Science & Technology* **2012,** *46* (24), 13471-13479.

103. Foley, M., Cheap Tubes, Inc. Ratio of Semiconducting to Metallic SWNT. 2016.

104. Zinder, S. H.; Anguish, T.; Cardwell, S. C., Selective inhibition by 2-bromoethanesulfonate of methanogenesis from acetate in a thermophilic anaerobic digester. *Applied and Environmental Microbiology* **1984,** *47* (6), 1343-1345.

105. Brochier-Armanet, C.; Boussau, B.; Gribaldo, S.; Forterre, P., Mesophilic crenarchaeota: proposal for a third archaeal phylum, the Thaumarchaeota. *Nature Reviews Microbiology* **2008,** *6* (3), 245-252.

106. Eriksson, J., Concentrations of 61 trace elements in sewage sludge, farmyard manure, mineral fertiliser, precipitation and in oil and crops. Swedish Environmental Protection Agency, **2001**.

107. Webster, T. M.; Smith, A. L.; Reddy, R. R.; Pinto, A. J.; Hayes, K. F.; Raskin, L., Anaerobic microbial community response to methanogenic inhibitors 2-bromoethanesulfonate and propynoic acid. *MicrobiologyOpen* **2016**, 1-13.

108. Janssen, P. H.; Kirs, M., Structure of the archaeal community of the rumen. *Applied and Environmental Microbiology* **2008,** *74* (12), 3619-3625.

109. Rozzi, A.; Remigi, E., Methods of assessing microbial activity and inhibition under anaerobic conditions: a literature review. *Reviews in Environmental Science and Bio/Technology* **2004,** *3* (2), 93-115.

110. Zhang, T. T.; Zhao, G. Y.; Zheng, W. S.; Niu, W. J.; Wei, C.; Lin, S. X., Effects of rare earth element lanthanum on rumen methane and volatile fatty acid production and microbial flora in vitro. *Journal of Animal Physiology and Animal Nutrition* **2015,** *99* (3), 442-448.

111. Zhao, Z. Q.; Zhang, Y. B.; Holmes, D. E.; Dang, Y.; Woodard, T. L.; Nevin, K. P.; Lovley, D. R., Potential enhancement of direct interspecies electron transfer for syntrophic metabolism of propionate and butyrate with biochar in up-flow anaerobic sludge blanket reactors. *Bioresource Technology* **2016,** *209*, 148-156.

112. Meador, J. P.; Yeh, A.; Young, G.; Gallagher, E. P., Contaminants of emerging concern in a large temperate estuary. *Environmental Pollution* **2016,** *213*, 254-267.

113. EPA, Significant New Use Rules: Certain Nonylphenols and Nonylphenol Ethoxylates. **2014**.

114. Soares, A.; Guieysse, B.; Jefferson, B.; Cartmell, E.; Lester, J. N., Nonylphenol in the environment: A critical review on occurrence, fate, toxicity and treatment in wastewaters. *Environment International* **2008,** *34* (7), 1033-1049.

115. Brix, R.; Hvidt, S.; Carlsen, L., Solubility of nonylphenol and nonylphenol ethoxylates. On the possible role of micelles. *Chemosphere* **2001,** *44* (4), 759-763.

116. Ahel, M.; Giger, W., Aqueous solubility of alkylphenols and alkylphenol polyethoxylates. *Chemosphere* **1993,** *26* (8), 1461-1470.

117. Frassinetti, S.; Isoppo, A.; Andrea, C.; Vallini, G., Bacterial attack of non-ionic aromatic surfactants: Comparison of degradative capabilities of new isolates from nonylphenol polyethoxylate polluted wastewaters. *Environmental Technology* **1996,** *17* (2), 199-205.

118. Barber, L. B.; Loyo-Rosales, J. E.; Rice, C. P.; Minarik, T. A.; Oskouie, A. K., Endocrine disrupting alkylphenolic chemicals and other contaminants in wastewater treatment plant effluents, urban streams, and fish in the Great Lakes and Upper Mississippi River Regions. *Science of the Total Environment* **2015,** *517*, 195-206.

119. Janex-Habibi, M. L.; Huyard, A.; Esperanza, M.; Bruchet, A., Reduction of endocrine disruptor emissions in the environment: The benefit of wastewater treatment. *Water Research* **2009,** *43* (6), 1565-1576.

120. Chang, B. V.; Yu, C. H.; Yuan, S. Y., Degradation of nonylphenol by anaerobic microorganisms from river sediment. *Chemosphere* **2004,** *55* (4), 493-500.

121. Stasinakis, A. S., Review on the fate of emerging contaminants during sludge anaerobic digestion. *Bioresource Technology* **2012,** *121*, 432-440.

122. Wang, Z.; Yang, Y. Y.; Dai, Y.; Xie, S. G., Anaerobic biodegradation of nonylphenol in river sediment under nitrate- or sulfate-reducing conditions and associated bacterial community. *Journal of Hazardous Materials* **2015,** *286*, 306-314.

123. Ejlertsson, J.; Nilsson, M. L.; Kylin, H.; Bergman, A.; Karlson, L.; Oquist, M.; Svensson, B. H., Anaerobic degradation of nonylphenol mono- and diethoxylates in digestor sludge, landfilled municipal solid waste, and landfilled sludge. *Environmental Science & Technology* **1999,** *33* (2), 301-306.

124. Bozkurt, H.; Sanin, F. D., Toxicity of nonylphenol diethoxylate in lab-scale anaerobic digesters. *Chemosphere* **2014,** *104*, 69-75.

125. Gejlsbierg, B.; Klinge, C.; Samsoe-Petersen, L.; Madsen, T., Toxicity of linear alkylbenzene sulfonates and nonylphenol in sludge-amended soil. *Environmental Toxicology and Chemistry* **2001,** *20* (12), 2709-2716.

126. Lenard, J., Mammalian hormones in microbial cells. *Trends in Biochemical Sciences* **1992,** *17* (4), 147-150.

127. Wang, Z.; Yang, Y. Y.; Sun, W. M.; Xie, S. G.; Liu, Y., Nonylphenol biodegradation in river sediment and associated shifts in community structures of bacteria and ammonia-oxidizing microorganisms. *Ecotoxicology and Environmental Safety* **2014,** *106*, 1-5.

128. Wang, Z.; Yang, Y. Y.; He, T.; Xie, S. G., Change of microbial community structure and functional gene abundance in nonylphenol-degrading sediment. *Applied Microbiology and Biotechnology* **2015,** *99* (7), 3259-3268.

129. Schreiber, C. A.; Meyn, L. A.; Creinin, M. D.; Barnhart, K. T.; Hillier, S. L., Effect of long-term use of nonoxynol-9 on vaginal flora. *Obstetrics and Gynecology* **2006,** *107* (1), 136-143.

130. Coates, J. D.; Ellis, D. J.; Gaw, C. V.; Lovley, D. R., Geothrix fermentans gen. nov., sp nov., a novel Fe(III)-reducing bacterium from a hydrocarbon-contaminated aquifer. *International Journal of Systematic Bacteriology* **1999,** *49*, 1615-1622.

131. Mehta-Kolte, M. G.; Bond, D. R., Geothrix fermentans Secretes Two Different Redox-Active Compounds To Utilize Electron Acceptors across a Wide Range of Redox Potentials. *Applied and Environmental Microbiology* **2012,** *78* (19), 6987-6995.

132. Nevin, K. P.; Lovley, D. R., Mechanisms for accessing insoluble Fe(III) oxide during dissimilatory Fe(III) reduction by Geothrix fermentans. *Applied and Environmental Microbiology* **2002,** *68* (5), 2294-2299.

133. Bond, D. R.; Lovley, D. R., Evidence for involvement of an electron shuttle in electricity generation by Geothrix fermentans. *Applied and Environmental Microbiology* **2005,** *71* (4), 2186-2189.

134. Zemb, O.; Lee, M.; Gutierrez-Zamora, M. L.; Hamelin, J.; Coupland, K.; Hazrin-Chong, N. H.; Taleb, I.; Manefield, M., Improvement of RNA-SIP by pyrosequencing to identify putative 4-n-nonylphenol degraders in activated sludge. *Water Research* **2012,** *46* (3), 601-610.

135. Ouattara, A. S.; Patel, B. K. C.; Cayol, J. L.; Cuzin, N.; Traore, A. S.; Garcia, J. L., Isolation and characterization of Desulfovibrio burkinensis sp. nov. from an African ricefield, and phylogeny of Desulfovibrio alcoholivorans. *International Journal of Systematic Bacteriology* **1999,** *49*, 639-643.

136. FischerRomero, C.; Tindall, B. J.; Juttner, F., Tolumonas auensis gen nov, sp nov, a toluene-producing bacterium from anoxic sediments of a freshwater lake. *International Journal of Systematic Bacteriology* **1996,** *46* (1), 183-188.

137. Harmon-Smith, M.; Celia, L.; Chertkov, O.; Lapidus, A.; Copeland, A.; Del Rio, T. G.; Nolan, M.; Lucas, S.; Tice, H.; Cheng, J. F.; Han, C.; Detter, J. C.; Bruce, D.; Goodwin, L.; Pitluck, S.; Pati, A.; Liolios, K.; Ivanova, N.; Mavromatis, K.; Mikhailova, N.; Chen, A.; Palaniappan, K.; Land, M.; Hauser, L.; Chang, Y. J.; Jeffries, C. D.; Brettin, T.; Goker, M.; Beck, B.; Bristow, J.; Eisen, J. A.; Markowitz, V.; Hugenholtz, P.; Kyrpides, N. C.; Klenk, H. P.; Chen, F., Complete genome sequence of Sebaldella termitidis type strain (NCTC 11300(T)). *Standards in Genomic Sciences* **2010,** *2* (2), 220-227.

138. Collins, M. D.; Shah, H. N., Reclassification of Bacteroides-termitidis Sebald (Holdeman and Moore) in a new genus Sebaldella, as Sebaldella termitidis comb nov. *International Journal of Systematic Bacteriology* **1986,** *36* (2), 349-350.

139. Lehman, R.; Lundgren, J.; Petzke, L., Bacterial Communities Associated with the Digestive Tract of the Predatory Ground Beetle, Poecilus chalcites, and Their Modification by Laboratory Rearing and Antibiotic Treatment. *Microbial Ecology* **2009,** *57* (2), 349-358.

140. Eisenberg, T.; Glaeser, S.; Kampfer, P.; Schauerte, N.; Geiger, C., Root sepsis associated with insect-dwelling Sebaldella termitidis in a lesser dwarf lemur (Cheirogaleus medius). *Antonie Van Leeuwenhoek International Journal of General and Molecular Microbiology* **2015,** *108* (6), 1373-1382.

141. Riviere, D.; Desvignes, V.; Pelletier, E.; Chaussonnerie, S.; Guermazi, S.; Weissenbach, J.; Li, T.; Camacho, P.; Sghir, A., Towards the definition of a core of microorganisms involved in anaerobic digestion of sludge. *Isme Journal* **2009,** *3* (6), 700-714.

142. Ueki, A.; Akasaka, H.; Satoh, A.; Suzuki, D.; Ueki, K., Prpvotella paludivivens sp nov., a novel strictly anaerobic, Gram-negative, hemicellulose-decomposing bacterium isolated from plant residue and rice roots in irrigated rice-field soil. *International Journal of Systematic and Evolutionary Microbiology* **2007,** *57*, 1803-1809.

143. Kushwaha, S. C.; Kates, M.; Sprott, G. D.; Smith, I. C. P., Novel polar lipids from the methanogen Methanospirillum hungatei GP1. *Biochimica Et Biophysica Acta* **1981,** *664* (1), 156-173.

144. Beckmann, S.; Lueders, T.; Kruger, M.; von Netzer, F.; Engelen, B.; Cypionka, H., Acetogens and Acetoclastic Methanosarcinales Govern Methane Formation in Abandoned Coal Mines. *Applied and Environmental Microbiology* **2011,** *77* (11), 3749-3756.

145. Parks, D. H.; Beiko, R. G., Identifying biologically relevant differences between metagenomic communities. *Bioinformatics* **2010,** *26* (6), 715-721.

APPENDIX

APPENDIX

Appendix Table 1. Image Credits for Fig. 1. Routes of Exposure for Emerging Contaminants in Anaerobic Systems

TV, Golf club, Fish, Water stick, Factories: **https://openclipart.org/**
"forage systems reseach center_0065" by "CAFNR" Licensed under Creative Commons. Accessed July 27, 2016 https://www.flickr.com/photos/cafnr/10580373474
"Mud" by "John-Paul Verkamp" Licensed under Creative Commons. Accessed July 27, 2016 https://www.flickr.com/photos/jpverkamp/4750369340
"Nanotube" by "Edumol Molecular Visualizations" Licensed under Creative Commons. Accessed July 27, 2016 https://www.flickr.com/photos/edumendo/15112442038
"Sewage treatment plant" by "eutrophication&hypoxia" Licensed under Creative Commons. Accessed July 27, 2016 https://www.flickr.com/photos/48722974@N07/4515205247
"Anaerobic Digesters" by "Rachel Schowalter" Licensed under Creative Commons. Accessed July 27, 2016 https://www.flickr.com/photos/mass_cec/8253337160
"Ready for sludge application" by "SuSanA Secretariat" Licensed under Creative Commons. Accessed July 27, 2016 https://www.flickr.com/photos/gtzecosan/6305612046

VITA

VITA

Leila Nyberg
Graduate School, Purdue University

Education

B.S., Biology 2001, Kansas State University, Manhattan, Kansas
M.S., Civil Engineering, 2008, Purdue University, West Lafayette, Indiana
Ph.D., Civil Engineering/ESE, 2016, Purdue University, West Lafayette, Indiana

Research Interests

Anaerobic ecosystems
Emerging contaminants
Molecular tools for microbial ecological assessment
Sustainable energy

Publications

Kim, Y.S., L. M. Nyberg, B. Jenkinson, and C. T. Jafvert. 2012. PAH Concentration Gradients and Fluxes through Sand Cap Test Cells installed *In Situ* over River Sediments containing Coal Tar. *Environ. Sci.: Processes Impacts*, 2013, 15 (8), 1601 – 1612.

Nyberg, L. Assessing the Impact of Nanomaterials on Anaerobic Microbial Communities. M.S Thesis Purdue University. May 2008.

Nyberg, L., R.F. Turco and L. Nies. 2008. Assessing the Impact of Nanomaterials on Anaerobic Microbial Communities. *Environmental Science and Technology,* 42:1938 - 1943.

Conference Presentations

Nyberg, L, R. F. Turco, and L. Nies. Investigating the effects of carbon nanotubes on structure and function of methanogenic microbial communities. Sustainable Nanotechnology Organization (SNO) Conference, Arlington, VA. November 4 – 6, 2012.

Nyberg, L. Impact of f-CNTs on Anaerobic Microbial Communities. EPA STAR Graduate Fellowship Conference, Washington, DC. September 19 - 20, 2011.

Nyberg, L, R. F. Turco, and L. Nies. Assessment of the impact of single-walled carbon nanotubes (SWNT) functionalized with –COOH and –PEG on an anaerobic microbial community. SETAC North America 2010 Annual Meeting, Portland, OR. November 7 – 11, 2010.

Nyberg, L, R. F. Turco, and L. Nies. Assessment of the impact of Carboxylated and PEGylated single-walled nanotubes (SWNT) in an anaerobic environment. China-US Annual Symposium (E3C), Beijing, Sept. 22-24, 2010.

Nyberg, L, L.A. Royer, K.M. Nichols, and M.S. Sepulveda. Partnering with Native Alaskan Villages: Scientific Salmon Monitoring Project. Center for the Environment Graduate Student Poster Competition, 2009.

Nyberg, L., R.F. Turco, and L. Nies. Assessment of the Impact of PEGylated Single-walled Nanotubes (SWNT) in an Anaerobic Environment. EmCon 2009: 2nd International Conference on Occurrence, Fate, Effects, and Analysis of Emerging Contaminants in the Environment. August 4-7, 2009. (Platform presentation)

Nyberg, L., R.F. Turco and L. Nies. Assessment of the impact of PEGylated single-walled nanotubes (SWNT) in an anaerobic environment. International Conference on Environmental Implications and Applications of Nanotechnology, Amherst, MA, June 9-11, 2009. (Platform presentation)

Nyberg, L., R.F. Turco and L. Nies. Assessment of the impact of PEGylated single-walled nanotubes (SWNT) in an anaerobic environment. 237th ACS National Meeting, Salt Lake City, UT, March 22-26, 2009. (Platform presentation)

Nyberg, L. and L. Nies, "Development of Molecular Tools to Assess the Impact of Nanomaterials on Anaerobic Communities", Presented at the Nanotechnology and the Environment Conference, Indianapolis, IN, August 5-6, 2008. (Platform presentation)

Nyberg L., V. Waranoski, L.F. Nies and R.F. Turco. Effect of carbon-based manufactured nanoparticles (CMNP) on anaerobic microbial communities presented at the Sigma Xi Graduate Student Poster competition, February 28, 2007. (Honorable Mention in Engineering Sciences category).

Nyberg, L.M., Z. Tong, M. Bischoff, L. F. Nies and R.F. Turco, Effect of carbon-based manufactured nanoparticles (CMNP) on microbial communities, Center for the Environment Graduate Student Poster Competition, 2006.

Nyberg, L.M., Z. Tong, M. Bischoff, L. F. Nies and R.F. Turco, Effect of carbon-based manufactured nanoparticles (CMNP) on microbial communities, Presented at the 229th ACS National Meeting, San Diego, CA, March 13-17, 2005. (Platform presentation).

Awards

(2013) Dr. James Etzel Endowment

(2012) Sustainable Nanotechnology Organization Student Travel Award

(2012) Joseph P. Chu Fellowship

(2010) SETAC Student Travel Award

(2010) EPA STAR Fellowship
(2010) Estus H. and Vashti L. Magoon Award for Excellence in Teaching
(2010) Matthew Edward Kern Environmental Engineering Scholarship
(2009) Joseph P. Chu Fellowship
(2008) Purdue University Office of Engagement Service Learning Grant for Students
(2008) Graduate Student Award for Outstanding Teaching
(2008) Ron Wukasch Environmental Engineering Scholarship
(2008) Nellie S. Munson Teaching Assistant Award
(2006) Center for the Environment Graduate Student Poster Competition, 2nd place
(2006) Matthew Edward Kern Environmental Engineering Scholarship
(2004) Lynn Fellowship